The Messenger

No. 191 | 2023

Sixty Years of Engagement Between ESO and Chile
Scientific Highlights from Ten Years of the MUSE Collaboration
The ESO Science Archive Facility: Status, Impact, and Prospects

ESO, the European Southern Observatory, is the foremost intergovernmental astronomy organisation in Europe. It is supported by 16 Member States: Austria, Belgium, the Czech Republic, Denmark, France, Finland, Germany, Ireland, Italy, the Netherlands, Poland, Portugal, Spain, Sweden, Switzerland and the United Kingdom, along with the host country of Chile and with Australia as a Strategic Partner. ESO's programme is focussed on the design, construction and operation of powerful ground-based observing facilities. ESO operates three observatories in Chile: at La Silla, at Paranal, site of the Very Large Telescope, and at Llano de Chajnantor. ESO is the European partner in the Atacama Large Millimeter/submillimeter Array (ALMA). Currently ESO is engaged in the construction of the Extremely Large Telescope.

The Messenger is published in electronic form twice per year. ESO produces and distributes a wide variety of media connected to its activities. For further information, contact the ESO Department of Communication at:

ESO Headquarters
Karl-Schwarzschild-Straße 2
85748 Garching bei München, Germany
Phone +498932006-0
information@eso.org

The Messenger
Editor: Mariya Lyubenova
Editorial assistant: Isolde Kreutle
Copy-editing and proofreading: Peter Grimley
Graphics, Layout, Typesetting: Lorenzo Benassi
Online Publishing: Mafalda Martins
Design: Jutta Boxheimer
messenger.eso.org

ISSN 0722-6691

Contents

Front Cover: Deep observations made with the MUSE spectrograph on ESO's Very Large Telescope have uncovered vast cosmic reservoirs of atomic hydrogen surrounding distant galaxies. The exquisite sensitivity of MUSE allowed for direct observations of dim clouds of hydrogen glowing with Lyman-α emission in the early Universe — revealing that almost the whole night sky is invisibly aglow. This composite image shows the Lyman-α radiation in blue superimposed on the iconic Hubble Ultra Deep Field image. Credit: ESO/Lutz Wisotzki et al., ESA/Hubble & NASA

DOI: 10.18727/0722-6691/5333

Sixty Years of Engagement Between ESO and Chile: Past, Present and Future

Xavier Barcons[1]

[1] ESO

On 6 November 1963 ESO and the Republic of Chile started a journey together that enabled the establishment in Chile of all ESO's observatories and telescopes so far. Despite all the challenges that the world went through over these six decades, a strong partnership between ESO and Chile has been forged. A vibrant user community in Chile has grown and matured, and ESO is proud to have accompanied this remarkable evolution. In this article I look at the past and present of the engagement between ESO and Chile and argue in favour of a future joint path.

How it began

It was very soon after the Convention to establish ESO as an intergovernmental organisation was signed in 1962 that the organisation decided to establish its (first) astronomical observatory in Chile. The signature of the *Agreement between the Government of Chile and the European Organisation for Astronomical Research in the Southern Hemisphere for the establishment of an astronomical observatory in Chile* on 6 November 1963[1] was a hallmark decision that set the scene for the coming decades of both European and Chilean astronomy.

The clear skies of the Atacama Desert were of course a key factor in selecting that option (Blaauw, 1991), but there was a lot more behind the decision: professional Chilean astronomy was beginning a path of growth and development[2]. While the study of the sky from northern Chile probably dates back to very ancient times, the development of professional astronomy in the country finds its roots in the middle of the nineteenth century. The very first astronomy centre in South America was established in Santiago around 1849, with the support of the President of Chile and important academic institutions. The National Astronomical Observatory (OAN) was created in 1852 by a presidential decree and has remained in Santiago since then. Pioneering scientific observations of the southern sky were performed using OAN's telescopes at various sites. In 1927 the OAN became part of the University of Chile, while another very powerful astronomy centre was taking off at the Pontificia Universidad Católica de Chile.

In the 1950s the excellence of the Chilean skies was known around the world, and Chile took the strategic decision to engage with international institutions in establishing their observatories in Chile. The 1963 agreement between ESO and Chile was therefore signed on very flourishing astronomical soil in Chile. The opening of astronomical observatories on La Silla (ESO) and of the Cerro Tololo Inter-American Observatory (CTIO) followed, both in 1969.

The current legal framework within which ESO and Chile cooperate on astronomy matters is also an international agreement: the *Interpretative, Supplementary and Amending Agreement* to the 1963 agreement, signed on 18 April 1995. This agreement led to the establishment of the Paranal Observatory to host the Very Large Telescope (VLT) and VLT Interferometer (VLTI), as well as to other very important elements, including site protection commitments, contributions to the development of Chilean astronomy, the granting of 10% of the observing time at all ESO facilities to meritorious proposals by astronomers from the Chilean community, and inclusion of Chilean astronomers in ESO's scientific advisory bodies.

ESO's observatories in Chile

Under the umbrella of the 1995 treaty, and under very similar principles, site agreements were signed not only for the VLT and VLTI (April 1995) but for the rest of ESO's observatories in Chile: APEX (August 2002), ALMA (October 2002), the Extremely Large Telescope (ELT, October 2011), and the Cherenkov Telescope Array (CTA-South, December 2018).

The reasons why ESO continued to establish all its current observatories in Chile are diverse. The driving criteria for the various site selections have invariably been of a technical nature. The exceptional conditions of the Atacama Desert for optical and infrared observations (for example, in Paranal weather losses rarely reach 10%, seeing is excellent and the dryness of the air secures a low median precipitable water vapour, critical for infrared observations) have driven the selection of first Paranal and then Armazones. The altitude, dryness and size of the Llano de Chajnantor have identified that site as unique for submillimetre observations.

Next to those criteria, the continued support of the Chilean authorities, in facilitating ESO organisational operations, in granting access and administration of the sites and engaging in their protection as well as in facilitating access to infrastructure, has played an important role, which is acknowledged and appreciated. And not to be overlooked, ESO's accumulated experience of working in Chile, the existing infrastructure and services established by the organisation over decades, and the potential synergies among the various programmes, were also of great relevance, in particular for the selection of the CTA-South site.

At some point ESO will be in a position to identify its next observatory-class project (in line with the ESO Vision and Strategy[3]), which could be a major upgrade of an existing one or a new one, either for ESO alone or in a partnership. If a new site needs to be identified and selected, technical requirements will obviously prevail and that may (or may not) require ESO to establish itself in a new place elsewhere in the world. That aside, at present the most powerful ground-based observatories that ESO has in its current programme, both in operation and under construction, are in Chile (see Barcons, 2022 for a review of ESO's programmatic views).

The evolution of Chilean astronomy

The presence of some of the most modern astronomical observatories in Chile (operated by ESO and others), specifically in the optical/infrared and millimetre/submillimetre wavelength domains, has been and remains a catalyser for the development of Chilean astronomy. University positions in astronomy have been created (in some cases supported by ESO development funds) and active

researchers, both Chilean and foreign nationals, have been recruited and have established competitive groups. Attracted by the opportunities offered by the guaranteed access to 10% of the observing time, these researchers constitute a very powerful and highly skilled task force able to exploit the observing opportunities offered by observatories at Chilean sites.

The Astronomical Society of Chile (SOCHIAS)[4] regularly releases statistics about institutions and astronomers in the country. In their 2022 statistics[5] they report that 23 institutions across the country are active in astronomy. In 2022 (2005) a grand total of 278 (58) professional astronomers worked in these institutions, made up of 170 (39) academic professionals plus another 108 (19) postdoctoral researchers. In addition, 256 (40) postgraduate students and more than 500 undergraduates are being trained in astronomy. The evolution of these figures in less than two decades is a clear testimony to the spectacular growth that the Chilean astronomical community has experienced.

The number of professional astronomers in Chile equates to 14.2 staff astronomers (including postdocs) per million inhabitants, which goes up to 36.3 per million when postgraduate trainees/ PhD students are added. These numbers are comparable with those for the ESO Member States, even higher in several cases.

In terms of publications in astronomy, according to the Scimago Journal and Country Rank[6], Chile ranks 14th in the world. When normalised to the population of the country, Chile has the 7th-highest number of publications in astronomy per capita in the world. The average citations per paper is also high (36), which compares favourably with ESO Member States, where it ranges from 44 to 21.

A significant fraction of the scientific publications by the Chilean community using ESO data are shared with astronomers from ESO Member States. In fact, 25% of the total yearly publications using data obtained by ESO's telescopes are co-authored by members of the Chilean community. This is a large number when compared to the 10% of the observing time granted, which underlines the successful collaborations between the astronomical communities of Chile and Europe.

The importance of the 10% of observing time granted to meritorious proposals by the Chilean community, as a tool to reach the current international standing, cannot be overstated. However, the actual observing time gained by the Chilean community on the VLT has exceeded 10% in about half of the periods since P80 (the record is in P109 with more than 15%). The competitiveness of Chilean proposals is well in line with that of the overall community, and therefore the observing time gained follows closely the observing time requested. Even in open competition, Chilean astronomers would normally obtain no less than 6–7% of the VLT observing time, with occasional excursions above 10%.

The emerging picture is that today there is a vibrant and productive astronomical user community in Chile and that international collaborations are significant and strong. ESO can be humbly proud of having contributed to that remarkable evolution.

Furthering the engagement between ESO and Chile

Taking note of the current astronomy landscape in the ESO Member States and in Chile, it is unavoidable to wonder about opportunities to further the existing engagement beyond the focus areas imprinted in the 1995 Agreement. That focus has been the support to the development of the astronomical community in Chile and the facilitation and support to ESO to establish its world-class observatories in the country. Success and co-evolution describe well the outcome of this joint venture.

ESO, as an intergovernmental organisation building and operating world-class research infrastructures (RIs), offers opportunities and generates impacts that go well beyond the perimeter of accessing scientific data[7]. Beyond enabling astronomical investigations through data obtained by world-class facilities, impacts in engineering through the design and development of advanced facilities, technology development, innovation and economic impacts, education, training and engagement with society through outreach are among the benefits stimulated by the 'ESO engine' in its Member States. The extent to which such benefits materialise depends strongly on how much the countries invest in and support the development of their Research, Development, Knowledge and Innovation (RDKI) ecosystem.

The strength and stature of the Chilean astronomical community is an existing asset in the Chilean ecosystem. A natural next step to further this engagement would be the participation of Chilean groups in instrument development consortia. In Chile this is referred to as Astro-engineering and has unfortunately been limited so far.

The *National Strategy of Science, Technology, Knowledge and Innovation*[8] presented to the President of Chile in 2022 is another important element. It acknowledges that astronomy offers opportunities for the development of the latest technologies and the provision of world-class scientific services and technologies, among other benefits. As one of the 13 challenges identified by that strategy, the *Integral exploitation of astronomy* quotes specific aspects, such as the need to engage with the supply chain of precision instrumentation, as well as others related to data management.

In December 2021 an ELT cooperation agreement was signed between ESO and ANID (the Chilean National Agency for Research and Development) to jointly fund cooperative projects of mutual interest around the ELT. Such projects would be related to smart operations, industry 4.0 tools, and other technical projects of significance to the future of ESO's observatories. They would also develop capacity building in the community around Paranal in technical areas and transfer knowledge to society. I consider this a very important step towards furthering the scope of the ESO-Chile partnership.

During a visit to CERN on 19 July 2023, the President of Chile announced the initiation of the process for Chile to become an Associate Member State of CERN[9]. The announcement acknowledges the added benefits of joining a RI like CERN,

including explicitly *"cooperation, expertise, investment and above all the growth of science and technology for the country"*. The President also confirmed the Chilean Government's intention to triple its investment in science, therefore providing further strategic support to the country's RDKI ecosystem.

In my view there is a path to the future with a broader scope for engagement between ESO and Chile, with Chile becoming a full ESO Member State on the horizon. A formal engagement with ESO as a full Member State by such an important partner as Chile would be indeed of the utmost importance for the organisation. As described above, there are signals that Chile may be reflecting on the added value of joining RIs, to partake in the potential opportunities they generate above and beyond user access. In the case of ESO, the context is: 1) a numerous and very competitive research astronomical community in Chile; 2) the acknowledgement of Chile's need to strengthen its RDKI ecosystem; 3) an existing and trusting relationship that has grown and consolidated for 60 years; and 4) ESO's continuing openness to welcoming Chile as a full Member State, should Chile be interested in that ultimate engagement.

Acknowledgements

This paper has benefited significantly from countless exchanges and discussions with many ESO colleagues (past and present) and members of the governing bodies, as well as colleagues, public servants, and authorities in Chile. To all of them, my sincerest thanks.

References

Barcons, X. 2022, The Messenger, 188, 3

Blaauw, A. 1991, ESO's early history (Garching: European Southern Observatory)[10]

Links

[1] ESO Basic Texts: https://www.eso.org/public/archives/books/pdf/book_0017.pdf

[2] Astronomy in Chile (1849–2000): https://www.memoriachilena.gob.cl/602/w3-article-100576.html#presentacion (In Spanish)

[3] The ESO Vision and Strategy: https://www.eso.org/public/about-eso/mission-vision-values-strategy/

[4] SOCHIAS website: https://sochias.cl

[5] SOCHIAS statistics for 2022: https://sochias.cl/astronomia-en-chile/censos-de-astronomos/

[6] SCIMAGO Journal and Country Rank: https://www.scimagojr.com/countryrank.php?area=3100&category=3103

[7] ESO's Benefits to Society: https://www.eso.org/public/products/brochures/brochure_0076/

[8] Chile's National Strategy of Science, Technology, Knowledge and Innovation: https://docs.consejoctci.cl/documento/estrategia-nacional-de-ciencia-tecnologia-conocimiento-e-innovacion-para-el-desarrollo-de-chile-2022 (in Spanish)

[9] Chile and CERN (press release): https://www.gob.cl/noticias/presidente-confirma-que-chile-esta-tramitando-su-incorporacion-como-estado-miembro-asociado-del-cern/

[10] ESO's early history: https://www.eso.org/sci/libraries/historicaldocuments/ESO_Early_History_Blaauw/ESO_Early_History.pdf

ESO/VPHAS+ team. Acknowledgement: CASU

This spectacular picture of the Sh2-284 nebula has been captured in great detail by the VLT Survey Telescope at ESO's Paranal Observatory. Sh2-284 is a star formation region, and at its centre is a cluster of young stars, dubbed Dolidze 25. The radiation from this cluster is powerful enough to ionise the hydrogen gas in the nebula. It is this ionisation that produces its bright orange and red colours.

DOI: 10.18727/0722-6691/5334

Ten Years of ALMA: Achievements and Future Perspectives

María Díaz Trigo[1]
Carlos De Breuck[1]
Evanthia Hatziminaoglou[1]
Silvio Rossi[1]
Erich Schmid[1]
Martin Zwaan[1]

[1] ESO

This year marks the 10th anniversary of the inauguration of the Atacama Large Millimeter/submillimeter Array (ALMA), the world's largest radio observatory. Over the past decade, ALMA, an international collaboration in which ESO, representing its Member States, is the European partner, has revolutionised our view of the Universe from the Solar System to the most distant galaxies. ALMA has produced iconic images that have attracted worldwide attention, such as that of the planet-forming disc around the young star HL Tau, and contributed to the first image of the shadow of a black hole at the heart of the galaxy M87. In this article we look back at the main achievements of ALMA and provide an outlook into the future.

ALMA, a worldwide collaboration

In 2001 representatives from Europe, Japan and North America signed a Resolution affirming their intent to construct and operate a giant radio telescope in cooperation with the Republic of Chile. With this Resolution three previous top-priority astronomical large projects aimed at observations at millimetre/submillimetre wavelengths in Europe, Japan and the United States united behind one of the most ambitious projects in the history of astronomy: the Atacama Large Millimeter/Submillimeter Array[a] (ALMA).

The many superlatives of ALMA

ALMA has a long history of records as an astronomical facility, from its construction and operation at an unprecedented altitude of 5000 metres to the 6569 m^2 total surface area of its antennas, its capability to observe the Sun, the more than 200 Terabytes of data stored every year in its archive, and the size of its scientific community.

ALMA's construction started in 2003 on the Chajnantor plateau, at 5000 metres above sea level in the Atacama Desert in Northern Chile. The site was chosen for its altitude and dryness, providing the best conditions for scientific observations of millimetre and submillimetre waves, which are heavily absorbed by water vapour in Earth's atmosphere in lower-altitude, more humid, environments. This choice, however, came with strict requirements related to the construction, maintenance, and operation of the facility in such a harsh environment.

More than one thousand kilometres of optical fibre had to be installed for data transmission from the Array Operations Site (AOS) at 5000 metres altitude to the Operations Support Facility (OSF) just below 3000 metres. Two 20-metre-long transporters of 130 tons and 1400 horsepower each, Otto and Lore, had to be built to transport the 66 high-precision antennas of the ALMA interferometer from the OSF to the plateau. These transporters were also part of a novel operations concept in which the antennas are relocated within the plateau to enable a continuously expanding and contracting array with baselines from 15 metres to 16 kilometres, capable of producing images with resolutions better than 10 milliarcseconds. To generate such images ALMA's main correlator (Escoffier et al., 2007), equipped with 134 million processors, combines the signals arriving at the antennas and detected in one of the receiver bands between 0.32 and 8.5 millimetres (Tan et al., 2009) at any given time, a task requiring up to 16 quadrillion operations per second. Not surprisingly, the computing effort on the part of a globally distributed team to develop the software with which ALMA operates resulted in about 5.7 million lines of code at the end of construction in 2013.

But ALMA would not be the success that it has come to be without its community

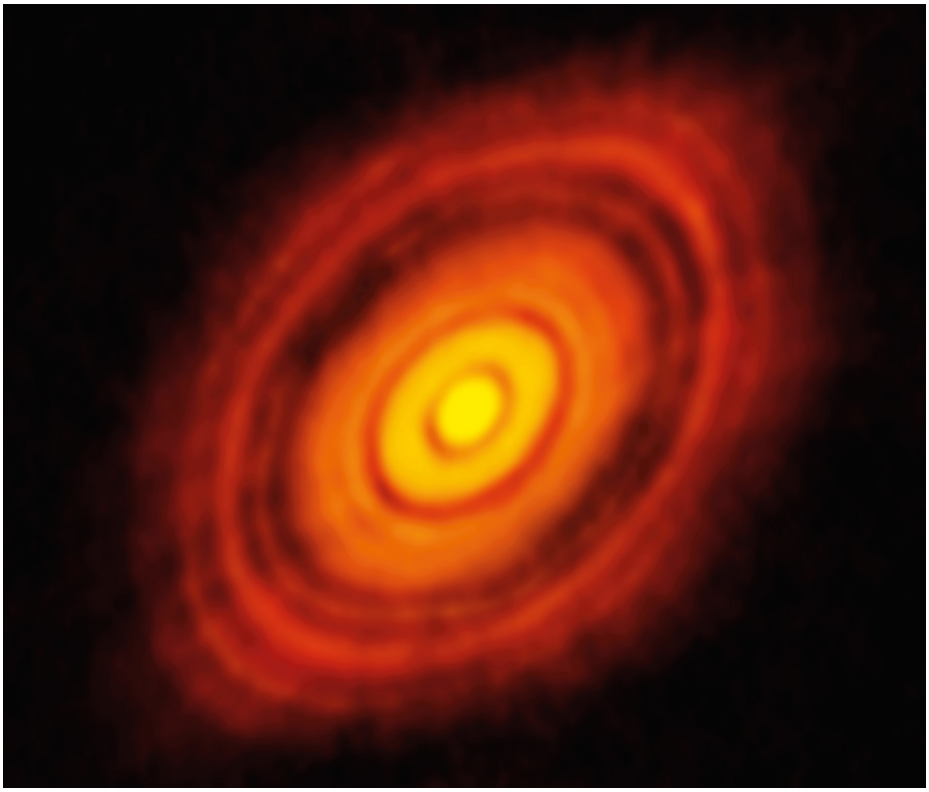

ALMA (ESO/NAOJ/NRAO)

Figure 1. This is the sharpest image ever taken by ALMA — sharper than is routinely achieved in visible light with the NASA/ESA Hubble Space Telescope. It shows the protoplanetary disc surrounding the young star HL Tauri. These new ALMA observations reveal substructures within the disc that have never been seen before and even show the possible positions of planets forming in the dark patches within the system.

Sangku Kim/ESO

Figure 2. ALMA, located in the Chilean Atacama desert, is the most powerful telescope for observing the cool Universe — molecular gas and dust. ALMA studies the building blocks of stars, planetary systems, galaxies and life itself. By providing scientists with detailed images of stars and planets being born in gas clouds near our Solar System, and detecting distant galaxies forming at the edge of the observable Universe, which we see as they were roughly ten billion years ago, it allows astronomers to address some of the deepest questions of our cosmic origins. ALMA can also be used to study Solar System objects.

of more than 11 000 ALMA registered users. More than 4000 principal investigators and co-investigators request time to perform astronomical observations with ALMA following the yearly ALMA call for proposals and in 2022 alone nearly 9000 scientists from more than 50 countries worldwide published scientific results using ALMA data. This global community is the result of ALMA's investment in creating data reduction and calibration pipelines and providing high-quality data products through an archive rivalling those of space observatories (Stoehr et al., 2022), and in providing users with an extensive support network with the goal of making the facility accessible to all astronomers regardless of their radio-interferometry expertise (Zwaan et al., 2021). In Europe, the user support has been set up as an internationally distributed network of European ALMA Regional Centre (ARC) nodes (Andreani & Zwaan, 2006; Hatziminaoglou et al., 2015). This highly successful model has provided yet more means for ALMA to establish direct contact with the community and to widen its support across Europe and has inspired the European network of VLTI Expertise Centres, aimed at extending the community behind optical interferometry.

Scientific highlights

ALMA's scientific leadership is demonstrated by more than 3000 refereed publications since the start of operations. The original goals for ALMA[b] had sensitivity and high-resolution and high-fidelity images at their base. Indeed, ALMA's investment in pursuing such goals was key to major discoveries such as the image of the planet-forming disc around the young star HL Tauri (ALMA Partnership, 2015) or the first ever image of a black hole shadow in 2017 (Event Horizon Telescope Collaboration, 2019), featuring more than 1000 and 2000 citations, respectively, to date.

Beyond our galaxy, ALMA has excelled at detecting both normal and bright galaxies at increasingly large distances and mapping their dust and cold gas reservoirs in exquisite detail at the high angular resolution needed to image the interstellar

S. Otarola/ESO

Figure 3. A photograph of an Atacama Large Millimeter/submillimeter Array (ALMA) antenna at the ALMA Operations Support Facility (OSF). Part of the Milky Way can be seen in the night sky above the antenna.

medium (ISM) and resolve molecular clouds at cosmic noon, thus enabling the study of distant dust-obscured star formation (see Hodge & da Cunha, 2020 and references therein). The Large Programmes ALPINE and REBELS (Le Fèvre et al., 2020 and Bouwens et al., 2022, respectively) focus now on going all the way back to the epoch of reionisation, thus allowing a precise determination of the evolution of the cosmic molecular gas mass density since the early times. The future is bright in this area thanks to the large galaxy samples that will arise from facilities like JWST, Euclid, Vera C. Rubin Observatory and ESO's ELT, to name just a few; those galaxies will need to have their redshifts determined, confirmed or refined, and also their gas and dust resolved and characterised, ensuring that ALMA will remain a key player.

Complementary efforts to those linking the physical process that govern star formation to galaxy properties have been also made in our vicinity. Molecular clouds in the Milky Way have been mapped in different environments at high angular and spectral resolution to show the rich structure of filaments and cores that collapse gravitationally to form protostars and their interplay with the ISM (see, for example, the Large Programmes FAUST and IMF; Codella et al., 2021 and Motte et al., 2022, respectively). In particular, studies of the chemical complexity of protostars are also providing clues to the emergence of complex organic molecules in the ISM and are the target of the recently approved Large Programme COMPASS.

Zooming-in to already formed protostars and the discs around them, a major ALMA discovery was brought about by the high spatial resolution image of the dust in the protoplanetary disc around HL Tau, revealing gaps and rings that indicated that planet formation is well under way at stellar ages of ~ 1 Myr. The morphology of protoplanetary discs has now been extensively studied with numerous ALMA observations, including the DSHARP (Andrews et al., 2018) and MAPS (Öberg et al., 2021) Large Programmes. The distribution of dust and molecules in the discs is providing insights into the physical characteristics of the disc with, for example, temperature or density being traced with different molecules and their transitions. The disc images have also revealed velocity kinks and unveiled planets that could not have been discovered otherwise as they were occulted by dust.

Finally, ALMA has also carried out studies of the Sun and the Solar System, neutron stars, supernovae and transient events, to name just a few, demonstrating that ALMA's reach at ten years has already gone far beyond expectations and paving the way for new discoveries in the next decades.

ALMA in the 2030s

Looking to the future, ALMA has just begun the most powerful upgrade in its history, the Wideband Sensitivity Upgrade (WSU). This upgrade addresses the first

priority of the ALMA 2030 development roadmap[1], a strategic plan for technical developments devised in consultation with the ALMA Science Advisory Committee and the scientific community and endorsed by the Astronet 2022–2035 roadmap[2].

The technical goals of the WSU are to broaden the system's bandwidth by at least a factor of two and up to four times the current value, and to upgrade the associated electronics and correlator. This will result in increases in ALMA's observing speed by at least a factor of three/six (for twice/four times the bandwidth) for observations at low spectral resolution and of up to a factor of 50 for spectral scans at high resolution, making ALMA even more powerful than it is today and setting the basis for more exciting discoveries in the next decades.

The first receiver band with wide bandwidth capability will be Band 2 (Yagoubov et al., 2020), covering the 67–116 GHz frequency range, for which the first receivers have just been successfully installed[3]. Band 2 completes ALMA's originally planned coverage of the atmospheric windows from 35 to 950 GHz and opens a new window at 67–84 GHz, enabling among other things the detection of complex organic molecules such as glycine, the characterisation of the fractionation of elements in our Solar System, evolved stars and young solar analogues, and the determination of completely new redshift ranges (Beltran et al., 2015; Fuller et al., 2016).

These goals are well aligned with the science drivers of ALMA 2030, arranged around the themes of origins of galaxies, origins of chemical complexity and origins of planets (Carpenter et al., 2022).

ALMA has detected gas in normal and bright galaxies across the history of the Universe, back to the time when the Universe was less than a billion years old, and it is now studying the structure and kinematics of such gas. Thanks to the wide bands afforded by the WSU and the improved sensitivity, the spectral scans needed to determine redshifts in unbiased galaxy surveys or to confirm photometrically determined redshifts will be 3.6 times faster than today. The gains in observing speed will be even higher for the high-spectral-resolution scans needed to advance further the study of the origins of chemical complexity across a vast range of astrophysical environments, enabling for instance comprehensive chemical inventories of filaments, cores and protostars in molecular clouds over all evolutionary states. Finally, building upon the revolutionary images of dust continuum in protoplanetary discs that reveal the presence of rings, gaps and spirals where planets are forming, the WSU will efficiently produce such images for a myriad of molecular lines. This will provide the means to advance towards a full understanding of the process of planet formation, since the gas contains most of the mass in protoplanetary discs and the morphology of different molecules can be used to determine the physical, chemical, and dynamical properties of the discs.

Concluding remarks

Ten years after its inauguration, ALMA has already transformed our understanding of the Universe, from the small to the largest scales. As the first of the 2020 decade's large facilities to become operational, ALMA has succeeded in having a scientific output comparable to those of other large facilities on the ground or in space, such as ESO's Very Large Telescope, ESA's XMM-Newton or the NASA/ESA Hubble Space Telescope at a similar age, while serving as a model for the operation and user support of future astronomical mega-facilities. Arguably, ALMA's most significant contribution to science may be that it was the first truly global astronomical facility. As outlined in the recent 2020 US Decadal Survey Report[4] "*Programmatically, the most dramatic development of the past decade has been the emergence of ALMA as a facility that engages the full (in terms of both wavelength and geography) astronomical community*". This is the best tribute to the dedication of all ALMA staff around the world who worked together to make ALMA happen. It is therefore time to celebrate: happy birthday ALMA!

Acknowledgements

M. Díaz Trigo thanks F. Stoehr for providing the statistics on the ALMA user community.

References

ALMA Partnership et al. 2015, ApJL, 808, L3
Andreani, P. & Zwaan, M. 2006, The Messenger, 126, 43
Andrews, S. M. et al. 2018, ApJL, 869, L41
Beltran, M. T. et al. 2015, arXiv:1509.02702
Bouwens, R. J. et al. 2022, ApJ, 931, 160
Carpenter, J. et al. 2022, ALMA memo 621
Codella, C. et al. 2021, FrASS, 8, 227
Escoffier, R. P. et al. 2007, A&A, 462, 801
Event Horizon Telescope Collaboration et al. 2019, ApJL, 875, L1
Fuller, G. A. et al. 2016, arXiv:1602.02414
Hatziminaoglou, E. et al. 2015, The Messenger, 162, 24
Hodge, J. A. & da Cunha, E. 2020, Royal Society Open Science, 7, 200556
Le Fèvre, O. et al. 2020, A&A, 643, A1
Motte, F. et al. 2022, A&A, 662, A8
Öberg, K. I. et al. 2021, ApJS, 257, 1
Stoehr, F. et al. 2022, The Messenger, 187, 25
Tan, G. H. et al. 2009, The Messenger, 136, 32
Yagoubov, P. et al. 2020, A&A, 634, A46
Zwaan, M. et al. 2021, The Messenger, 184, 16

Links

[1] ALMA 2030 development roadmap: https://almaobservatory.org/en/publications/the-alma-development-roadmap/
[2] ASTRONET 2022–2035 roadmap: https://www.astronet-eu.org/wp-content/uploads/2023/05/Astronet_RoadMap2022-2035_Interactive.pdf
[3] New ALMA receivers that will probe our cosmic origins successfully tested: https://www.eso.org/public/announcements/ann23013
[4] 2020 US Decadal Report: https://science.nasa.gov/astrophysics/decadal-2020/2020-decadal-survey

Notes

[a] ALMA is a partnership of ESO (representing its Member States), the National Science Foundation in the USA and the National Institutes of Natural Sciences in Japan, together with the National Research Council (Canada), the Ministry of Science and Technology and the Academia Sinica Institute of Astronomy and Astrophysics (Taiwan) and the Korea Astronomy and Space Science Institute (Republic of Korea), in cooperation with the Republic of Chile.
[b] ALMA's original goals were:
- the ability to detect spectral line emission from CO or C+ in a normal galaxy like the Milky Way at a redshift of $z = 3$, in less than 24 hours of observation;
- the ability to image the gas kinematics in a solar-mass protoplanetary disc at a distance of 150 pc, enabling one to study the physical, chemical, and magnetic field structure of the disc and to detect the tidal gaps created by planets undergoing formation; and
- the ability to provide precise images at an angular resolution of 0.1 arcseconds.

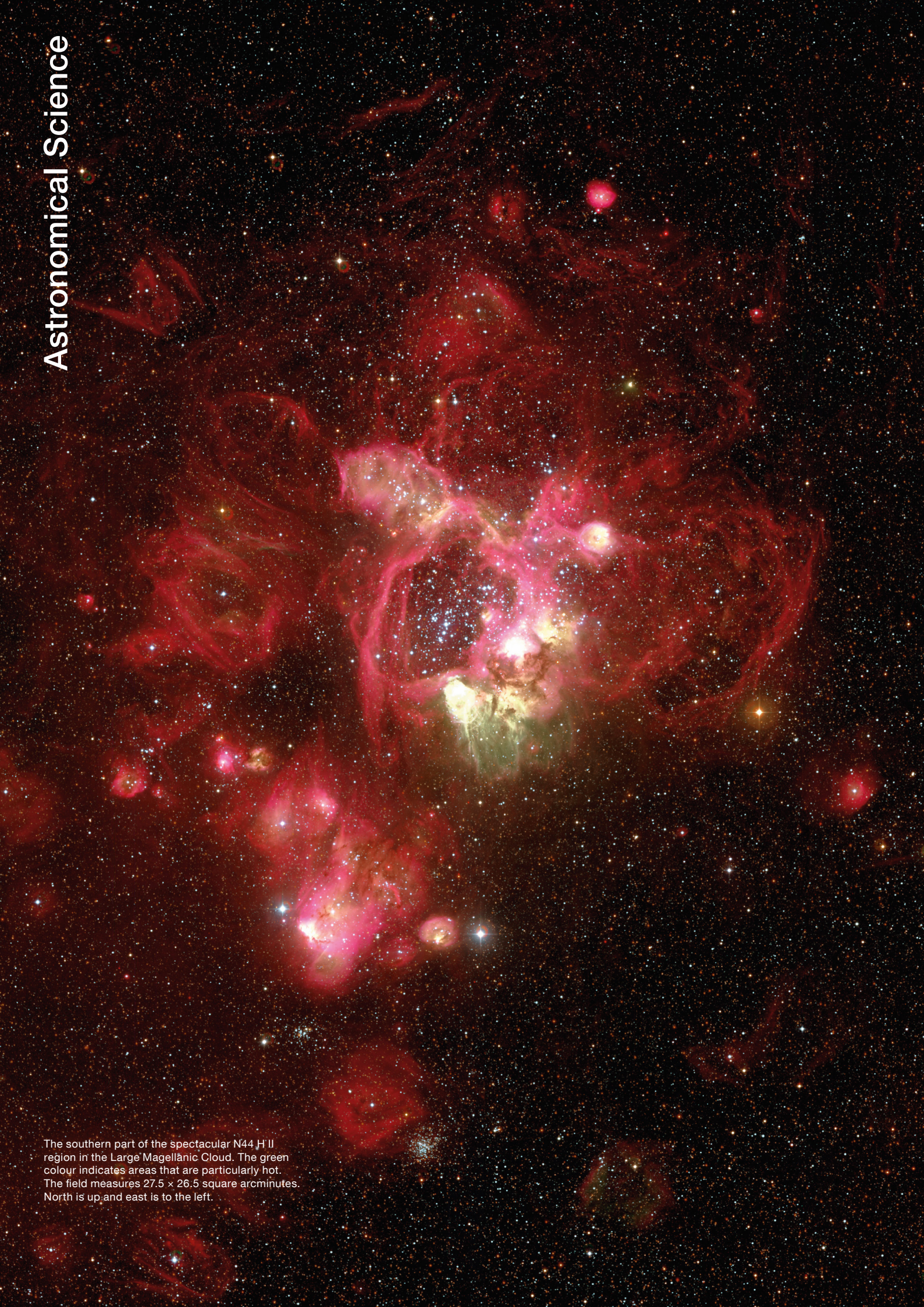

The southern part of the spectacular N44 H II region in the Large Magellanic Cloud. The green colour indicates areas that are particularly hot. The field measures 27.5 × 26.5 square arcminutes. North is up and east is to the left.

DOI: 10.18727/0722-6691/5335

Scientific Highlights from Ten Years of the MUSE Collaboration

Roland Bacon[1]
Jarle Brinchmann[2]
Nicolas Bouché[1]
Thierry Contini[3]
Sebastian Kamann[4]
Davor Krajnović[5]
Ana Monreal Ibero[6]
Johan Richard[1]
Tanya Urrutia[5]
Lutz Wisotzki[5]
and the MUSE collaboration

[1] Lyon Astrophysics Research Centre, University of Lyon, CNRS, France
[2] Institute of Astrophysics and Space Science, University of Porto, Portugal
[3] Institute for Research in Astrophysics and Planetology, CNRS, University of Toulouse, France
[4] Astrophysics Research Institute, Liverpool John Moores University, UK
[5] Leibniz Institute for Astrophysics, Potsdam, Germany
[6] Leiden Observatory, Leiden University, the Netherlands

We present the scientific highlights of ten years of exploitation of the Multi Unit Spectroscopic Explorer (MUSE) Guaranteed Time Observations performed in the context of the MUSE collaboration. These ten years have been particularly rich in discoveries and have resulted in more than 120 refereed papers. In this article we focus on the main results, grouped into four broad topical categories: resolved stellar populations, nearby galaxies, galaxy demographics, and the circumgalactic medium.

Introduction

About 20 years ago we proposed building the Multi-Unit Spectroscopic Explorer (MUSE) as a second-generation instrument for ESO's Very Large Telescope (VLT). MUSE was conceived to combine the qualities of a sensitive high-resolution imager with those of a powerful integral field spectrograph, capable of not only single-object studies but also opening up the possibility of conducting spectroscopic surveys in deep fields and crowded regions without any target preselection (Bacon et al., 2010). After 10 years of designing, planning, and manufacturing, MUSE was successfully deployed at the VLT's Unit Telescope 4 (UT4) in January 2014 (Bacon et al., 2014) and almost instantly started to produce science-grade data of a hitherto unknown quality (and file sizes). MUSE has now been in regular operation since October 2014 and has become one of the most in-demand ESO instruments. In 2017 and 2018 its performance was further enhanced by the addition of the Adaptive Optics Facility at UT4 (deploying ground layer adaptive optics and laser tomography adaptive optics).

After handing over the keys to ESO we, the MUSE consortium, decided to stay together as a team and exploit our 255 nights of Guaranteed Time Observations (GTO) in a collaborative effort. Ultimately this effort stretched over nearly 10 years — always absorbing only a small fraction of the total time available for MUSE — and was finally concluded (in the sense of recording the very last GTO photons) only a few weeks before finishing this article. Here we take the opportunity to give an overview of the science projects that we focused on within GTO, and to summarise the key accomplishments.

We present these results grouped into four broad topical categories: resolved stellar populations, nearby galaxies, galaxy demographics, and the circumgalactic medium. While each topic encompasses a variety of target types, observing strategies, and detailed science goals, the projects within a category share at least several methodical aspects of the data analysis. Furthermore, the observational data obtained in GTO have often served multiple, sometimes very different, scientific purposes. This is particularly the case for our MUSE surveys in fields with deep Hubble Space Telescope (HST) and multiwavelength data, where we performed 'spectroscopy of everything' down to unprecedented depths. And although this observing strategy was already largely decided before MUSE went on sky, we encountered many surprises, including some of the most influential MUSE discoveries.

Resolved stellar populations

MUSE has been a game-changer in terms of our ability to study stellar populations in the local Universe. By combining precise astrometric information with algorithms to recover the point spread function (PSF), tools like PampelMuse (Kamann, Wisotzki & Roth, 2013) enabled us for the first time to gather large spectroscopic samples even in the crowded environments of massive star clusters or nearby galaxies. This novel approach of 'crowded field spectroscopy' has led to several breakthrough results, as highlighted below.

In a core GTO programme we performed a stellar census of Galactic globular clusters, presented by Kamann et al. (2018).

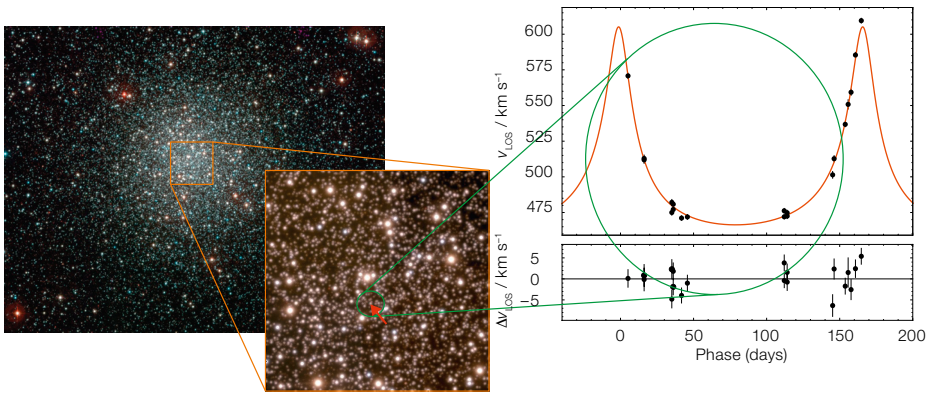

Figure 1. Discovery of a dormant stellar-mass black hole in the Galactic globular cluster NGC 3201. The left panel shows a wide-field image of the cluster taken with the ESO/MPG 2.2-metre telescope at La Silla. Outlined in orange are the contours of a 2 × 2 MUSE mosaic shown in the centre of the Figure. The companion to the stellar-mass black hole is indicated with a red arrow and its phase-folded radial velocity curve is shown to the right. The red line shows the Keplerian motion predicted if the unseen companion is a black hole with a minimum mass of 4.2 $M_{\odot}$.

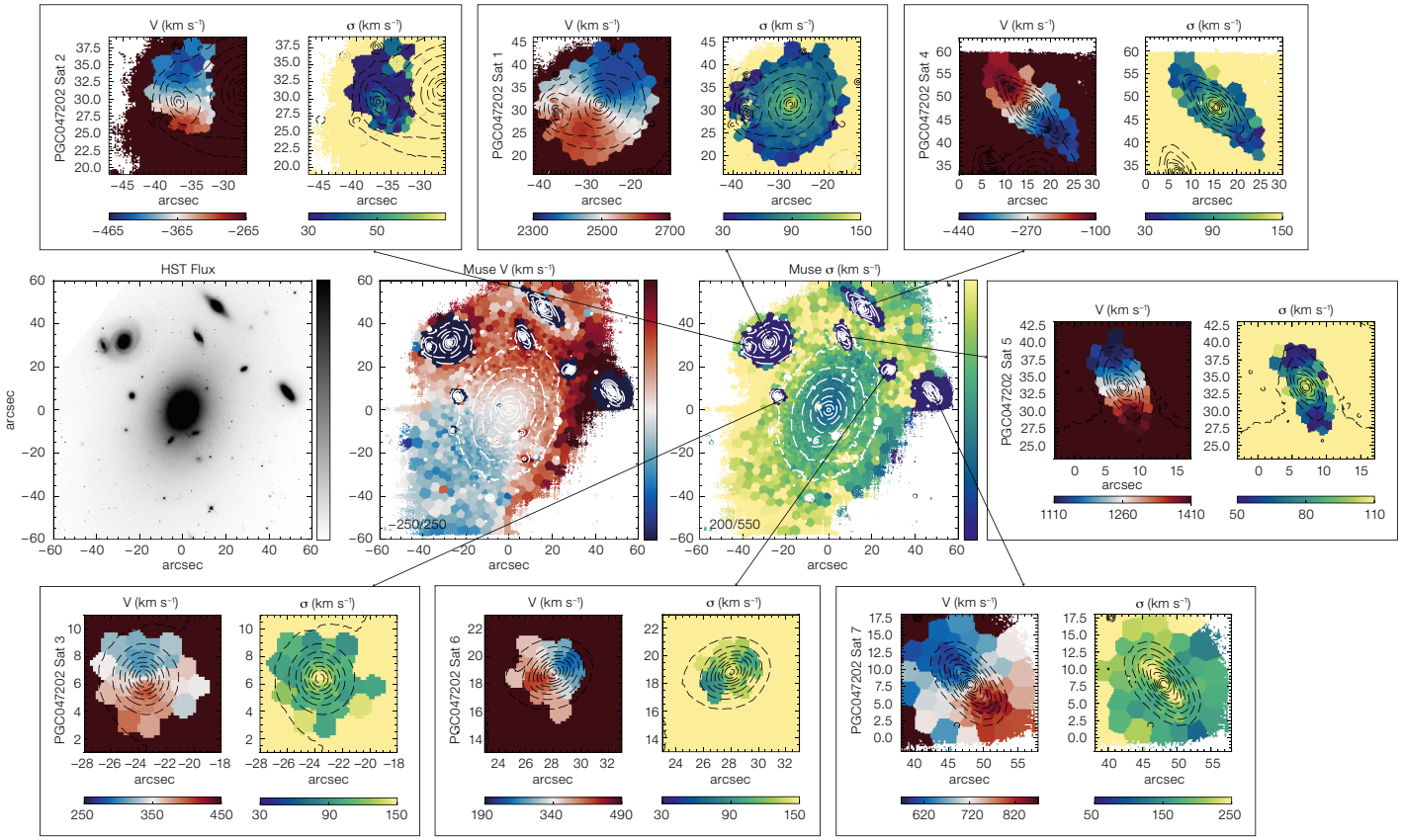

Figure 2. MUSE mosaic of 2 × 2 pointings mapping PGC047202, the BCG in the cluster Abell 3558. The large central panels show the HST/ACS/F814W image, the MUSE mean velocity and the velocity dispersion maps of the stellar component. The velocity limits are given in the lower right corner. The smaller maps show the stellar velocity and velocity dispersion of the satellite galaxies of PGC047202. Their velocities (shown under the maps) are given with respect to the systemic velocity of the main galaxy (set to zero).

For a sample of about 25 clusters we studied the kinematics and chemistry of up to 50 000 cluster stars, and we monitored their radial velocities over eight years in search of variations that would reveal binaries. This campaign led to the detection of a dormant stellar-mass black hole (and two additional candidates) in the globular cluster NGC 3201, presented by Giesers et al. (2018, 2019; see Figure 1). This was not only the first detection of a quiescent black hole in a star cluster, but also the very first dynamical detection of a stellar-mass black hole. It proves that massive star clusters are able to retain sizable black hole populations, which makes them prime candidates to host binary black hole mergers, observable in gravitational waves.

MUSE also allowed us to study the kinematics of globular clusters in unprecedented detail. Kamann et al. (2018) showed that the majority of massive clusters rotate, and that their angular momenta scale with their relaxation times. Star clusters evolving in the tidal fields of their host galaxies will lose angular momentum as stars escape, and the rate of escaping stars is linked to their relaxation times. Therefore, the link between the two suggests that the rotation we observe today is only a fraction of the clusters' natal rotation. In this way MUSE has already improved our understanding of the conditions in which globular clusters — which represent some of the oldest constituents of our Milky Way — formed.

Another relic from the infancy of the Milky Way is the population of ultra-faint dwarf galaxies (UFDs) surrounding it. UFDs are dominated by dark matter and notoriously poor in stars, but are nevertheless challenging to target with multi-object spectrographs because of the low contrast between member stars and surrounding stars and galaxies, and, in some cases, the stellar crowding near their centres. By adopting the crowded field spectroscopy technique we could bypass the challenge of sample pre-selection and efficiently measure radial velocities for faint stars, using their kinematic and dynamical signatures to place constraints on dark matter models. With this goal in mind we carried out MUSE-Faint, a survey of UFDs with MUSE. In the first paper of this survey we used observations of Eridanus 2 to show that the overdensity present in the galaxy is actually a star cluster hosted by this galaxy (Zoutendijk et al., 2020). We then used the existence of this cluster to place constraints on the fraction of dark matter in massive compact halo objects.

Since the UFDs have little baryonic matter, any significant core in the dark matter density profile would present a challenge to the cold dark matter (CDM) model.

Zoutendijk et al. (2021a) carried out the first test of this using data from Eridanus 2 and found that its density profile is consistent with CDM. This work was extended by Zoutendijk (2022) and a forthcoming paper analyses the dark matter density profiles of all five UFDs from Zoutendijk et al. (2021b), providing even stronger constraints on dark matter models.

Located almost an order of magnitude further away than the UFDs at a distance of 1.9 Mpc, the galaxy NGC 300 has been the target of a GTO programme to identify and classify a multitude of discrete objects, again adopting the new approach of crowded field spectroscopy. A pilot study (Roth et al., 2018) revealed several emission line nebulae — H II regions, supernova remnants and planetary nebulae — alongside a large variety of luminous stellar sources such as carbon- and oxygen-rich asymptotic giant branch stars, and symbiotic and other emission-line stars. Hot massive stars are of particular interest for probing the theory of stellar evolution, chemical enrichment and feedback, and as progenitors to black holes. González-Torà et al. (2022) performed quantitative spectroscopy of 16 BA supergiants in a single MUSE pointing and we were able to place these stars into the Hertzsprung–Russell diagram, extending the so-called flux-weighted gravity luminosity relationship to higher surface gravity, and enabling us to obtain a new estimate of the distance modulus of the galaxy, $(m–M)_{FGLR} = 26.34 \pm 0.06$.

Nearby galaxies

We devoted several GTO programmes to the study of galaxies in the nearby Universe, to investigate the role of star formation at different levels and the dynamics of their stellar and gaseous components. Here we use the qualifier ‘nearby’ to denote objects close enough to resolve their inner structures over scales of less than 1 kpc, but already too far away to resolve their contents into individual sources. Within this category, however, the definition of the various samples and the typical properties in these samples vary quite substantially.

At the high end of the distribution of star formation rates, we observed around thirty Luminous and Ultraluminous Infrared Galaxies. A primary target among them was the Antennae system, one of the most iconic galaxies known and the closest (at 22 Mpc) ongoing major merger. We mapped its main body together with the tip of one of the tidal tails at a spatial scale of 100 pc arcsec^{-1}, allowing us to systematically separate H II regions from the diffuse ionised gas (DIG). Combining the measured Hα luminosities with HST photometry of young star clusters we inferred that the dominant ionisation mechanism of the DIG is UV radiation leaking from the main sites of star formation, with escape fractions (from the H II regions, not from the galaxy as a whole) of up to 90%; there is no need for additional sources of ionising photons (Weilbacher et al., 2018). This study was complemented by age-dating the stellar populations in the H II regions in the system (Gunawardhana et al., 2020). A surprising result was the detection of two diffuse interstellar bands, spectral absorption features of mysterious origin, at various locations across the galaxy (Monreal-Ibero, Weilbacher & Wendt, 2018) — the first time that these features had been mapped beyond the Local Group.

We also observed several blue compact dwarf galaxies to probe the impact of extreme star formation on the interstellar medium of galaxies at much lower masses and lower metallicities. An illustrative example is UM 462, a nearby galaxy with properties similar to the so-called green pea galaxies, where we could use the rich information content of a MUSE datacube to disentangle its complex gas structures and the impact of stellar feedback (Monreal-Ibero et al., 2023).

Moving to more typical systems, we mapped a sample of about 40 spiral galaxies on the stellar mass – star formation rate main sequence to investigate the relation of the diffuse interstellar gas to denser gas responsible for star formation. Erroz-Ferrer et al. (2019) showed that these two gas components have different metallicities (star-forming gas being more metal-rich than diffuse gas), but with similar radial variations. Subsequently, den Brok et al. (2020) demonstrated that the star forming gas and the DIG differ in their kinematic properties: while the rotation curves follow a similar trend, the diffuse gas is slower and has higher velocity dispersion. The ‘dynamically hotter’ nature of the DIG was confirmed by dynamical modelling, suggesting that the DIG gas is distributed in a disc-like structure that is considerably thicker than the thin disc holding the star forming gas.

At the other extreme of the range of star formation rates are the quenched systems, i.e. those with little or no star formation activity. Such objects are particularly common among very massive galaxies. As part of our GTO programme we conducted the MUSE Most Massive Galaxies (M3G) survey which targetted some of the most massive galaxies in the nearby Universe. We focused on a sample of Brightest Cluster Galaxies (BCGs) together with a selection of massive ($> 10^{12}\ M_{\odot}$) neighbours, all located in very dense clusters (see Figure 2). While presently not completely devoid of gas (Pagotto et al., 2021), these systems show a high fraction (75–90%) of accreted stars, suggesting an assembly history dominated by merging (Spavone et al., 2021).

The detailed kinematic and dynamical properties revealed by MUSE provide important clues towards understanding which type of mergers were involved in the assembly of these galaxies. Their kinematics is often very complex, with multiple spin reversals and generally low stellar angular momentum. Remarkably, about 50% of BCGs in the sample show evidence of rotation around their major axis (Krajnović et al., 2018), suggested to be the signature outcome of major ‘dry’ (similar mass, gas free) mergers. Such mass assembly pathways are also confirmed by looking at the internal orbital structures: the most massive galaxies are all strongly triaxial systems containing all major orbital families, with co- and counter-rotating spin orientations, resulting in truly spectacular observed kinematics (den Brok et al., 2021).

Galaxy demographics

Among the great scientific successes of the MUSE GTO programme are undoubtedly the MUSE surveys in deep fields, which exploited the multiplexing capability of the instrument in completely new ways. A substantial fraction of our

invested observing time was focused on a systematic spectroscopic mapping of the area in and around the Hubble Ultra Deep Field (HUDF), selected only on the basis that it had the best available multi-band HST coverage to complement the MUSE data (Bacon et al., 2017, 2023; Urrutia et al., 2019). In other fields we took advantage of the presence of strong lensing clusters in the foreground (Bina et al., 2016; Richard et al., 2021). We also surveyed several galaxy groups in the COSMOS area (Epinat et al., 2023).

A key ingredient of our 'spectroscopy of everything' approach adopted for these MUSE deep fields was the development of dedicated software to perform 'blind' searches for emission-line sources. This enabled us to build large samples of objects with extremely faint continuum levels, way below the limit for inclusion in a photometrically selected sample. We are thus probing star-forming galaxies down to extremely low stellar masses. In conjunction with the redshift-dependent survey volume corresponding to a fixed field of view, the two emission lines most frequently selected are [O II] λ3727 and Lyman-α λ1216. The former is detectable with MUSE at (roughly) $0.3 < z < 1.5$, the latter at $2.9 < z < 6.7$. In the following we denote these two redshift intervals as 'intermediate' and 'high' redshifts. In between the two domains there is a region from $z = 1.5$ to 2.9 where galaxies do not show strong emission lines, clearly visible as a 'redshift desert' in the overall redshift distribution (see Figure 3). Here we report on some key results of these deep field surveys, with an emphasis on galaxy demographics and scaling relations.

In the high-redshift range the dominant population studied with MUSE consists of star-forming Lyman-α-emitting galaxies (LAEs), which because of their low stellar masses are far more numerous than the relatively massive 'Lyman-break galaxies' (LBGs). In contrast to narrowband surveys for LAEs or broadband surveys for LBGs, MUSE provides substantial samples of spectroscopically confirmed galaxies in a single observational pass, without any need to preselect targets. Even with a single hour of observing time per pointing, as adopted in the MUSE-Wide survey, we detect typically 11 LAEs in a single MUSE field of 1 arcmin^2 (Herenz et al., 2017). Of course this number increases with exposure time, reaching densities of almost 400 LAEs per arcmin^2 in our deepest dataset encompassing 140 hours — the MXDF (Bacon et al., 2023). Altogether we have already identified several thousand LAEs which we can study in detail.

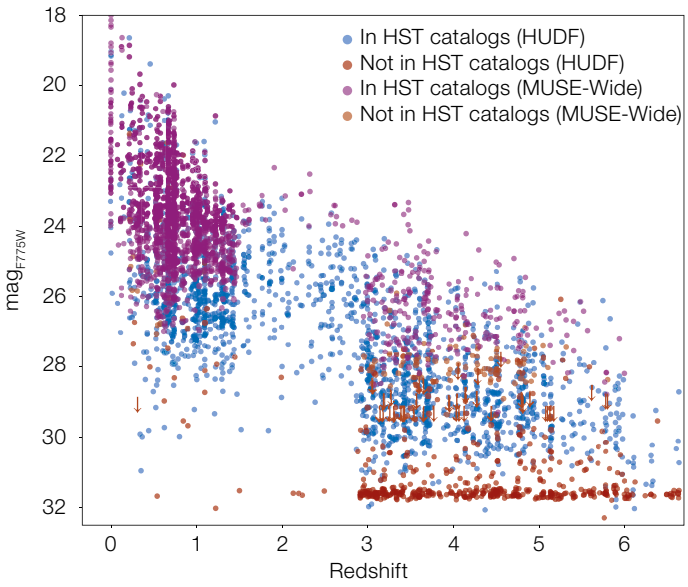

Figure 3. Magnitude–redshift scatter plot for well over 4000 sources in both the HUDF and the surrounding MUSE-Wide fields (adapted from Bacon et al., 2023 and Urrutia et al., 2019). As the shallower MUSE-Wide survey covers a larger volume, more low-redshift sources are spectroscopically identified, while the deeper HUDF data identify more LAEs. Nevertheless, even in the 1-hour data, over 20% of LAEs do not have a catalogued HST counterpart.

One of the most important tools with which to characterise galaxy populations is the luminosity function. For LAEs this quantity is related to the production and escape of H-ionising photons. Getting the correct shape and redshift evolution of the LAE luminosity function, especially at the faint end, is therefore imperative for determining which galaxies dominate the cosmic ionisation budget. One of the challenges that we faced was that the generally very extended nature of Lyman-α emission (see below) impacts the detectability of LAEs. Taking this into account when constructing the survey selection function, we found the faint-end slope of the LAE luminosity function to be considerably steeper than it would have been if we had assumed point sources (Drake et al., 2017; de La Vieuville et al., 2019; Herenz et al., 2019).

Since our blind emission line search technique is not bound to any photometric pre-selection, we are sensitive to finding objects with even extremely high Lyman-α equivalent widths. It turns out that such objects exist in surprisingly large numbers. Almost 20% of the LAEs do not have a counterpart even in the deepest existing HST images, implying very low stellar masses and extreme equivalent widths of > 240 Å (Hashimoto et al., 2017; Maseda et al., 2018; Kerutt et al., 2022). These objects challenge traditional star formation models (for example, Charlot & Fall, 1993; Schaerer, 2002), except for the most extreme stellar populations with low metallicities and a top-heavy initial mass function. In combination with Spitzer infrared photometry to infer Hα luminosities of a subset of these objects, we obtained extremely high H-ionising photon production rates, suggesting that such ultra faint LAEs are a major contributor to the metagalactic UV radiation field (Maseda et al., 2020).

While Lyman-α is usually the most prominent spectral feature in our high-redshift objects, several spectra also show other UV emission and absorption lines. Some of them are valuable for probing the ionisation states of LAEs, the two most prominent being C III] λ1909, a typical tracer for extreme star formation (Maseda et al., 2017) and, intriguingly, He II λ1640, which requires high ionisation parameters to be as strong as observed (Nanayakkara et al., 2019). We have characterised the global UV emission line properties of our high-redshift samples by stacking (Feltre

et al., 2020) and also object-by-object (Schmidt et al., 2021), finding several indications of extreme star formation, young ages and low gas-phase metallicities.

About a third of our blindly detected emission line sources are intermediate-redshift [O II] emitters at $z < 1.5$, for which MUSE also delivers full spectra, often with additional emission lines apart from the detected line. Exploiting the ionised gas kinematics for spatially resolved galaxies, we extended the Tully–Fisher Relation (TFR) to low stellar masses, showing a high scatter around this relation that is due to the frequent presence of dispersion-dominated galaxies in this mass regime (Contini et al., 2016). However, the environment in which galaxies reside does not have a significant impact on the slope or zero-point of the TFR (Abril-Melgarejo et al., 2021; Mercier et al., 2022). Moreover, we found that the regular stellar kinematics of disc galaxies observed in the local Universe was already in place 4–7 Gyr ago and that their gas kinematics traces the gravitational potential of the galaxy, and therefore is not dominated by shocks and turbulent motions even at sub-kpc scales (Guérou et al., 2017; Patricio et al., 2019).

The main sequence of star-forming galaxies in the low-mass regime follows a sub-linear relation with a steeper slope and higher scatter than in the high-mass regime, in agreement with simulations implementing supernova feedback processes in low-mass halos (Boogaard et al., 2018). Mercier et al. (2022) further showed that the main sequence is offset by ~ 0.2 dex in dense environments, suggesting that the star formation activity is reduced by a factor of ~ 1.5 with respect to field galaxies at $z \sim 0.7$.

We further investigated the relationship between the angular momentum of disc galaxies and their stellar masses, also known as the ‘Fall relation’ (FR). Contini et al. (2016) showed that the FR of star-forming galaxies at intermediate redshifts forms a contiguous transition from spirals to ellipticals, according to the dynamical state of the gas. The redshift evolution of the FR is consistent with simulations but the scatter is also a strong function of the dynamical state of the galaxies (Bouché et al., 2021). These results suggest that star-forming galaxies experience a dynamical transformation and lose their angular momentum, i.e., they become dispersion-dominated, before their morphological transformation to passive galaxies.

Thanks to extreme depth of the MXDF we were able to probe the dark matter content in several galaxies within this single field, for the first time in the low-mass regime at these intermediate redshifts (Bouché et al., 2022). Individual rotation curves up to three effective radii show that dark matter fractions are high, typically around 60–95% (see Figure 4), contrary to what has been found in more massive galaxies at higher redshifts.

Circumgalactic medium

As a wide-field integral field unit with exquisite sensitivity, MUSE is a very powerful line imager, and as such it turned out to be a game charger for studies of the circumgalactic medium (CGM), both for mapping it in emission and for studying it with background sources. For these reasons, we dedicated several GTO programmes specifically to improving our understanding of the gas outside galaxies. These programmes targeted quasars, either to use them as background light sources to probe the CGM in absorption and connect the absorption signal with foreground galaxies detected in MUSE (the MUSEQuBES and MEGAFLOW programmes), or to investigate the quasar environments directly. In addition, several of the deep-field observations (including cluster and galaxy group pointings) turned out to provide important new constraints on the CGM — sometimes based on serendipitous discoveries — over a wide range of dark matter halo masses, ranging from small (10^9) to large (10^{14}) halo masses (illustrated in Figure 5). All transverse sizes given in the following refer to physical, not comoving, distances.

Of key importance here is MUSE’s unprecedented sensitivity to low-surface-brightness signals, enabled by the winning combination of high instrument throughput, the advantage of having dispersed data with very low background, and the often very long exposure times. This has facilitated the detection of the CGM in emission in a wide variety of environments, down to a surface brightness of 1×10^{-18} (3×10^{-20}) erg s^{-1} cm^{-2} arcsec^{-2} in exposure times of 1 hr (140 hr).

Our standard cosmological model predicts that the bulk of the baryons in the Universe should reside in a ‘Cosmic Web’ of intergalactic filaments at $z = 3$ which trace the overall mass distribution. By specifically looking at a few overdense regions within the MXDF, the deepest MUSE-GTO field of 140 hours exposure, such filamentary structures have been revealed at very faint levels in Lyman-α emission (Bacon et al., 2021). By itself, UV fluorescence cannot explain the observed emission levels, and one possible

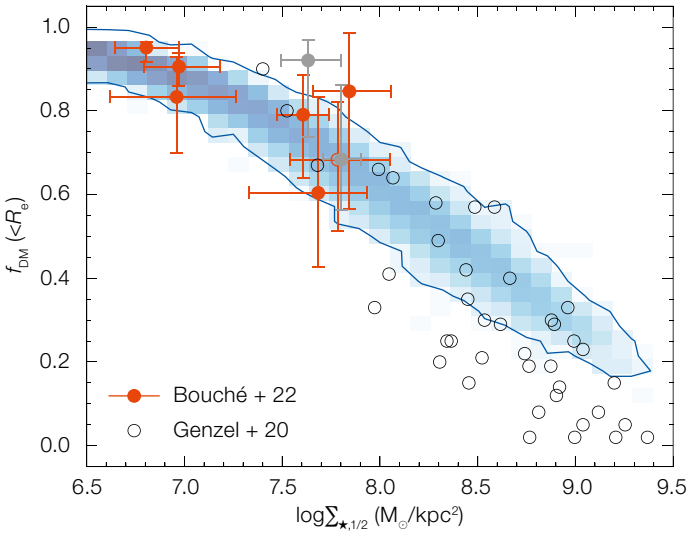

Figure 4. Dark matter fraction (within half-light radius) as a function of stellar mass surface density for nine low-mass star-forming galaxies in the MUSE eXtremely Deep Field. Error bars are 95% confidence intervals, and open circles correspond to the sample of Genzel et al. (2020). The shaded (blue contours) histogram shows the location of $z \sim 1$ central star-forming galaxies in the TNG100 simulations. Adapted from Bouché et al. (2022).

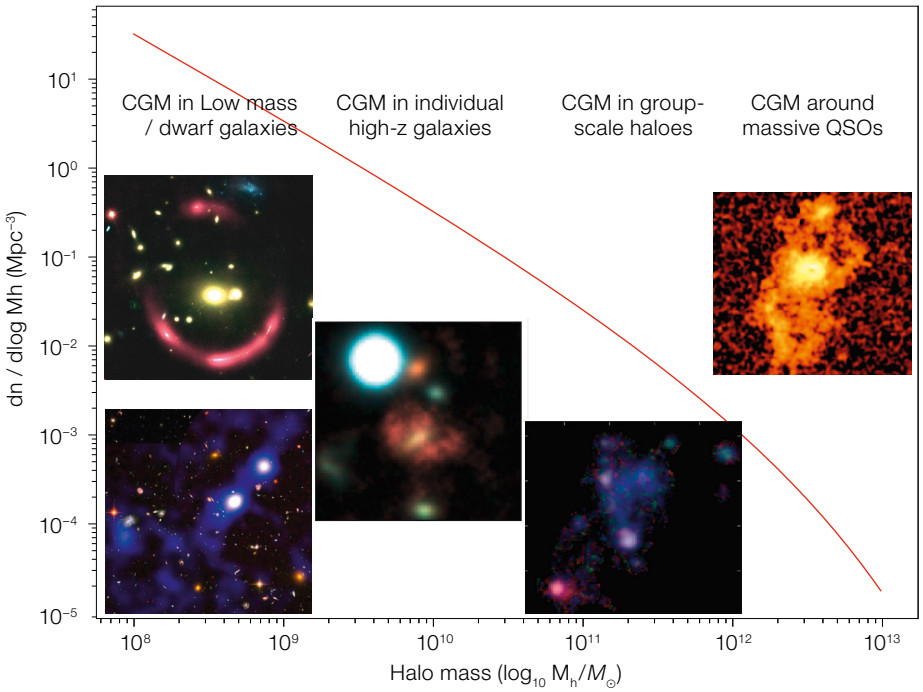

Figure 5. MUSE detections of CGM nebular emission at different mass scales, shown against the halo mass function at z = 3 (red curve). From left to right: extended Lyman-α gas emission around low mass dwarf galaxies found in lensing clusters and ultra-deep fields, anisotropic Mg II emission observed in individual galaxies identified through QSO absorption, diffuse CGM gas found in the intra-group medium, Lyman-α halo surrounding bright QSOs at high redshift.

origin is a very large population of individually undetected 'extreme dwarf' star-forming galaxies with star formation rates per galaxy down to 10^{-4} $M_\odot$ yr^{-1}.

Investigating the Lyman-α emission around 17 quasars at $z \approx 3$, we found very extended structures, sometimes stretching out over more than 100 kpc, in snapshot observations of 1 hr exposure time (Borisova et al., 2016). Remarkably, the detection rate of such Lyman-α quasar nebulae was 100%, very much in contrast to the results of previous (pre-MUSE) surveys using less sensitive instruments. These Lyman-α-bright structures generally have narrow line profiles, and the lack of widespread extended He II and C IV emission suggests that a large fraction of the gas around such massive halos is in the form of cold (T ~ 10^4 K), small (< 20 pc), and metal-poor clumps (Cantalupo et al., 2021).

On the scale of galaxy groups, Leclercq et al. (2022) unveiled extended cold gas shining as Mg II λ2800 emission in a z = 1.31 compact group, distributed over scales of more than 30 kpc, including a low-surface-brightness bridge between two galaxies which suggests that tidal stripping from galaxy interactions is enriching the intragroup medium in the deep MXDF field. At z = 0.7, Epinat et al. (2018) discovered a large gaseous structure in [O II] inside a group in the COSMOS region. The nebula has a radius of more than 150 kpc and contains over 10^{10} $M_\odot$ of ionised gas. We also found several cases of extended ionised gas in massive structures surrounding bright quasars (Johnson et al., 2018, 2022).

On the scale of galaxies ($M_* \approx 10^{10}$ $M_\odot$), Zabl et al. (2021) reported the detection of extended Mg II emission in a deep (11-hr) field around a highly inclined galaxy which happened to be located only 40 kpc from a background quasar observed with high-resolution spectroscopy. The Mg II emission is strongest around the projected minor axis of the galaxy, consistent with gas being ejected from the host by a supernova-driven outflow. A probably related case was noted by Finley et al. (2017) who found evidence for fluorescent Fe II* emission in a galaxy at z = 1.29 which was also aligned with the minor axis.

Around low-mass galaxies ($M_* \approx 10^8$ $M_\odot$), one of the main results from deep MUSE observations is that essentially every Lyman-α-bright high-redshift galaxy shows an extended Lyman-α halo with a characteristic scale ~ 10 times larger than its corresponding stellar continuum emission (Wisotzki et al., 2016; Leclercq et al., 2017). Together with the high spatial density of high redshift galaxies detected, this ubiquity of Lyman-α halos produces an overall background of Lyman-α emission with almost 100% sky coverage (Wisotzki et al., 2018; Kusakabe et al., 2022). When compared to the statistics of Lyman-α absorption against bright background quasars, this result suggests that most circumgalactic atomic hydrogen at these redshifts has now been detected in emission.

Thanks to gravitational lensing by massive galaxy clusters we managed to probe even fainter galaxies and Lyman-α halos, albeit in small volumes. We found that the trends in CGM properties (scale radii, surface brightness profiles) seen in the general (unlensed) deep fields persist down to these low luminosities (Claeyssens et al., 2022). Occasionally the magnification is so strong that the galaxy is stretched out into a giant arc in such a way that we could probe the CGM even at sub-kpc scales, revealing the complexity of its structure in morphological and spectroscopic properties (Claeyssens et al., 2019). One of the most important results was the discovery of significant spatial offsets between the continuum and CGM emission, which possibly indicates the presence of bright star-forming clumps or satellite galaxies surrounding the main CGM halos (Claeyssens et al., 2022).

Using targeted quasar sight-lines with strong metal absorption lines (Mg II with rest-frame equivalent width > 0.5 Å), the MEGAFLOW survey demonstrated that the metals are not distributed isotropically around galaxies (Zabl et al., 2019), but are instead concentrated around the polar and major axis of galaxies out to 60–80 kpc. Furthermore, the metallicity and/or dust content seems enhanced in polar directions (Wendt et al., 2021), consistent with the idea that supernova-driven outflows play a major role in enriching the

CGM. Employing the power of MUSE to find Lyman-α emitters, the MUSEQuBES blind survey of fields around quasars with high-quality spectra of the Lyman-α forest revealed excess H I and C IV absorption near LAEs out to 250 kpc in the transverse direction and 500 km s^{-1} along the line of sight (Muzahid et al., 2021).

Conclusion

The GTO data collection phase is complete, but we still have a long way to go with exploiting the richness of our MUSE data cubes. Analysis is going further for several of the above-mentioned endeavours, and that will keep us busy for some years to come. The astronomical community has also indirectly benefited from our continued involvement in observing with MUSE. We have triggered repeated upgrades of the MUSE Data Reduction System (Weilbacher et al., 2020), and those have played a major role in making MUSE such a popular instrument. We further invested significant effort into developing advanced data analysis software specifically tuned for MUSE science, most of it now in the public domain. We have provided extensive catalogues and user-friendly data access interfaces for several of our deep field surveys and will continue to do so for the remaining fields. Last but not least, all MUSE data including GTO are freely available via the ESO Science Archive Facility. There is undoubtedly still much more science to be conducted with those data, and many discoveries to be made.

References

Abril-Melgarejo, V. et al. 2021, A&A, 647, A152
Bacon, R. et al. 2010, Proc. SPIE, 7735, 773508
Bacon, R. et al. 2014, The Messenger, 157, 13
Bacon, R. et al. 2017, A&A, 608, A1
Bacon, R. et al. 2021, A&A, 647, A107
Bacon, R. et al. 2023, A&A, 670, A4
Bina, D. et al. 2016, A&A, 590, A14
Boogaard, L. A. et al. 2018, A&A, 619, A27
Borisova, E. et al. 2016, ApJ, 831, 39
Bouché, N. F. et al. 2021, A&A, 654, A49
Bouché, N. F. et al. 2022, A&A, 658, A76
den Brok, M. et al. 2020, MNRAS, 491, 4089
den Brok, M. et al. 2021, MNRAS, 508, 4786
Cantalupo, S. et al. 2019, MNRAS, 483, 5188
Charlot, S. & Fall, S. M. 1993, ApJ, 415, 580
Contini, T. et al. 2016, A&A, 591, A49
Drake, A. B. et al. 2017, A&A, 608, A6
Claeyssens, A. et al. 2019, MNRAS, 489, 5022
Claeyssens, A. et al. 2022, A&A, 666, A78
Epinat, B. et al. 2018, A&A, 609, A40
Epinat, B. et al. 2023, submitted to A&A
Erroz-Ferrer, S. et al. 2019, MNRAS, 484, 5009
Feltre, A. et al. 2020, A&A, 641, A118
Finley, H. et al. 2017, A&A, 605, A118
Genzel, R. et al. 2020, ApJ, 902, 98
Giesers, B. et al. 2018, MNRAS, 475, L15
Giesers, B. et al. 2019, A&A, 632, A3
González-Torà, G. et al. 2022, A&A, 658, A117
Guérou, A. et al. 2017, A&A, 608, A5
Gunawardhana, M. L. P. et al. 2020, MNRAS, 497, 3860
Hashimoto, T. et al. 2017, A&A, 608, A10
Herenz, E. C. et al. 2017, A&A, 606, A12
Herenz, E. C. et al. 2019, A&A, 621, A107
Johnson, S. D. et al. 2018, ApJL, 869, L1
Johnson, S. D. et al. 2022, ApJL, 940, L40
Kamann, S., Wisotzki, L. & Roth, M. M. 2013, A&A, 549, A71
Kamann, S. et al. 2018, MNRAS, 473, 5591
Kerutt, J. et al. 2022, A&A, 659, A183
Krajnović, D. et al. 2018, MNRAS, 477, 5327
Kusakabe, H. et al. 2022, A&A, 660, A44
de La Vieuville, G. et al. 2019, A&A, 628, A3
Leclercq, F. et al. 2017, A&A, 608, A8
Leclercq, F. et al. 2022, A&A, 663, A11
Maseda, M. V. et al. 2017, A&A, 608, A4
Maseda, M. V. et al. 2018, ApJL, 865, L1
Maseda, M. V. et al. 2020, MNRAS, 493, 5120
Mercier, W. et al. 2022, A&A, 665, A54
Monreal-Ibero, A., Weilbacher, P. M. & Wendt, M. 2018, A&A, 615, A33
Monreal-Ibero, A. et al. 2023, A&A, 674, A210
Muzahid, S. et al. 2021, MNRAS, 508, 5612
Nanayakkara, T. et al. 2019, A&A, 624, A89
Pagotto, I. et al. 2021, A&A, 649, A63
Patrício, V. et al. 2019, MNRAS, 489, 224
Richard, J. et al. 2021, A&A, 646, A83
Roth, M. M. et al. 2018, A&A, 618, A3
Schaerer, D. 2002, A&A, 382, 28
Schmidt, K. B. et al. 2021, A&A, 654, A80
Spavone, M. et al. 2021, A&A, 649, A161
Urrutia, T. et al. 2019, A&A, 624, A141
Wendt, M. et al. 2021, MNRAS, 502, 3733
Weilbacher, P. M. et al. 2018, A&A, 611, A95
Weilbacher, P. M. et al. 2020, A&A, 641, A28
Wisotzki, L. et al. 2016, A&A, 587, A98
Wisotzki, L. et al. 2018, Nature, 562, 229
Zabl, J. et al. 2019, MNRAS, 485, 1961
Zabl, J. et al. 2021, MNRAS, 507, 4294
Zoutendijk, S. L. et al. 2020, A&A, 635, A107
Zoutendijk, S. L. et al. 2021a, A&A, 651, A80
Zoutendijk, S. L. et al. 2021b, arXiv:2112.09374
Zoutendijk, S. L. 2022, PhD Thesis, Leiden University

A photograph showing most of the telescopes that make up ESO's Very Large Telescope. At the centre, to the right of the setting Sun, Unit Telescope 1 stands ready to observe. It started operating 25 years ago.

DOI: 10.18727/0722-6691/5336

The VISTA Star Formation Atlas (VISIONS)

Stefan Meingast[1]
João Alves[1]
Herve Bouy[2]
for the VISIONS collaboration

[1] Institute for Astrophysics, University of Vienna, Austria
[2] Astrophysics Laboratory, University of Bordeaux, France

VISIONS is a public survey that explores five nearby star-forming molecular cloud complexes. The observing programme finished in March 2022, after collecting more than one million individual images in the near-infrared passbands *J*, *H*, and K_S over a period of five years. VISIONS aims to provide a comprehensive legacy archive similar to the Two Micron All Sky Survey. In addition, multi-epoch observations facilitate proper motion measurements for sources inaccessible to Gaia. VISIONS addresses science cases related to the identification of young stars, their 3D motions, the evolution of embedded star clusters, and the characteristics of interstellar dust.

ESO/Meingast et al. 2023a

Scientific context

Stars form deep within cold, filamentary molecular cloud complexes whose dust content shrouds young stars from observation at visible wavelengths. As a consequence, ESO facilities in particular continue to play a pivotal role in deepening our understanding of this intricate process, offering as they do large-aperture telescopes together with state-of-the-art instrumentation capable of high-resolution infrared imaging. The star formation sites in the solar neighbourhood have been popular targets for observational studies since they provide the only environment where the star formation process can be physically resolved, thereby enabling the study of individual sources.

VISIONS[1,a] (Meingast et al., 2023a,b) is a Cycle 2 Public Survey with the Visible and Infrared Survey Telescope for Astronomy (VISTA), which closely follows in the footsteps of a previous ESO observing programme, the Vienna Survey in Orion (Meingast et al., 2016; programme ID 090.C-0797A). The primary goal of these earlier observations was to characterise the young stellar object (YSO) population and the characteristics of dust in the Orion A molecular cloud. VISIONS substantially expands this pilot programme, as regards both the scientific context and the number of observed star formation sites.

VISIONS targets a total of five nearby star-forming complexes in the near-infrared (NIR) wavelength regime, using the VISTA telescope and the now decommissioned infrared camera VIRCAM[2] (Emerson, McPherson & Sutherland, 2006). Together, these sites harbour thousands of YSOs (see, for example, Evans et al., 2009; Dunham et al., 2015; Großschedl et al., 2019) which are themselves embedded in more than a hundred thousand solar masses of molecular gas and dust (see, for example, André et al., 2010; Lombardi, Alves & Lada, 2011; Alves, Lombardi & Lada, 2014). The targeted star-forming regions inherit their names from the constellations against which they are projected on the sky: Chamaeleon, Corona Australis, Lupus, Ophiuchus, and Orion. Figure 1 displays four *RGB* images assembled from the NIR VISIONS data. These examples showcase the Lupus III molecular cloud (top left), the spectacular infrared sources IRAS 11051-7706 (top right) and HH 909 A (bottom left) in Chamaeleon, and the Coronet cluster (bottom right), which is embedded in the Corona Australis molecular cloud complex[b].

Figure 1. Colour images assembled from VISIONS observations in the near-infrared bands *J* (blue channel), *H* (green channel), and K_S (red channel). The top left panel displays the Lupus III molecular cloud. At the top right, the infrared source IRAS 11051-7706 is visible. HH 909 A in the bottom left features a remarkable, cone-shaped reflection cavity. The bottom right depicts the Coronet cluster in the Corona Australis star-forming complex where it illuminates parts of the surrounding gas and dust.

The primary goal of VISIONS is to establish a NIR legacy archive, similar in structure and content to the Two Micron All Sky Survey (2MASS; Skrutskie et al., 2006). Particularly, the increased sensitivity limits (~ 6 magnitudes fainter than 2MASS), the sub-arcsecond resolution, and the provided absolute astrometry at the milliarcsecond level make VISIONS a valuable foundation for future observations conducted at ESO. In particular, ESO's Extremely Large Telescope will also benefit from the survey for photometric and astrometric cross-calibration and for target selection purposes.

A key aspect of the survey relates to its design, that enables the proper motions of deeply embedded young stars to be measured, as well as sources with sub-stellar masses in the vicinity of the observed regions. VISIONS is therefore highly complementary to the Gaia mission (Gaia Collaboration et al., 2016), which has already proven to be instrumental in our understanding of local star-forming processes and the shape of the interstellar medium on large scales (see, for example, Zucker et al., 2022 and references therein). Yet, owing to the nature of Gaia's optical observations, the 3D dynamics of the most deeply embedded sources, which are still dynamically coupled to their natal molecular cloud, as well as of the low-mass stellar field population, remain largely unexplored as of today.

As regards the difficulty of making ground-based proper motion measurements, VISIONS was designed to be complementary to the VISTA Hemisphere Survey (VHS; McMahon et al., 2013), a previous-generation VISTA Public Survey which covers the entire southern hemisphere. Given that VHS observations began in 2009, for some areas VISIONS has access to a time baseline of more than 10 years. Based on previous experience (for example, Bouy et al., 2013), VISIONS was designed to reach a proper motion measurement precision on the order of 1 mas yr^{-1} for bright sources (H < 16 mag), corresponding to a physical velocity of 0.5 km s^{-1} at a distance of 100 pc. Based on VISIONS data obtained for a 1.5 × 1 degree large field in the Corona Australis region, Figure 2 shows the measured preliminary proper motion accuracy as a function of H-band magnitude. Results for about 30 000 sources are shown for both VISIONS data alone and the combination of VISIONS and VHS data. For a robust estimation of errors, the ordinate in this figure displays the standard deviation of the difference between VISIONS and Gaia proper motions, for sources detected in both surveys. The figure not only reveals that using VHS data is crucial to the accuracy of the proper motion measurements, but also that in this experiment VISIONS delivers proper motions with errors below 1 mas yr^{-1} only in an H-band magnitude range from about 11 mag to 16 mag. The cutoff at the bright end is a consequence of saturation, while the faint limit is given by the single-exposure sensitivity limit. In future we expect to reach similar precision for proper motions of fainter stars when using stacked image data. We note here that the used VHS data were reprocessed with the VISIONS pipeline for a much improved astrometric solution.

Another central pillar of the VISIONS science goals is related to the identification and characterisation of YSOs. The excellent quality of the optical system, that together with the excellent observing conditions at Paranal delivers images at sub-arcsecond resolution, permits the meticulous investigation of YSO morphology. In particular, light scattered off nebulae surrounding YSOs can be a useful tool for confirming their protostellar nature. Moreover, high-velocity jets and outflows, which are characteristic of early YSO evolutionary stages, are also accessible through the high-quality NIR imaging data.

Furthermore, with VISIONS it becomes possible to explore cluster formation processes and properties of the initial mass function. The survey's ability to detect young sources with masses of only a few M_{Jupiter} allows for a robust sampling of all star formation products, also enabling a study of regional variations in the mass function at the lowest substellar mass ranges. Furthermore, the interplay between localised feedback effects and the production of low-mass stars, and connection between the maximum stellar mass and the cluster size can be investigated.

Another integral aspect of the VISIONS scientific objectives addresses the dust content of the observed molecular clouds. In this regard, the high-sensitivity NIR observations of the VISIONS programme enable a comprehensive census of the background field population and consequently

Figure 2. VISIONS proper motion performance as a function of H-band magnitude. The performance metric σ_μ is calculated as the standard deviation of the difference between Gaia proper motions and VISIONS measurements, which were obtained from single (unstacked) exposures. The black line depicts σ_μ when calculated only from VISIONS data. The red line shows the performance when VHS data, which significantly extends the time baseline, are included. The cutoff at the bright end is due to saturation, the faint end is limited by the signal-to-noise ratio.

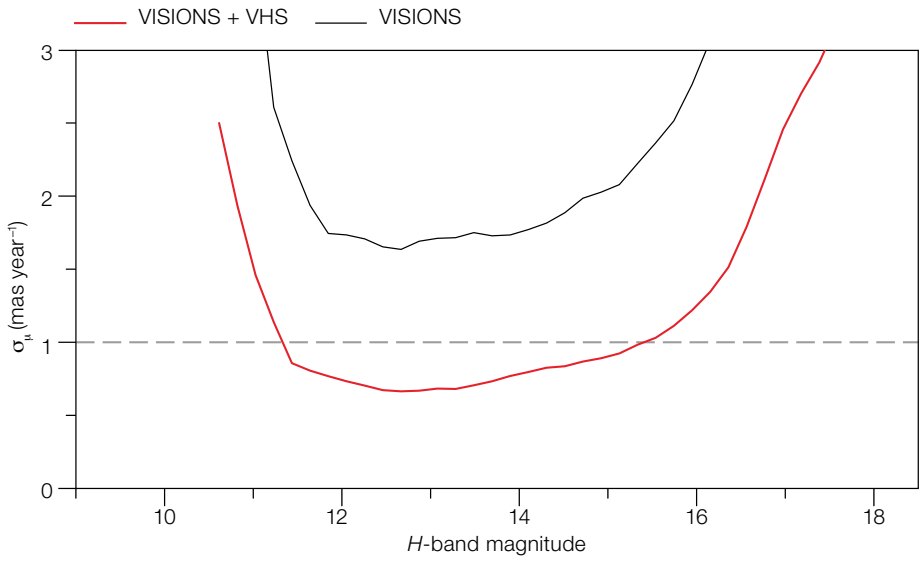

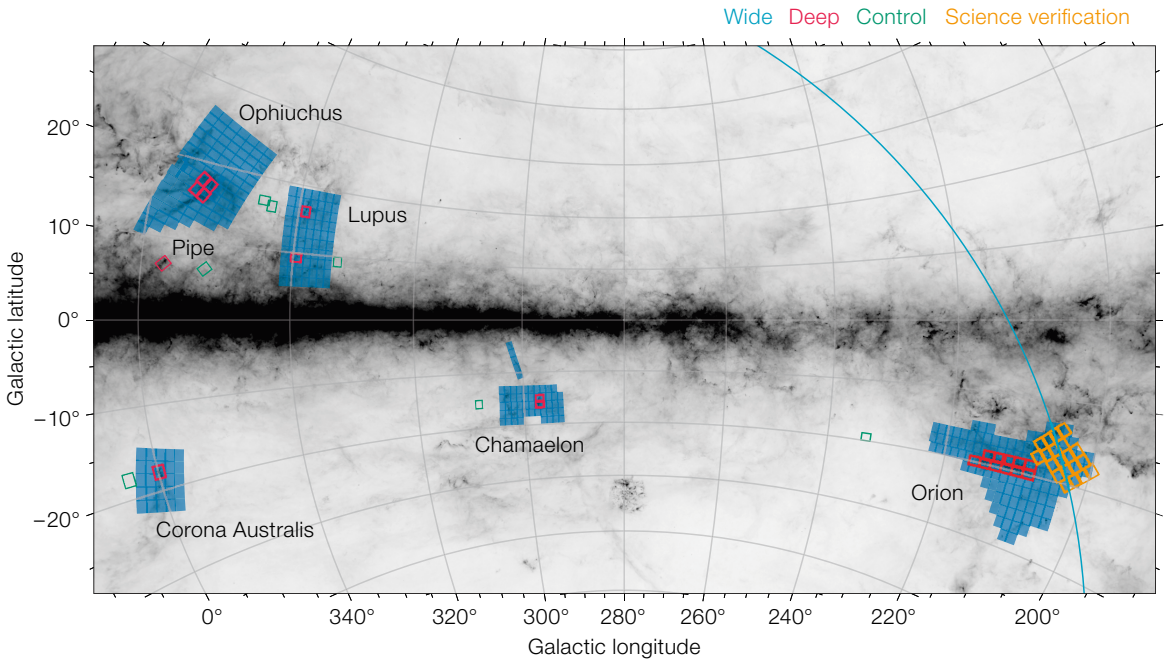

Figure 3. Spatial coverage of VISIONS. The filled blue boxes represent individual VIRCAM tiles in the wide subsurvey. These were revisited a total of six times over the course of the survey. The red boxes depict the pointings in the deep subsurvey, which includes high-sensitivity observations of the regions with the highest column-densities. The green boxes mark the control subsurvey which targeted areas with minimal dust extinction for statistical comparisons. Figure adapted from Meingast et al. (2023a)

the construction of high-resolution extinction maps using well-established methods (for example, Lombardi & Alves, 2001). These maps will enable an unbiased and well-sampled view of the clouds' core mass functions for comparison with their stellar counterparts. The maps will also help with investigating properties of dense cores, establishing a connection between dense cores and YSOs, and mapping their spatial distribution within clouds. In this context, VISIONS also aims to examine the universality of the NIR reddening law and the dust properties of the molecular clouds. The targeted regions are particularly well suited for this task, since they are largely isolated and found well outside the Galactic plane where multiple cloud complexes overlap along the line of sight. Combining the extinction data with emission maps obtained by the Herschel and Planck missions will also allow the ratio of the submillimetre dust opacity to the NIR extinction coefficient to be studied.

Survey overview

VISIONS observations include five prominent star-forming molecular cloud complexes that are situated within a distance of 500 pc (for example, Zucker et al., 2020). The observations were carried out between April 2017 and March 2022, acquiring more than 19 TB of raw data comprising more than a million individual images. The total covered area measures more than 650 deg^2 with a total on-sky exposure time of about 50 hours in the NIR passbands J (1.25 μm), H (1.65 μm), and K_S (2.15 μm).

The spatial coverage of the VISIONS survey is globally divided into three complementary subsurveys, referred to as wide, deep and control. Figure 3 displays the VISIONS coverage, separated into the subsurveys, on top of Planck 857-GHz data (Planck Collaboration et al., 2011). The figure shows the survey setup for the wide programme in blue, deep observations in red, and control data in green. In addition, the Orion B VISTA science verification data, captured in 2009, are shown in orange (Petr-Gotzens et al., 2011).

The wide subsurvey comprises the bulk of the VISIONS observing programme and covers the star-forming complexes on scales of several degrees. This part of the programme was executed six times during the survey in order to provide multiple epochs so as to facilitate measurements of stellar proper motions. Owing to its large extent, the observations were designed to be carried out swiftly with an effective on-sky exposure time of one minute. Additionally, all observations within the wide subsurvey were carried out in the H band. In this way, these data are complementary to the J- and K_S-band VHS observations. The 5-sigma sensitivity limit for these data was determined to be about 20 mag, albeit with a relatively large spread of about 0.5 mag, depending on atmospheric conditions during the observations.

The deep subsurvey includes observations in the J, H and K_S bands and targets areas with the highest column densities within the star-forming regions. This subsurvey utilises long exposure times to reach a sensitivity limit that is similar to that of the Orion A observations published by Meingast et al. (2016). The covered area amounts to about 36 deg^2 which is substantially smaller than for the wide observations. Moreover, to limit the execution time of the observation blocks, each deep field pointing was observed twice for a total exposure time of 10 minutes. These observations typically reach sensitivity limits six magnitudes fainter than 2MASS, or about 21.5 mag, 21 mag, and 19.5 mag in J, H and K_S, respectively.

Finally, the control subsurvey was designed to map regions with minimal dust extinction, collecting data on unextincted stellar field populations for

statistical comparisons to the other observations in VISIONS. The individual field pointings were selected to collect data at the same galactic latitudes as the deep observations for each region, albeit shifted in galactic longitude to map largely extinction-free areas. With a coverage of only about 16 deg^2, the control observations comprise the smallest part of VISIONS.

Data processing and data releases

All data acquired within the VISIONS programme are processed with an optimised pipeline package that was specifically developed for the requirements of this survey. Details of the pipeline are given by Meingast et al. (2023b). Here we provide only an abbreviated overview of all procedures involved, particularly highlighting the performance with respect to image quality, photometry and astrometry. The pipeline itself is implemented in Python and relies heavily on vectorised computations for the required performance and on open source software, where, foremost, the AstrOmatic software tools are employed for source detection and extraction, computation of astrometric solutions, and optimised image stacking (Bertin & Arnouts, 1996; Bertin 2010a,b). The package is publicly available on GitHub[3] and can be easily accessed in a virtual environment provided by a Docker image[4].

The pipeline is designed to work out of the box with raw data downloaded from the ESO Science Archive[5]. It also generates its own calibration frames and tables, including bad pixel masks, dark frames, flat fields, non-linearity coefficients, gain and read-noise tables, weight maps, and illumination corrections. Furthermore, Gaia DR3 (Gaia Collaboration et al., 2021) and 2MASS serve as astrometric and photometric references, respectively. The science frames undergo a series of processing steps which largely remove the instrumental signature and employ a sophisticated multi-step background subtraction routine. In comparison to VIRCAM data products processed by other pipeline environments (for example those provided by the Cambridge Astronomical Survey Unit[6] [CASU]), we identify three major differences in our workflow.

Firstly, we employ a sophisticated resampling algorithm that uses Lanczos kernels, in contrast to bilinear interpolation, as employed by the CASU workflow. This leads to an improved resolution in the stacked data products where our methods typically produce 20% narrower point-source FWHMs.

Secondly, the astrometric solution is computed against an adaptive reference catalogue, generated from the Gaia DR3 database. Before cross-correlating sources detected on the VIRCAM images with the Gaia reference catalogue, our approach warps the reference frame to the epoch of the observations, a method that has only recently become possible thanks to the superb astrometric data quality provided by Gaia. In this way, our image products are not calibrated against a specific mean epoch given by the reference catalogue (for example, approximately J2000 for 2MASS, or J2016.0 for Gaia DR3). Instead, the VISIONS source position epochs correspond to the actual date of the observations. This not only enables a much more robust and precise astrometric calibration, but also offers the possibility of considering our position measurements absolute. Figure 4 visualises this characteristic, which shows the difference between source positions (right ascension and declination) measured on the (fully calibrated) Corona Australis control field and Gaia DR3. While Gaia DR3 positions refer to epoch J2016.0, VISIONS recorded these specific data at epoch J2018.36. This difference of about two years becomes evident in the offset of the shown distribution, which does not centre on the origin in this graph, but instead aligns well with the offset expected from the mean proper motion of this field (marked as dashed lines). Moreover, the standard deviation of this distribution is on the order of 10 milliarcseconds for all sources (and about 3 milliarcseconds for bright sources), highlighting the extraordinary performance of VISIONS astrometry.

Thirdly, because of the slightly different filter systems, VIRCAM measurements typically require a colour transformation to obtain photometry compatible with the 2MASS system (for example, Coccato, Freudling & Retzlaff, 2021). In contrast, our pipeline is principally designed to calibrate all photometric data against the 2MASS source catalogue and also produces only negligible residual colour terms (see Figure 8 of Meingast et al., 2023b).

So far, the VISIONS team has produced two major data releases. Data Release 1[7] includes only the deep and control field data for the Ophiuchus field. Data Release 2[8] features an already substantially larger data volume and was published in March 2022. This latest release includes all observed data in the three subsurveys related to the Corona Australis complex. All data (images and source catalogues) are available through the ESO Science Archive Facility. Details of the contents of these releases are available in the respective release documentation.

Outlook

The majority of the VISIONS observations have yet to be published. At the time of

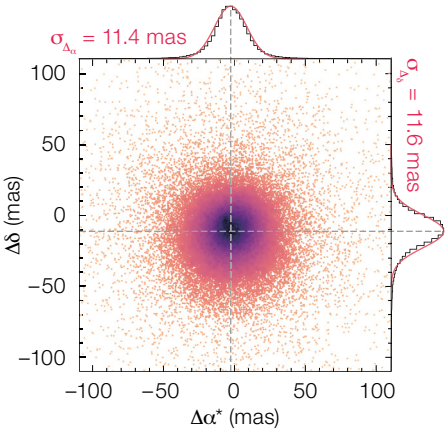

Figure 4. Comparison of source coordinates as determined by VISIONS and the Gaia DR3 catalogue for the Corona Australis control field. The axes represent the differences in right ascension (y-axis) and declination (x-axis) between the two datasets. All astrometric solutions for VISIONS were calculated against a Gaia frame (J2016.0) adjusted to the epoch of the VISIONS observation (J2018.36). Consequently, the distribution is not centred on the origin, but aligns with the expected mean shift, marked by grey dashed lines. The black histograms at the top and on the right of the plot align well with a Gaussian distribution (highlighted in red) that has a mean at the anticipated shift and a standard deviation that matches the statistical error as reported during the astrometric calibration. Figure adapted from Meingast et al. (2023b)

writing the VISIONS team is simultaneously working on future data releases, as well as testing proper motion measurements. Specifically, the team plans to publish all data for each star-forming region in separate data releases, with Data Release 3 focusing on the Chamaeleon observations. The order of subsequent publications is currently set by the expected data volume, i.e., Lupus will follow Chamaeleon (DR4), followed by Ophiuchus (DR5), and lastly the Orion data will be made public (DR6). In addition, the VISIONS team plans to reprocess the Orion A and B fields obtained by Meingast et al. (2016) and the VISTA Science verification efforts. Furthermore, in addition to the data releases through the ESO archive, we plan to reformat all source catalogues to match the 2MASS convention (with similar quality flags, for example), reprocess VHS observations with the VISIONS pipeline, and publish a band-merged catalogue via CDS[9].

Acknowledgements

We thank the ESO Survey Team and the Archive Science Group for their helpful and constructive feedback and collaboration during the preparation, execution, and data publication phases of the survey.

References

André, Ph. et al. 2010, A&A, 518, L102
Alves, J., Lombardi, M. & Lada, C. J. 2014, A&A, 565, A18
Bertin, E. & Arnouts 1996, S. A&AS, 117, 393
Bertin, E. 2010a, ascl.soft, ascl:1010.063
Bertin, E. 2010b, ascl.soft, ascl:1010.068
Bouy, H. et al. 2013, A&A, 554, A101
Coccato, L., Freudling, W. & Retzlaff, J. 2021, The Messenger, 183, 20
Dunham, M. M. et al. 2015, ApJS, 220, 11
Emerson, J., McPherson, A. & Sutherland, W. 2006, The Messenger, 126, 41
Evans, N. J. et al. 2009, ApJS, 181, 321
Gaia Collaboration et al. 2016, A&A, 595, A1
Gaia Collaboration et al. 2021, A&A, 649, A1
Großschedl, J. E. et al. 2019, A&A, 622, A149
Lombardi, M. & Alves, J. 2001, A&A, 377, 1023
Lombardi, M., Alves, J. & Lada, C. J. 2011, A&A, 535, A16
McMahon, R. G. et al. 2013, The Messenger, 154, 35
Meingast, S. et al. 2016, A&A, 587, A153
Meingast, S. et al. 2023a, A&A, 673, A58
Meingast, S. et al. 2023b, A&A, 673, A59
Petr-Gotzens, M. et al. 2011, The Messenger, 145, 29
Planck Collaboration et al. 2011, A&A, 536, A1
Skrutskie, M. F. et al. 2006, AJ, 131, 1163
Zucker, C. et al. 2020, A&A, 633, A51
Zucker, C. et al. 2022, arXiv, arXiv:2212.00067

Links

[1] VISIONS homepage: http://visions.univie.ac.at
[2] VIRCAM webpage: https://www.eso.org/sci/facilities/paranal/instruments/vircam.html
[3] Pipeline GitHub repository: https://github.com/smeingast/vircampype
[4] Docker platform: https://www.docker.com/
[5] ESO Science Archive Facility: http://archive.eso.org/
[6] Cambridge Astronomical Survey Unit (CASU): http://casu.ast.cam.ac.uk/
[7] DR1 description: https://www.eso.org/rm/api/v1/public/releaseDescriptions/123
[8] DR2 description: https://www.eso.org/rm/api/v1/public/releaseDescriptions/190
[9] Centre de Données astronomiques de Strasbourg https://cds.unistra.fr/

Notes

[a] VISIONS programme ID 198.C-2009
[b] The RGB images displayed in Figure 1 were published as an ESO press release (ID eso2307; https://www.eso.org/public/news/eso2307/)

Despite its name, ESO's Very Large Telescope, the VLT, is not a single telescope! It is in fact made up of an array of four 8.2-metre-diameter Unit Telescopes (UTs) (one of which is shown here) and four additional, movable, 1.8-metre-diameter Auxiliary Telescopes (ATs) (three of which are visible on the right side of this image).

Each UT has its own individual name in the Mapuche (Mapudungun) language. The star of this image is Antu (or UT1, the first of the UTs), and is pictured here sitting atop Cerro Paranal in Chile. This polychromatic image, taken by ESO Photo Ambassador Petr Horálek, also captures the beautiful colours of the cloudy night sky encircling Antu.

Many night-sky objects are visible here. Starting from the left we see the pink California Nebula, the Pleiades star cluster, the fiery river of the Milky Way, the constellation of Orion and its famous Belt, the looping Gum Nebula, the Carina Nebula and the Southern Cross. The most curious features are the green bands or stripes to the right of Antu's enclosure. They are atmospheric gravity waves, generated by storms forming ripples in the greenish layer of Earth's airglow in the upper atmosphere. This image also appeared in an ESOcast dedicated to Red Sprites, which can occur under similar conditions as gravity waves.

P. Horálek/ESO

This image from the Wide-Field Imager on the MPG/ESO 2.2-metre telescope shows the starry skies around a galaxy cluster named PLCKESZ G286.6-31.3. The cluster itself is difficult to spot initially, but shows up as a subtle clustering of yellowish galaxies near the centre of the frame.

Telescopes and Instrumentation

It might look like the opening scene from The Lion King, but this stunning image was actually taken in the Chilean Atacama Desert rather than the African savannas. Taking centre stage is ESO's Extremely Large Telescope (ELT), or part of it, at least.

The ELT's steel dome is about 80 metres tall and one day it will play host to the world's biggest eye on the sky. When finished, the dome will weigh some 6100 tonnes and be capable of rotating 360 degrees on a set of 36 stationary trolleys.

E. Garcés/ESO. Acknowledgements:. N. Dubost

DOI: 10.18727/0722-6691/5337

ERIS Science Verifications

Alice Concas[1]
Ric Davies[2]
Monika G. Petr-Gotzens[1]
Marianne Heida[1]
Harald Kuntschner[1]
Bruno Leibundgut[1]
Michaël Marsset[1]
Robert J. De Rosa[1]
Lowell Tacconi-Garman[1]
Zahed Wahhaj[1]
Thomas Wevers[1]
Diego Parraguez[1]
Israel Blanchard[1]

[1] ESO
[2] Max Planck Institute for Extraterrestrial Physics, Garching, Germany

The Enhanced Resolution Imager and Spectrograph (ERIS) is the new near-infrared instrument at the Cassegrain focus of Unit Telescope 4 (UT4) of ESO's Very Large Telescope. Its Science Verification (SV) was scheduled from 2 to 6 December 2022 during which time conditions were mostly good. Most of the planned SV observing programme could be accomplished. Out of 87 submitted proposals 23 observing programmes were scheduled for a total of 40 hours of observations. The allocation had assumed observations in four nights (eight hours each) and included a slight oversubscription. Five of the seven top-ranked proposals could be fully completed, the other two received partial data. In total, eleven programmes could be completed, seven were partially observed and three programmes could not be started. Some smaller technical problems with the adaptive optics affected parts of the observations.

Brief instrument description

ERIS has two arms: SPIFFIER, the refurbished version of the Spectrometer for Infrared Faint Field Imaging (SPIFFI), and the Near Infrared Camera System (NIX). SPIFFIER is a medium-resolution integral field spectrograph covering the *J* to *K* bands. NIX is capable of imaging between the *J* and *M* bands, and offers coronagraphic and *L*-band long-slit capabilities. ERIS is designed to be used in conjunction with UT4's deformable secondary mirror and delivers diffraction-limited spatial resolution with Strehl ratios of better than 0.6 for $\lambda > 2$ µm. The atmospheric turbulence can be sensed with either a natural guide star, or a single artificial star generated with the Adaptive Optics Facility (AOF). ERIS replaces and expands the capabilities of the decommissioned Nasmyth Adaptive Optics System (NAOS) – COudé Near-Infrared CAmera (CONICA) combination (together known as NACO) and Spectrograph for INtegral Field Observations in the Near-Infrared (SINFONI) in a single instrument. A full description of ERIS can be found in Davies et al. (2023).

Proposal solicitation and submission

The call for ERIS Science Verification (SV) proposals[1] was issued on 16 September 2022. With the call, the ERIS SV webpage[2] was launched. Eighty-seven proposals were received by the deadline on 14 October 2022 requesting in total 215 hours. This was the highest demand for recent instrument SVs. The SV team ranked the proposals according to scientific interest and the final selection was discussed at a meeting on 3 November 2022. Twenty-three projects were selected for a total of 40 hours of execution time. Two proposals were rejected entirely, and one target was rejected from a third, because of conflicts with submitted P111 proposals. The approved projects oversubscribed the available time slightly to account for atmospheric conditions and target visibility. The proposers were informed about the outcome of the selection on 8 November 2022. Owing to a technical problem at the end of the last commissioning run in November 2022, NIX's pupil wheel mechanism was left fixed in the imaging position. This precluded the execution of any approved SV programme requesting use of the apodising phase plate coronagraph. Three projects were therefore not feasible, and the PIs were informed accordingly on 23 November. The Phase 2 deadline for the submission of the observing blocks was 25 November 2022.

Proposed scientific topics included galaxy structures across redshift space, kinematic searches for signatures of stellar-mass black holes or binary supermassive black holes in galaxy centres, observations of gravitational lenses, characterisation of emission-line objects, for example young stars, and searches for exoplanets using different high-contrast methods. Integral-field spectroscopy and high-contrast imaging were in high demand.

Observations

The ERIS SV nights were scheduled from 2 to 6 December 2022. In general, the conditions were quite good, i.e. mostly photometric and clear. The first night had poor seeing (up to 1.5 arcseconds), but substantially better observing conditions were encountered during the following three nights.

ERIS performed well, although some difficulties with the adaptive optics (AO) were experienced during the first night. The third night suffered from a loss of time that was due to an instrument cryogenic alarm, which needed to be investigated. The beginning of the last night was affected by a failure of the telescope guide camera, which delayed the start of observing by one hour. Some programmes were affected by glitches (for example errors associated with the Standards Platform for Adaptive optics Real Time Applications[3] (SPARTA); AO loop opening) and only received partial data. The collaboration between the science operations on Paranal and the support team in Garching (via the Garching Remote Access Facility) worked well and we also received technical support from the team at Arcetri Observatory who developed the AO subsystem for ERIS.

As in previous cases, ERIS SV provided an excellent opportunity to test and diagnose issues related to the operability of the instrument, especially the acquisition of faint targets and crowded regions. Valuable lessons were learned and provided the opportunity to implement fixes/changes before the instrument started regular operations with P111 (in April 2023).

Data processing

All raw data are publicly available through the ESO science archive. The ERIS SV webpage[2] provides direct links to the raw data in the archive. A preliminary version

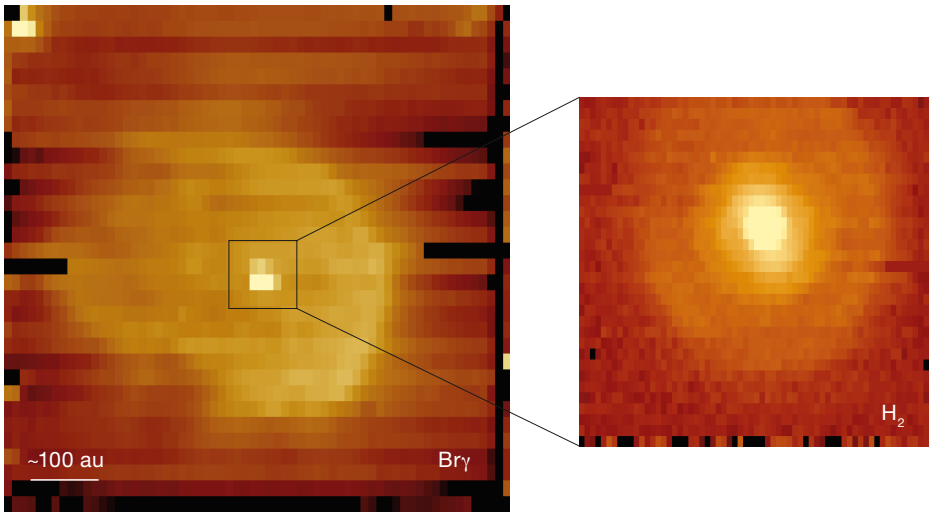

Figure 1. Two ERIS views of the planetary disc around θ^2 Ori A. The left image shows the Brγ emission in a field of view of 8 × 8 arcseconds, while the right image shows details of the planetary disc in H_2 in a field of view of 0.8 × 0.8 arcseconds. In both images north is up and east to the left.

of the ERIS data reduction pipeline was made available to the PIs through the SV Web page. In the meantime, the ERIS pipeline has been released[4].

Some early SV results

First results of some of the SV observations are presented below. They have been kindly provided by the research teams.

Protoplanetary discs

The evolutionary pathways of individual protoplanetary discs can differ, depending on the surrounding environment, especially in the presence of massive stars (see the review by Parker, 2020). The UV radiation from O-type stars in massive clusters can photo-evaporate discs and strongly affect their size, mass, and survival timescale (for example, Winter & Haworth, 2022).

ERIS/SPIFFIER obtained a spatially and spectrally resolved image of the large irradiated protoplanetary disc (proplyd) 244-440 in the Orion Nebula Cluster (Figure 1). The proplyd, illuminated by the O-type star θ^2 Ori A, was observed with two spaxel scales: the larger field of view (8 x 8 arcseconds) covered the whole object, and the smaller one (0.8 × 0.8 arcseconds) zoomed-in to the central protoplanetary disc.

ERIS can resolve the various components of the proplyd in greater detail and better constrain their density and temperature than the instruments it replaces. The observations with ERIS are complementary to those with the Multi Unit Spectroscopic Explorer (MUSE) and the JWST and help to create a comprehensive view of the structure and physical conditions of 244-440.

Outflows from forming stars

Forming stars drive jets and outflows. These outflows are often detected in optical emission lines that are excited in shocks or molecules entrained in the outflow. In massive star-forming regions, jets and outflows are illuminated by external UV photons that dissociate molecules and ionise atoms, changing the observational picture. The template irradiated outflow is HH 900, located in the Carina star-forming region. The cold molecular outflow is clearly seen inside its natal globule in CO with the Atacama Large Millimeter/submillimeter Array (ALMA) but ends abruptly at the edge of the globule (Reiter et al., 2020). Outside the globule, classic jet-sensitive lines like Hα and [S II] seen with MUSE trace an ionised wide-angle outflow that extends smoothly from the end of the CO outflow and surrounds a collimated jet seen in [Fe II] (Reiter et al., 2019). ERIS/SPIFFIER reveals the transition between the purely molecular and fully ionised components where molecules in the outflow are rapidly dissociating (see Figure 2). Understanding this dissociating component is an important step towards accounting for the full mass-loss in irradiated jets and outflows. Results from this programme (Reiter et al., submitted to MNRAS) will guide the interpretation of

Figure 2. Outflow from the HH 900 tadpole at various wavelengths.

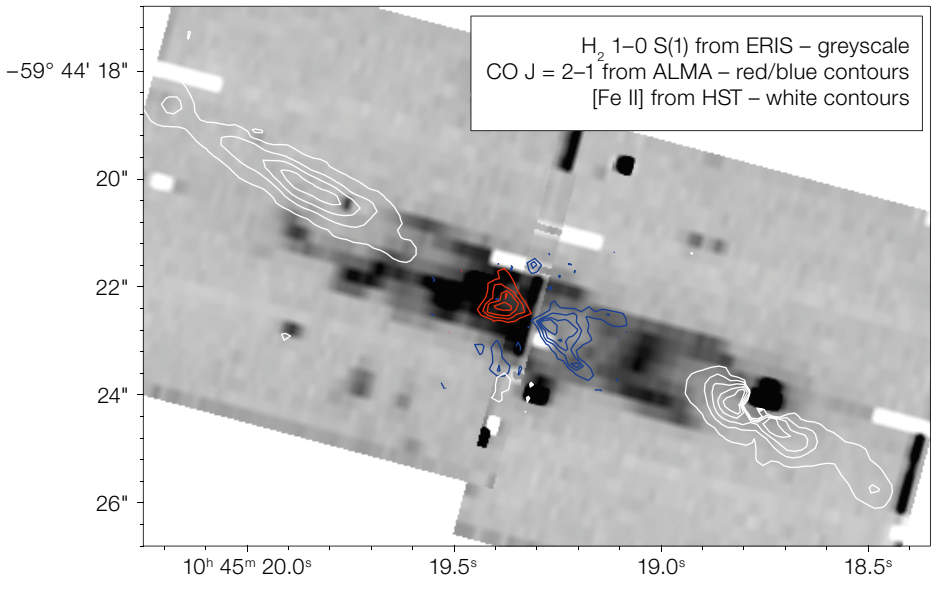

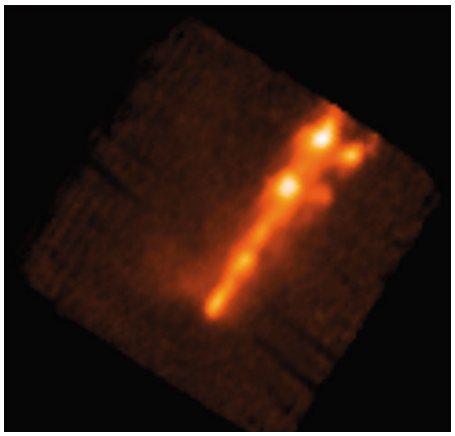

Figure 3. Image slice of the ERIS data cube in the 1.6435 µm emission line of [Fe II]. The knotty structure of HH1 jet is clearly visible. It is crossed in projection by the fainter HH501 jet. The field of view is 8 × 8 arcseconds. North is up, and east is to the left.

near-infrared observations of jets and outflows in massive star-forming regions (for example with the JWST) and provide a template for the further development of models of irradiated jets and outflows (for example, Estrella-Trujillo et al., 2021).

The prototypical jet HH1

Protostellar outflows play a crucial role in the formation and evolution of stars since they remove excess angular momentum from the star-disc system and return material into the surrounding cloud (Frank et al., 2014). The Herbig-Haro 1 (HH1) jet represents a prototypical Class 0 jet with interesting kinematical features. It has been traced in H_2 2.121 µm (for example, Garcia Lopez et al., 2008) and [Fe II] 1.64 µm (for example, Erkal et al., 2021) as close as 1–2 arcseconds from its driving source VLA1, a deeply embedded Class 0 protostar.

Observations were carried out with the SPIFFIER arm of ERIS, using the laser guide star (LGS) mode with a nearby star for tip-tilt corrections. The grating configurations J_middle, H_middle, and K_middle were observed, giving spectral resolutions of about 10 000, 10 400, and 11 200, respectively. The 250-milliarcsecond plate scale was used, giving spaxels of 125 × 250 milliarcseconds, and a total field of view of 8 × 8 arcseconds. In the three datacubes a total of 21 lines of [Fe II], eight lines of H_2, two lines of [Ti II], and one line each of [P II], He I and Paschen β could be detected. Figure 3 shows the HH1 jet in the strong 1.6435 µm line of [Fe II]. A series of five knots, connected by fainter inter-knot emission, is visible, extending in a north-westerly direction. The high spatial resolution of the image reveals that in fact there are two jets crossing each other in projection. The fainter HH501 jet becomes visible just north of the HH1 jet and is crossing it in projection. The series of knots along these jets are resolved into small bow shocks. The large number of iron lines and H_2 lines enables a detailed analysis of the increasing extinction towards the jet source VLA1 and of the excitation state of the outflowing jet gas with both its atomic and its molecular components.

Exoplanet characterisation

ERIS was operated in the LGS mode to resolve the young (~ 2.5 Myr) Taurus system 2M0347 consisting of a 0.15–0.18 $M_\odot$ star and a 3–5 M_{Jup} exoplanet. SPIFFIER produced datacubes in the *K* band providing the spatial and spectral diversity at R = 5000 resolution needed to remove the stellar halo, reveal the emission of the faint ($K \approx 17$ mag) exoplanet (Figure 4), and look for molecular absorptions (H_2O, CO) in the atmosphere of the object. The observations demonstrate the potential of the instrument to capture images and spectra of substellar companions and circumstellar discs in the vicinity of stellar and substellar host stars.

Lensed galaxy spectrum

ERIS observed a strongly lensed hyper-luminous infrared galaxy, PJ0116–24, at z = 2.125 (Figure 5). The different galaxy images are aligned in a near-perfect circle. The galaxy has a magnified infrared luminosity of $L_{IR} \approx 1 \times 10^{14}\ L_\odot$ and an intrinsic star formation rate of *SNR* 1820 ± 460 $M_\odot\ yr^{-1}$ (Kamieneski et al., 2023), and it is a member of the rare class of hyper-luminous infrared galaxies that are usually thought to be extremely dust obscured.

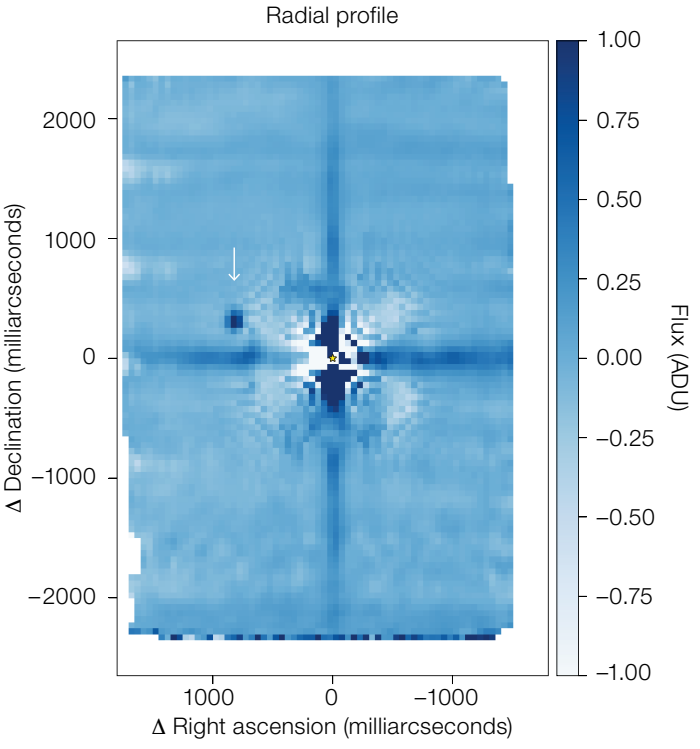

Figure 4. Detection of a 3–5 Jupiter-mass planet around 2M0347. The image is the collapsed cube of a SPIFFIER observation and will enable direct spectroscopy of the planet.

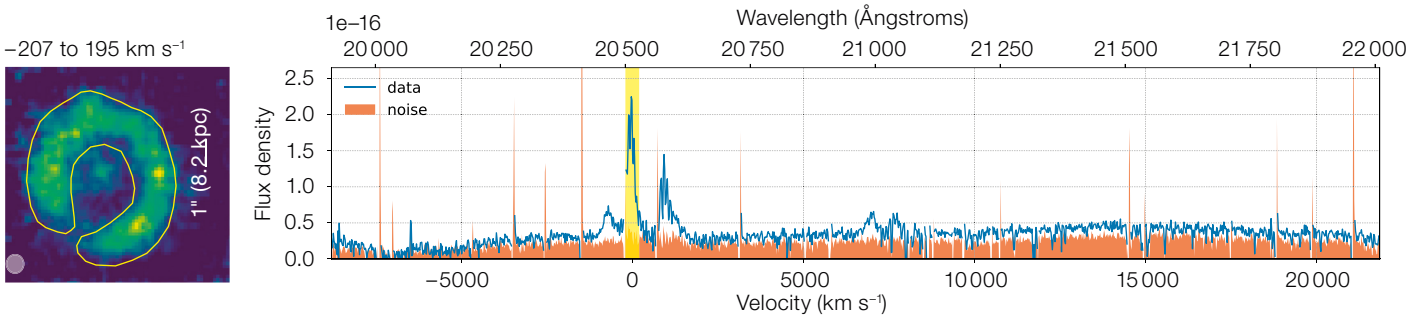

Figure 5. Left: ERIS Hα line integrated intensity image at a seeing-limited angular resolution with ~ 0.67 hours of on-source exposure in the *K* band. Right: ERIS *K*-band spectrum integrated over the highlighted area in the left panel. Prominent Hα, (N II) and (S II) lines are observed with a wide line width indicating outflows.

Summary

ERIS operations started with P111 in April 2023. The SV data give an early indication of what scientific topics can be addressed with near-infrared integral field spectroscopy with SPIFFIER and the imaging provided by the NIX camera. It can be expected that ERIS will continue to build on the successful campaigns of NACO and SINFONI.

Acknowledgements

We would like to thank Mari-Liis Aru, Megan Reiter, Thomas J. Haworth, Suzanne Ramsay, Pamela D. Klaassen, Anna F. McLeod, Dominika Itrich, Jochen Eislöffel, Mickaël Bonnefoy and Daizhong Liu for sharing their early results in this article.

References

Davies, R. et al. 2023, A&A, 674, A207
Erkal, J. et al. 2021, ApJ, 919, 23
Estrella-Trujillo, D. et al. 2021, ApJ, 918, 75
Frank, A. et al. 2014, in Protostars and Planets VI, ed. Beuther, H., Klessen, R. S., Dullemond, C. P. & Henning, T., (Tucson: University of Arizona Press), 451
Garcia Lopez, R. et al. 2008, A&A, 487, 1019
Kamieneski, P. S. et al. 2023, arXiv:2301.09746
Parker R. J. 2020, Roy. Soc. Open Sci., 7, 201271
Reiter, M. et al. 2019, MNRAS, 490, 2056
Reiter, M. et al. 2020, MNRAS, 496, 394
Winter, A. J. & Haworth, T. J. 2022, EPJP, 137, 1132

Links

[1] ERIS call for SV proposals: https://www.eso.org/sci/publications/announcements/sciann17516.html
[2] ERIS SV webpage: http://www.eso.org/sci/activities/vltsv/erissv.html
[3] SPARTA: https://www.eso.org/sci/facilities/develop/ao/tecno/sparta.html
[4] VLT instrument pipelines: http://www.eso.org/sci/software/pipelines/

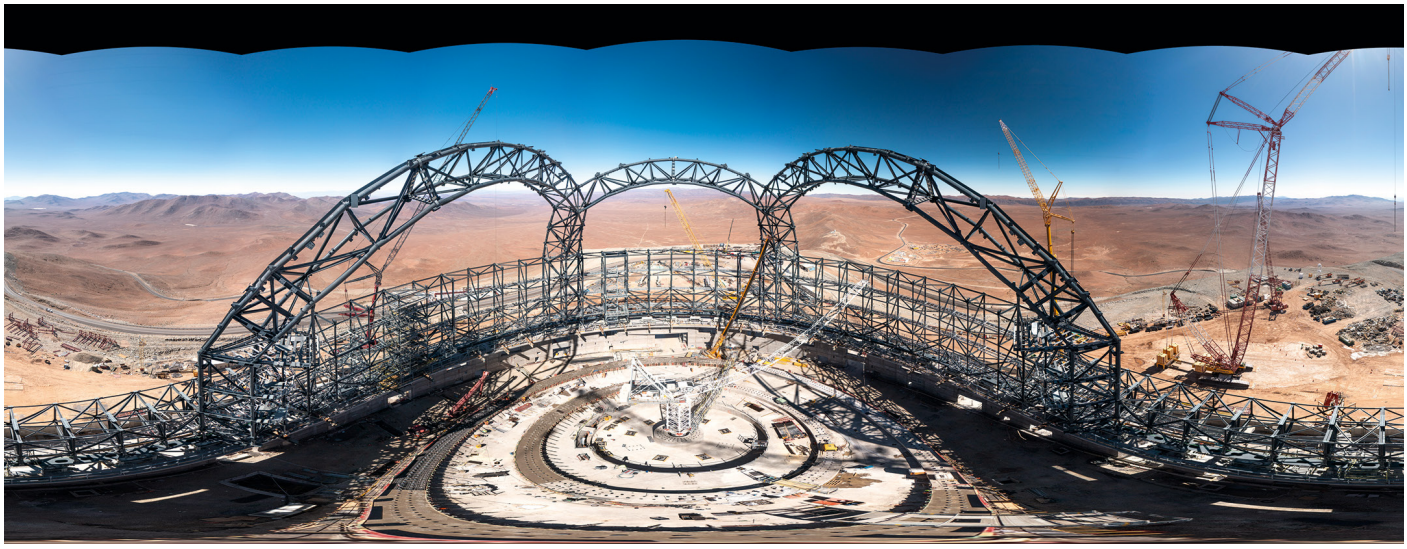

G. Hüdepohl (atacamaphoto.com)/ESO

A panoramic view taken from the top of the dome of ESO's Extremely Large Telescope (ELT) in early August, 2023. When completed, the dome will be 80 metres high, weigh more than 6100 tonnes and rotate 360 degrees on 36 trolleys.

DOI: 10.18727/0722-6691/5338

The ESO Science Archive Facility: Status, Impact, and Prospects

Martino Romaniello[1]
Magda Arnaboldi[1]
Mauro Barbieri[2]
Nausicaa Delmotte[1]
Adam Dobrzycki[1]
Nathalie Fourniol[1]
Wolfram Freudling[1]
Jorge Grave[1]
Laura Mascetti[2]
Alberto Micol[1]
Jörg Retzlaff[1]
Nicolas Rosse[2]
Tomas Tax[2]
Myha Vuong[2]
Olivier Hainaut[1]
Marina Rejkuba[1]
Michael Sterzik[1]

[1] ESO
[2] Terma GmbH

Scientific data collected at ESO's observatories are freely and openly accessible online through the ESO Science Archive Facility. In addition to the raw data straight out of the instruments, the ESO Science Archive also contains four million processed science files available for use by scientists and astronomy enthusiasts worldwide. ESO subscribes to the FAIR (Findable, Accessible, Interoperable, Reusable) guiding principles for scientific data management and stewardship. All data in the ESO Science Archive are distributed according to the terms of the Creative Commons Attribution 4.0 International licence (CC BY 4.0).

Introduction

The science data collected at ESO's La Silla Paranal Observatory (LPO) are accessible through the ESO Science Archive Facility (SAF). The observatory comprises three sites in northern Chile's Atacama region, namely La Silla[1], Paranal[2] and the Chajnantor plateau (the Atacama Pathfinder EXperiment, or APEX telescope[3]). Data from the Atacama Large Millimeter/submillimeter Array (ALMA) observatory[4] are also directly accessible from the ESO Science Archive, so that they can be conveniently queried together with the data from LPO. In addition, ESO also hosts and operates the European copy of the dedicated ALMA Science Archive[5], which provides extended search capabilities tailored to these data; it was recently described by Stoehr et al. (2022).

At the time of writing, the ESO Science Archive contains, in a uniform and consistent form, data from more than 30 instruments (and counting), covering a wide range of observing techniques, data types and formats, and their metadata. It stores all the raw science data and the related calibrations. A growing selection of processed data is also available, on which science measurements can be readily performed. The archive home page is at: archive.eso.org. User support and a knowledgebase database are provided at support.eso.org.

ESO has a long tradition of fostering 'Open Access' to scientific data, and it endorses the European EOSC initiative[6]. As an overarching principle, ESO subscribes to the FAIR[7] (Findable, Accessible, Interoperable, Reusable) guiding principles for scientific data management and stewardship (Wilkinson et al., 2016). Access to the ESO Science Archive is regulated by policy[8]. In general terms, the Principal Investigators (PIs) of successful proposals for observing time on ESO telescopes, along with their delegates, have exclusive access to their scientific data for a proprietary period, after which the data are accessible to all users in the worldwide community. The default proprietary period is set by the ESO Director General and communicated at the time of proposing for observing time[9]. It is typically one year, but may depend on the observing programme type, as detailed in the policy (for example, Public Survey raw data are immediately public). Processed data distributed via the ESO Science Archive retain the same proprietary protections as the raw data they were derived from. All data in the ESO archive retain ESO's copyright and are distributed according to the terms of the Creative Commons Attribution 4.0 International licence (CC BY 4.0[10]). The use of ESO data, for example in publications, either downloaded directly from the ESO Science Archive or via third parties, must be acknowledged[8].

Data content and access

Over the course of the last 25 years, a large fraction of the accessible sky has been observed by ESO telescopes. The density map coverage of the science raw data available in the ESO Science Archive as of June 2023 is shown in Figure 1. Given the wide variety of data distributed over such a large area, it may be a challenge to find the data needed. The Science Archive provides several means to do so, tailored to the different use cases.

The raw data can be queried by basic instrumental, target, observing programme and scheduling criteria through a unified form[11]. Specialised query forms for individual instruments, which expose many more detailed technical and scientific search parameters, are also available[12]. Once a user has selected the raw science data of interest, relevant calibration files can be associated automatically prior to download. The service is tuned to provide the calibrations as defined in the instrument's Calibration Plan[13]. At this stage, users can choose whether they want raw and/or pre-processed master calibrations. They can also select to include night-log information, such as weather conditions and notes from the observer. Once downloaded, users can process raw data along with the associated calibrations to remove signatures from the telescope, instrument and Earth's atmosphere, and to calibrate the resulting data products in physical units. For this, dedicated software tools to process and organise the data and the execution sequence are made available[14]. At this point, the data are ready for extraction of the science signal and its subsequent analysis.

The current era in astronomy research is characterised by an abundance of data and the need to combine them across facilities, wavelengths, and messengers. It is, therefore, imperative to lower as much as possible the user's access barrier to the data. The goal is to reach as wide an audience as possible, providing a complete overview of the content of the archive, while requiring as little overhead as possible on the part of the researcher. To this end, the ESO Science Archive provides access to processed data. Via this route, users can download data that

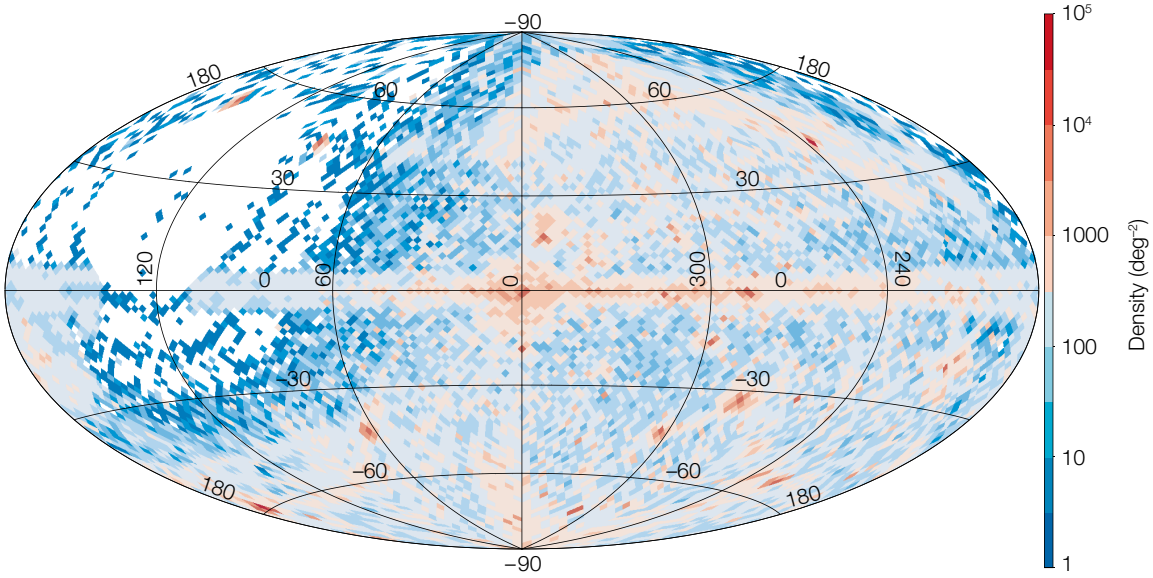

Figure 1. Sky density map of the raw data content of the ESO Science Archive Facility as of June 2023. Popular locations on the sky, such as the Galactic centre or the Magellanic System, clearly stand out, as do the footprints of some of the Public Surveys. The few observations close to the Celestial North Pole are clearly the result of errors in metadata content.

have already gone through most of the processing needed in preparation for extracting the science signal and are thus free from atmospheric and instrumental effects and are calibrated in physical units. The main science files are accompanied and complemented by ancillary ones that provide additional information useful to their exploitation (for example, 2D calibrated spectra are often provided with the main 1D product to allow a custom spectrum extraction; and white-light images go with data cubes). Each data collection comes with extensive textual documentation in the form of a Release Description. In most cases, processed data from the archive are directly ready for science analysis.

There are two main sources of such processed data. One is provided by users who carried out the processing, typically, but not always, for their own projects, and returned the results to the SAF. This is mandatory for observing programmes that require large, coordinated amounts of telescope time, namely Public Surveys[15] and Large Programmes[16], as well as for Hosted Telescopes where there is a signed agreement with ESO for this. In these cases, generating data, both raw and processed, with a long-lasting legacy value is an important criterion in the programme selection process. Voluntary contributions from individual users are much encouraged; this provides a great way to give data, and their authors, enhanced visibility and citeability. To this end, each data collection in the ESO Science Archive is assigned a unique persistent Digital Object Identifier[17] (DOI). Its processing is tailored to the science case(s) of the originating observing programmes, and results are often described and used by the team in refereed publications. Typical data products include calibrated deep and/or mosaicked images and data cubes, stacked spectra, and flux maps. In several cases, these are used to generate source catalogues. These are the highest-level processed data and contain directly the physical parameters of the celestial sources.

The other main channel of influx of processed data for the Science Archive is carried out at ESO. Here, the data histories of instruments, or instrument modes, are processed as consistently and as completely as possible and ingested into the SAF. By its very nature, this data processing is not tailored to any specific science case, but is focused on removing the instrumental and atmospheric signatures and on calibrating in physical units large, coherent datasets. The tools used in-house to process the data are the same ones that are made publicly available[14]. The impact of archival processed data is discussed further below.

Stewardship of science data product: the Phase 3 process

At the time of writing, the ESO Science Archive contains four million processed science files from nearly 80 data collections, covering virtually all data types and observational techniques enabled by the slew of more than 30 instruments that ESO operates at LPO. They cover a correspondingly large range of observing techniques, data types, formats, and metadata.

Without science-oriented data stewardship, curation and homogenisation, the archive would be just a big bucket of bits and bytes, where finding data would be exceedingly hard and reserved to a few experts. Therefore, before ingestion into the archive, the processed data undergo an auditing process for completeness, compliance, consistency, and documentation[18] (Arnaboldi et al., 2011). This process is a collaborative effort between the data provider and ESO and is called Phase 3, reflecting the fact that it closes the loop after the solicitation and handling of observing proposals (Phase 1) and the observation preparation and execution at the telescope (Phase 2).

To ensure data consistency and accessibility throughout this broad variety of archive holdings, the Phase 3 process enforces the use of the ESO Science Data Product Standard[19], an interface

document that defines the data format and metadata (content and definition) for the various types (images, spectra, cubes, interferometric visibilities, catalogues, and so on). It specifies how to encode the level of calibration, scientific quality, originating files (provenance), ancillary data and product versioning. Its content is continuously evolving to reflect the evolving data landscape, for example to incorporate new data types produced by different observing techniques and facilities. The ESO Science Data Product Standard incorporates accepted Virtual Observatory (VO) standards, making ESO data interoperable with the other VO resources. Compliance with the standard is a fundamental requirement which ensures that data can be easily located among the broader ESO holdings and in the general global data scenario. This is a must in the current era of multi-instrument, multi-wavelength, multi-messenger astronomy.

The Archive Science Portal

An important driver for the metadata curation and homogenisation ensuing from the Phase 3 process is that data can be presented and queried uniformly across collections, independently of their origins and specificities. We have built different ways to browse the processed data in the SAF, namely web interfaces, and programmatic and scripted access.

The web interfaces offer a low-barrier access by presenting the data and metadata in an intuitive graphical interface[20]. Query parameters are represented by elements in the page that have the dual function of visually expressing the content of the archive and rendering the user's choices. The results are then rendered on the backdrop of the celestial sphere and included in a tabular form, which summarises their main characteristics (see Figure 2, top panel). Given the underlying compatibility with VO protocols, the results can be sent to VO-aware tools, such as, for example, TOPCAT or Aladin.

Upon request, individual datasets can be explored in detail through previews that are customised by data type. As an example the preview of a Multi Unit Spectroscopic Explorer (MUSE) datacube is shown in the right panel of Figure 2.

A dedicated web interface is available to query source catalogue data[21]. Once users select the catalogue they are interested in, they can constrain the search on any combination of its columns.

Repetitive or otherwise particularly demanding tasks can be coded and automatised by using the provided programmatic access[22]. It too makes extensive use of VO protocols, thus ensuring interoperability and a high level of standardisation. Extensive documentation and example ADQL and TAP queries, Python scripts and Jupyter notebooks are provided to guide users in their first steps, and throughout some more complex cases.

A forum platform is available for archive researchers to exchange ideas and questions[23].

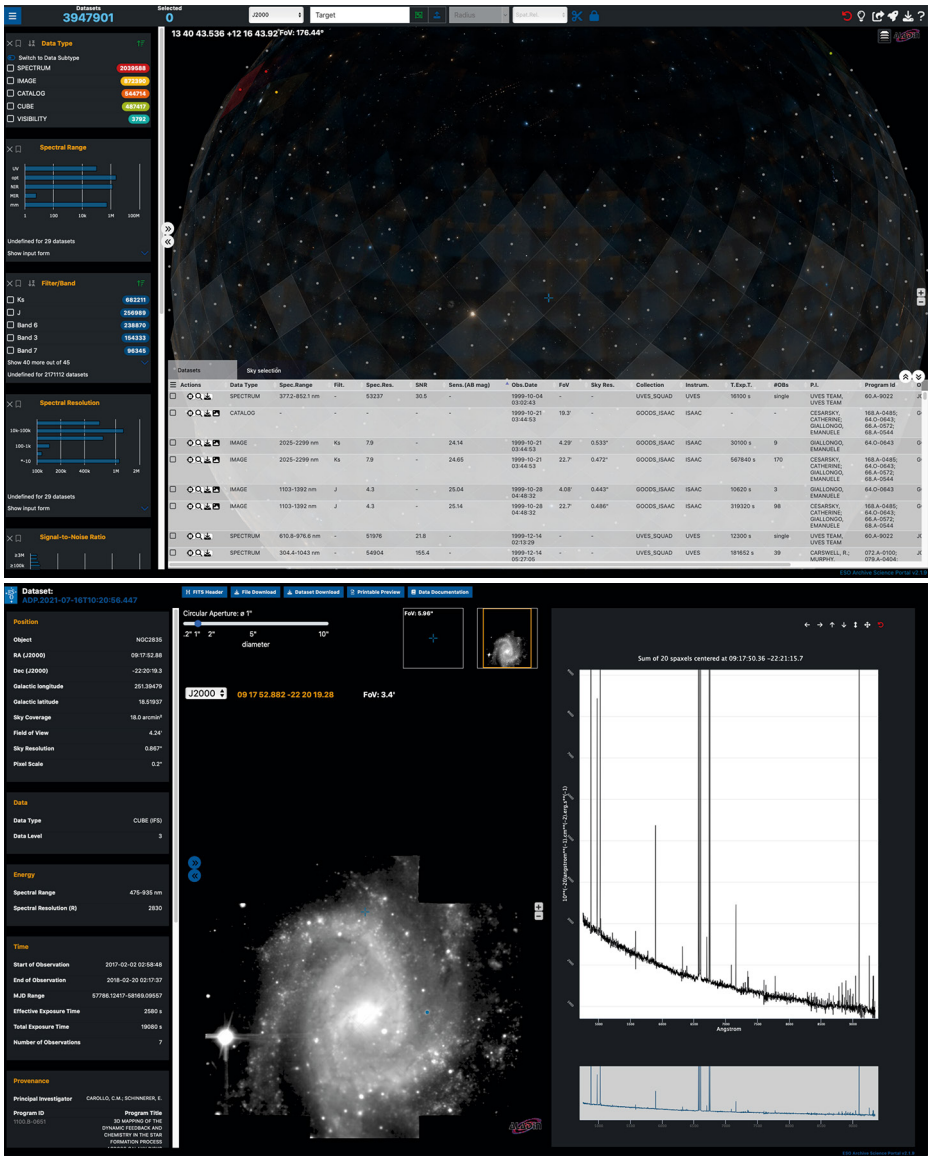

Figure 2. Top panel: The landing page of the web interface to the ESO Archive Science Portal[20]. Bottom panel: Example of the web page where individual datasets can be explored in detail. In this case, the file is a MUSE datacube.

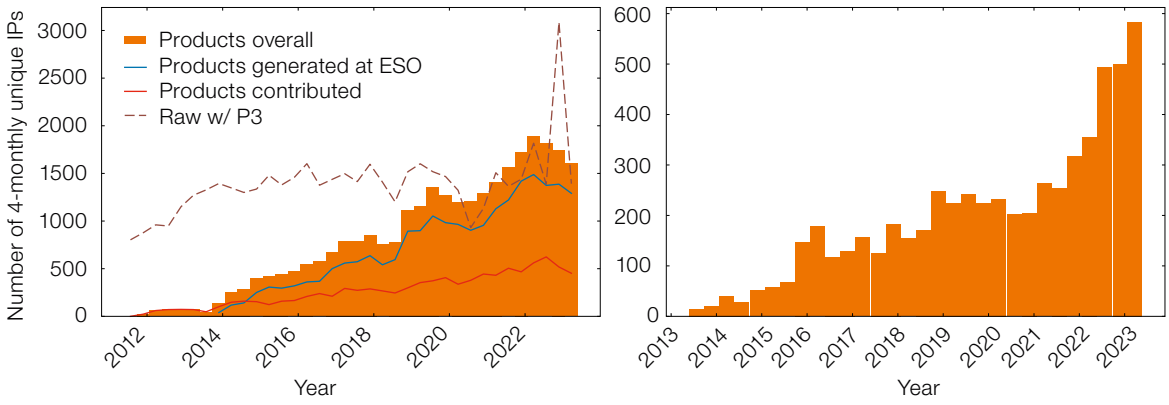

Figure 3. The differential number of unique IP addresses as a function of time from which processed files (left panel) and source catalogues (right panel) in the ESO Science Archive are accessed. The IP addresses are a proxy for the number of users, with each using on average 1.5 IPs. Resorting to IP addresses as a proxy for users is made necessary by the fact that the vast majority of downloads are anonymous.

The impact of the ESO Science Archive Facility

All of the assets in the ESO SAF, i.e., raw data and products generated at ESO or contributed by the community and catalogues, are in great and increasing demand. This is shown in Figure 3, where the number of unique IP addresses, a proxy for the users downloading data, is plotted as a function of time for processed files and source catalogues (left and right panel, respectively). Interestingly, the increase in the download of processed data did not come at the expense of the access to raw data, just as the fast increase in the number of users of data processed by ESO has not hindered the need for data generated externally (bottom panel in Figure 3). The different types of data are, then, highly complementary.

Figure 4 shows the contribution of the SAF to the science output of LPO. This is expressed in terms of the fraction of refereed papers using LPO data that made use of the archive (a referred paper is classified by the ESO Library as archival if there is no overlap between its authors and the members of the original observing proposal[24]). There is a clear upward trend since the inception of the ESO Science Archive in its current form at the end of the 1990s. Currently, about 4 papers out of 10 utilising LPO data make use of the ESO Science Archive.

The ESO Science Archives, both LPO and ALMA, featured as a Special Topic at the 47th meeting of the ESO Users Committee, which was held on 20 and 21 April 2023[25]. The high level of user satisfaction with the archives was confirmed in the discussions during the meeting, as well as in the Committee's report[26], which is based on a poll of the science community.

What's next

As discussed above, the availability of processed data has led to a tangible boost to the access and usefulness of the ESO Science Archive. The engagement of the community at large in providing reduced data has been very successful, and the archive now provides more than 60 out of 80 collections secured in this way. This number is, of course, poised to increase as the policy mandating the delivery of processed data for new Public Surveys, Large Programmes and Hosted Telescopes/Instruments continues and will also include data from ESO's Extremely Large Telescope (ELT) in the future.

In addition to maintaining support for the Phase 3 process for data provided by internal and external users, we are also exploring new ways of collaborating with the community that are not linked to specific observing programmes. Prominent examples include the data stream for the Precision Integrated-Optics Near-infrared Imaging ExpeRiment (PIONIER; Le Bouquin et al., 2011), and the VISTA EXtension to Auxiliary Surveys (VEXAS; Spiniello & Agnello, 2019) and Ultraviolet and Visual Echelle Spectrograph Spectral QUasar Absorption Database (UVES SQUAD; Murphy et al., 2019) collections. We have established a collaboration with the High Contrast Data Center[27] (HC-DC, previously the SPHERE Data Center) in Grenoble. Data from the Spectro-Polarimetric High-contrast Exoplanet REsearch instrument (SPHERE) are regularly processed there, leveraging the considerable science expertise available, and delivered to ESO for wide dissemination (a public archive copy is also maintained

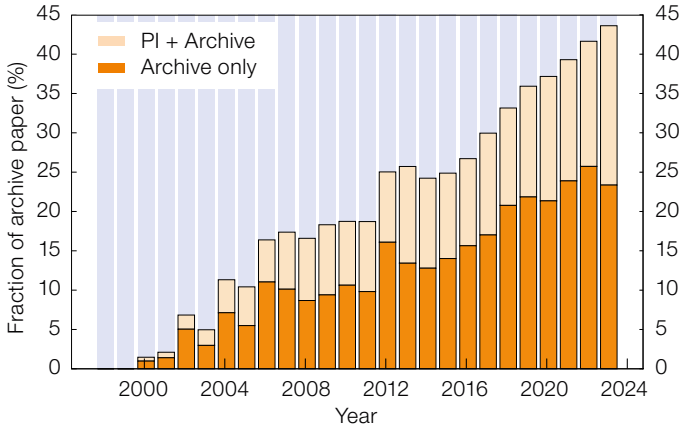

Figure 4. The fraction of refereed publications using La Silla Paranal data that made use of the archive, entirely (dark orange bars) or partially (light yellow bars). Source: ESO Telescope Bibliography[24].

at the HC-DC). The first data products were published in December 2022 in the ESO Science Archive Facility and include imaging data from the InfraRed Dual Imaging and Spectrograph (IRDIS) subsystem, observed during the ESO Periods 103 and 104, i.e., acquired between April 2019 and March 2020. Both the time and the instrumental modes covered will expand in future releases. Similarly, a new collaboration is being set up with the Very Large Telescope Interferometer (VLTI) Expertise Centres of the OPTICON Radionet Pilot[28]. In this case, the processing of GRAVITY data up to calibrated visibilities is performed at ESO, while the Expertise Centres provide scientific guidance and quality control.

The evolution of data generated internally at ESO for publication in the archive will be along two main directions. Firstly, we are working towards making the processed data for the new instruments available much sooner than was possible in the past. The goal is to do so at the same time as the raw data first become public, typically about a year after the start of science operations. This initial delay is determined by the need to characterise the data calibration and processing well enough to provide products of known and documented quality and accuracy. And secondly, to increase the quality of the data processed at ESO we are implementing a more extensive in-depth quality control aimed at identifying ways to improve the products. This is complementing the reprocessing of entire data streams in case of significant improvement of the pipeline and/or calibrations.

With the data content increasing in quality, quantity and complexity, the archive tools to browse and access them must evolve too. As an example, the spectroscopic surveys with the 4-metre Multi-Object Spectrograph Telescope (4MOST) alone will return each year more than three times as many individual processed files as we have collected in the last ten years. The main drivers for this evolution are towards a unification of the web query interfaces to the data, and towards querying the archive content by (selected) physical properties of the astronomical sources. The former aims to reduce the complexity for users by providing as far as possible a single experience where currently different interfaces are in place (for example for processed data[20] and source catalogues[21]). With the latter, we instead aim to provide query capabilities that are closer to the science questions that archive users have. In both cases, the overarching objective is to help scientists to get quickly, efficiently and accurately to the data of interest among the millions of assets that are stored and preserved in the treasure trove which is the ESO Science Archive.

Acknowledgements

The list of people who have made possible the growth and success of the ESO Science Archive Facility goes far beyond the authors of this article. We would like to extend our thanks to the ESO colleagues who have worked with us throughout the years, especially the software development and testing team (Vincenzo Forchì, Ahmed Mubashir Khan, Uwe Lange, Stanislaw Podgorski, Fabio Sogni, Malgorzata Stellert, and Stefano Zampieri). The work, time and dedication of colleagues from the scientific community who have provided processed data to the ESO Science Archive is gratefully acknowledged: their contributions represent a truly invaluable science resource. This article is dedicated to the memory of our colleague Jörg Retzlaff. His hard work, dedication and talent were fundamental in making the ESO Science Archive Facility the powerful science resource for the whole community that it is today. It was an honour and a pleasure to work with him, he will be fondly remembered.

References

Arnaboldi, M. et al. 2011, The Messenger, 144, 17
Le Bouquin, J.-B. et al. 2011, A&A, 535, A67
Murphy M. T. et al. 2019, MNRAS, 482, 3458
Spiniello, C. & Agnello, A. 2019, A&A, 630, A146
Stoehr, F. et al. 2022, The Messenger, 187, 25
Wilkinson, M. D. et al. 2016, Sci. Data, 3, 160018

Links

[1] ESO La Silla: https://www.eso.org/public/teles-instr/lasilla
[2] ESO Paranal: https://www.eso.org/public/teles-instr/paranal-observatory
[3] APEX: https://www.eso.org/public/teles-instr/apex
[4] ESO ALMA webpage: https://almascience.eso.org
[5] ESO ALMA Science Archive: https://almascience.eso.org/aq
[6] EOSC website: https://eosc.eu
[7] FAIR principles: https://www.go-fair.org/fair-principles
[8] ESO Science Archive data access policy: http://archive.eso.org/cms/eso-data-access-policy.html
[9] ESO Phase 1 Call for Proposals: https://www.eso.org/sci/observing/phase1.html
[10] CC BY 4.0 attribution: https://creativecommons.org/licenses/by/4.0
[11] ESO raw data query form: http://archive.eso.org/eso/eso_archive_main.html
[12] ESO instrument-specific query forms: http://archive.eso.org/cms/eso-data/instrument-specific-query-forms.html
[13] ESO instrument calibration plan: https://www.eso.org/sci/observing/phase2/SMGuidelines/CalibrationPlan.generic.html
[14] ESO VLT instrument pipelines: https://www.eso.org/sci/software/pipelines
[15] ESO Public Surveys: https://www.eso.org/sci/observing/PublicSurveys/sciencePublicSurveys.html
[16] ESO Large Programmes: https://www.eso.org/sci/observing/teles-alloc/lp.html
[17] ESO Science Archive DOIs: https://archive.eso.org/wdb/wdb/doi/collections/query
[18] ESO Phase 3 process: https://www.eso.org/sci/observing/phase3.html
[19] ESO Science Data Products Standard: http://www.eso.org/sci/observing/phase3/p3sdpstd.pdf
[20] ESO Archive Science Portal: http://archive.eso.org/scienceportal
[21] ESO catalogue query: https://www.eso.org/qi
[22] ESO Science Archive programmatic access: http://archive.eso.org/programmatic
[23] ESO archive community forum: esocommunity.userecho.com
[24] ESO Telescope Bibliography: https://telbib.eso.org
[25] ESO Users Committee 47th meeting: https://www.eso.org/public/about-eso/committees/uc/uc-47th.html
[26] ESO Users Committee report of 47th meeting: https://www.eso.org/public/about-eso/committees/uc/uc-47th/UC47_2023_UCreport.pdf
[27] High Contrast Data Center: https://sphere.osug.fr/spip.php?rubrique16&lang=en
[28] OPTICON RadioNet Pilot: https://www.orp-h2020.eu

DOI: 10.18727/0722-6691/5339

Telluric Correction of VLT Spectra: The New Graphical Interface to Molecfit

John Pritchard[1]
Lodovico Coccato[1]
Wolfram Freudling[1]
Alain Smette[1]

[1] ESO

The removal of absorption features due to Earth's atmosphere is a fundamental and delicate process in the reduction of spectroscopic observations, in particular in the near- and mid-infrared. In this paper we present the new graphical user interface of Molecfit, a package that aims to model the full atmospheric transmission by fitting key absorption features in spectra.

Some of the light from astronomical sources is absorbed by Earth's atmosphere. The atmosphere is completely opaque in some regions of the spectrum, where the signal from the source is therefore unavailable to ground-based telescopes. In other regions, however, the absorption occurs only at specific wavelengths and a series of absorption lines, called 'telluric absorption lines', contaminate the spectra of the observed sources. The correction of these telluric absorption features is a crucial step in the reduction of spectroscopic data. This is particularly relevant for near- and mid-infrared observations, where the depth, number and density of telluric absorption features are high and significantly contaminate the spectrum, blending with the intrinsic spectroscopic features in the spectrum of the object. Figure 1 shows the atmospheric transmission from 0.3 mm to 2.6 mm.

Telluric correction

There are two main strategies to remove telluric absorptions from a spectrum. The first is to observe a source (a telluric standard star) with no intrinsic features. The spectrum of the telluric standard star, normalised to its continuum level, can be used to remove the atmospheric signatures from other spectra taken under the same conditions and with the same instrument and instrument setup. The advantage of this method is that it delivers a telluric transmission convolved with the same spectral resolution as the scientific target(s). The main disadvantages are that it requires taking dedicated observations close in time to the scientific target(s) and that the telluric standards are not observed at the same time as the science exposures, so any changes in the atmosphere will introduce artifacts in the corrected source spectrum.

The second strategy is to generate a model of the atmospheric transmission starting from measurements of humidity and pressure and the column densities of the molecules that shape the telluric features. The last of those can be obtained by measuring specific absorption features on a reference spectrum, which could be either a telluric standard star or the science target itself if it is bright enough. The advantage of this strategy is that, in principle, dedicated telluric standard star observations can be avoided, or at least minimised. The disadvantage is that the method relies on the goodness of the underlying physical ingredients (such as correct treatment of the molecules and how they interact with each other, and how the pressure, temperature and humidity vary with altitude) and instrument-related components such as the line spread function and the goodness of the wavelength calibration.

Molecfit

ESO provides a general tool, named Molecfit (Smette et al., 2015; Kausch et

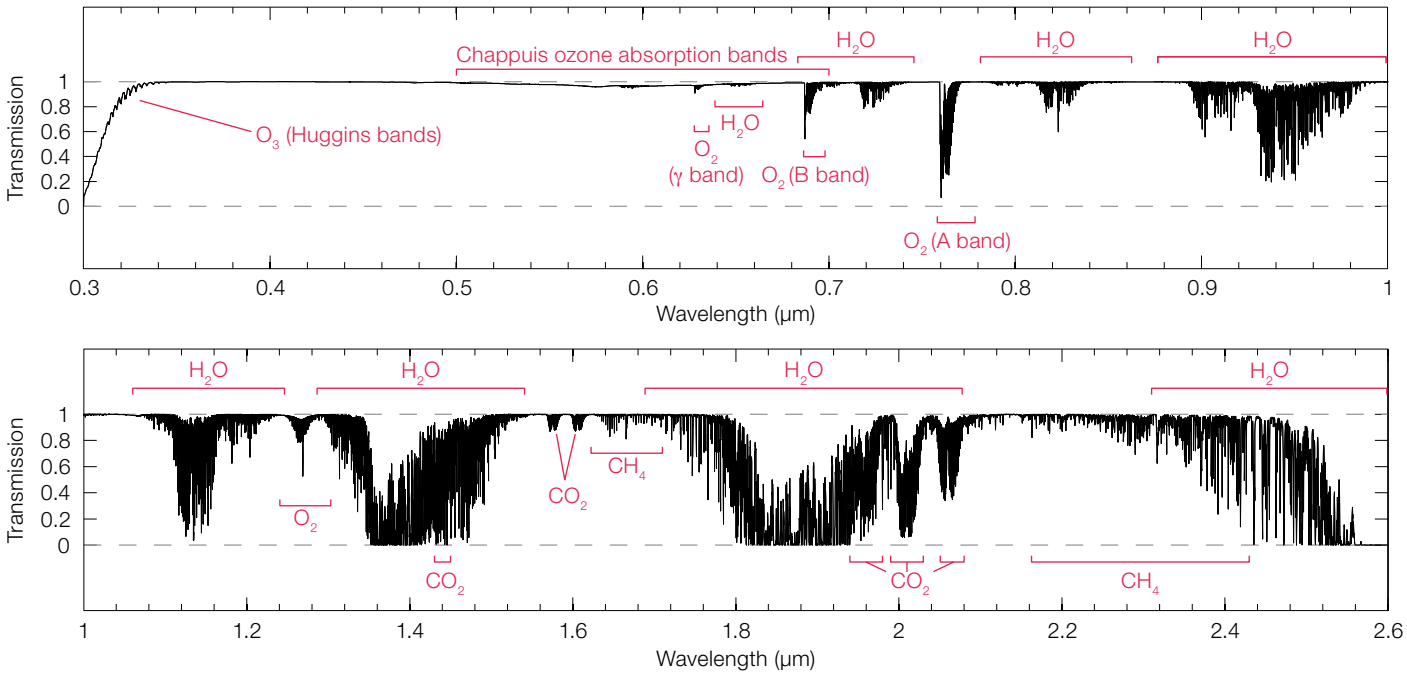

Figure 1. Atmospheric transmission in the optical and near-infrared (from Smette et al., 2015).

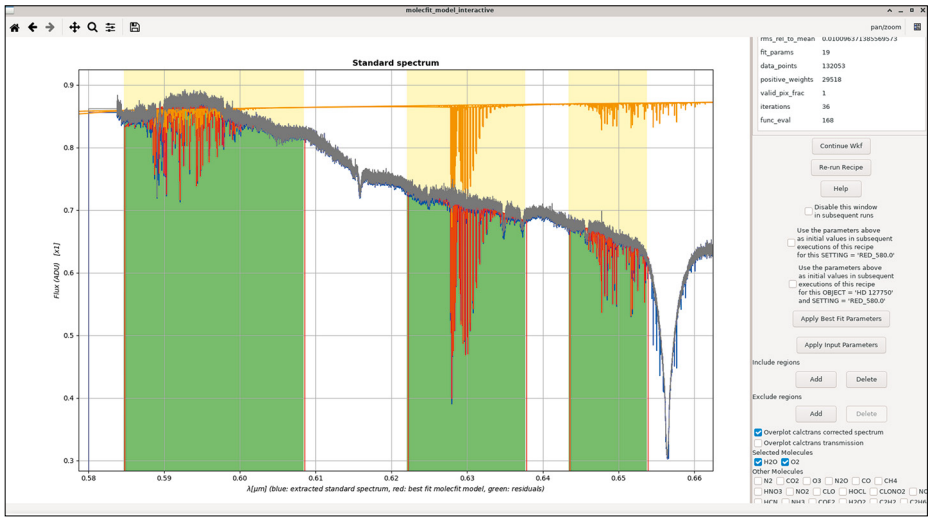

Figure 2. Interactive window of the Molecfit model. The left-hand panel shows the input reference spectrum (blue), the typical transmission curve for H_2O and O_2 (orange), the best fit model (red), the telluric corrected spectrum (grey), and the wavelength regions used in the fit (green). The right-hand panel allows the user to change the recipe parameters.

al., 2015), which aims to remove telluric absorptions using the modelling approach. Molecfit was released on 1 April 2014 as three stand-alone 'executables' and a graphical user interface (GUI) that guides the user through the process of removing telluric features.

As Molecfit was created to be used with most spectrographs, it includes a large number of user parameters. However, although well-tuned to the underlying executables, the way the original GUI was coded made it difficult to maintain and to integrate with the ESO pipeline environment.

Therefore, to facilitate future developments and maintenance and to improve compatibility with existing ESO data and instrument pipelines, Molecfit has been integrated into the ESO data processing infrastructure as a pipeline package[1]. The original stand-alone code is still distributed, but is not supported anymore[2].

Like the original suite, the new version of Molecfit consists of three 'recipes': molecfit_model fits — possibly small — regions of a spectrum, accounting for the shape of the continuum in these regions, spectral resolution and systematics in the wavelength scale, and derives the column densities of the molecules included in the atmosphere; molecfit_calctrans constructs the atmospheric transmission over the whole spectral range of the input spectrum taking account of the atmospheric composition determined by the previous fit, adapting it to the spectrum to be corrected by taking account of any difference in airmass between the spectrum used to derive the model and the spectrum to be corrected; and molecfit_correct applies the above mentioned correction to a scientific spectrum. These recipes can be executed, like any other ESO recipe, from the command line with the esorex command or via an EsoReflex workflow[a] (Freudling et al., 2013).

The first version of Molecfit to be released as a pipeline package and EsoReflex workflow (version 3.0.0) was released in 2020. As the focus of that release was the implementation of the underlying modelling engine, many of the more user-friendly aspects of the GUI of the original version were not implemented in the first version of the workflow.

Since then the underlying engine has been updated and improved and the Molecfit workflow has been overhauled, so that it now includes advanced features that enhance the user's experience of making an efficient telluric correction; this is the topic of this paper.

The most critical aspect of Molecfit is to determine the various parameters that accurately reproduce the transmission spectrum of the atmosphere as seen by the spectrograph: the column densities of the various molecules contributing to the telluric features, the parameters of the line spread function of the spectrograph, the coefficients of the polynomial representing correction of the wavelength calibration, and a good representation of the continuum in the selected regions to be modelled. The workflow overhaul therefore concentrated on the GUI associated with the molecfit_model recipe.

Before starting the workflow, the user must set some basic parameters, such as:

– the directories where the data are located and where the final products will be stored. As for all EsoReflex workflows, the input directories are scanned and files in them are classified. For each science spectrum to be corrected the 'closest-in-time' telluric standard (if present) observed with the same instrumental setup is associated.
– the reference spectrum for the model. The user can decide to fit the atmospheric model on the science file to correct itself (this strategy works best for spectra of high signal-to-noise), or on the associated telluric standard (if present).
– the instrument the data were taken with. The workflow currently recognises data from five instruments (ESPRESSO, GIRAFFE, UVES, VISIR, and X-shooter) and automatically adapts the output files of the ESO pipelines of these instruments into Molecfit-compatible formats (if necessary). It sets robust recipe parameters for these instruments and their configurations, such as molecules and wavelength regions to consider in the fit. The user can change them through the interactive windows that will pop up during the analysis. Data from other instruments, including non-ESO instruments, can also be corrected. However, in such cases adapting the input files to Molecfit-compatible formats (if necessary) and the setup of the recipe parameters are left to the user, either interactively when running the workflow, or by implementing a set of Python methods specific to the instrument in question. Support for more (ESO) instruments is under development[3].

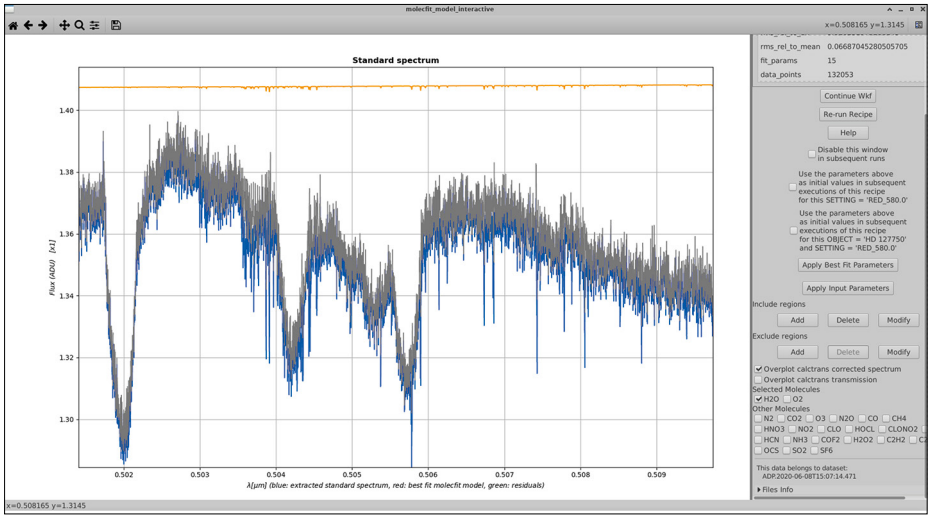

Figure 3. Zoom-in of Figure 2. Note that the corrected spectrum (grey) has the telluric lines removed (blue) even in this wavelength region that was not included in the fit. The power of the method is that one can consider only strong telluric features to determine the model for the entire wavelength range of the data, minimising the contamination from noise or the intrinsic features of the source.

To correct each dataset, the workflow first presents the molecfit_model GUI, with which the user can fine tune the parameters and their initial guesses to use in the first execution of the molecfit_model recipe. The GUI shows the reference spectrum together with pre- or auto-defined wavelength regions and pre- or auto-defined molecules to fit. The user can display a typical transmission curve for each molecule to evaluate whether it has an impact on the telluric absorption in the reference spectrum and therefore to include or exclude it from the model. The wavelength regions can be defined and edited with the mouse. Although there are still more than 100 parameters that control every aspect of the model, they have been grouped into several tabs by experience level to guide users from novice to expert.

Once happy with the initial recipe parameters, the user can run the molecfit_model recipe to compute the fit. Upon completion of the recipe, the GUI is presented again, this time also displaying the fitted model and residuals. It displays the computed corrected spectrum over the full wavelength range of the input spectrum (Figures 2 and 3), allowing the user to further fine tune parameters and rerun the recipe as many times as necessary to obtain an optimum model. The parameter setup can be stored and re-used for other datasets from the same instrument configuration.

Once an optimal model has been computed, the workflow uses the model to construct the telluric correction for the target spectrum. If the reference spectrum used for the model was a telluric standard, Molecfit accounts for the airmass and Precipitate Water Vapour difference between the two spectra. Optionally, the user can provide a function describing the instrumental line spread function at each wavelength, which will be considered when constructing the transmission curve. Finally, the spectrum is corrected. The products of the workflow reflect the format of the input data: if the input spectra comply with the format of the ESO archival standard (known as the phase3 standard), so do the products.

References

Freudling, W. et al. 2013, A&A, 559, A96
Kausch, W. et al. 2015, A&A, 576, A78
Smette, A. et al. 2015, A&A, 576, A77

Links

[1] ESO Pipelines: https://www.eso.org/sci/software/pipelines/
[2] Molecfit: http://www.eso.org/sci/software/pipelines/skytools/molecfit
[3] Molecfit Experimental Version: https://support.eso.org/kb/articles/molecfit-experimental-version

Notes

[a] Integration with the GASGANO GUI, however, has not been implemented, neither is it foreseen.

ESO/P. Horálek

The bright light in the centre of this picture, shining below the Milky Way's dark, pinkish belt, is the planet Jupiter. It is flanked by two hills hosting ESO's Very Large Telescope (left) and VISTA (right) in the Atacama Desert in Chile.

DOI: 10.18727/0722-6691/5340

Ultra-wideband Cryogenic Low Noise Amplifiers: a Cool and Crucial Component for Future Submillimetre Radio Telescopes

Isaac López-Fernández[1]
Juan Daniel Gallego[1]
Carmen Diez[1]
Inmaculada Malo[1]
Ricardo I. Amils[1]
Gie Han Tan[2]

[1] Yebes Observatory, Spain
[2] ESO

This article reports on the evolution in designing state-of-the-art cryogenic, wideband, low-noise amplifiers as used in the intermediate frequency stages of ALMA receivers. The most recent designs are presented which demonstrate exceptional bandwidth and noise performance; those are crucial in enabling the planned ALMA Wideband Sensitivity Upgrade.

Introduction

For radio telescopes like the Atacama Large Millimeter/submillimeter Array it is crucial to optimise performance parameters such as sensitivity and observation bandwidth in order to keep pace with the developing needs of the astronomical user community. Since current receiver systems at these short wavelengths already demonstrate very low noise performance, on the order of a few times the quantum limit hν/k, further improvement of that parameter is practically very limited. An alternative way to enhance sensitivity is to increase the instantaneous bandwidth. This must be achieved across the entire astronomical signal chain, both the analogue signal path and the digital signal processing, interfaced by suitable high-speed digitisers (Quertier et al., 2021). In the analogue section of the receiver, a humble but critical component in this respect is the intermediate-frequency cryogenic low-noise amplifier. In this article we report on the latest developments that enable further increase of the instantaneous bandwidth.

Maximising the instantaneous bandwidth

Almost since the beginning of radio astronomy one of the permanent items in the wish list of radio astronomers has been to enlarge the instantaneous bandwidth processed by the instruments, which is intrinsically linked to an increase in observation efficiency. For continuum (total power) observations this means increasing the sensitivity or needing less integration time, since fluctuations in power measurements diminish in proportion to the square root of the bandwidth. For spectral-line observations a wider frequency range is accessible at once so more lines or transitions of the same species can be observed in less time, and blind redshift observations are facilitated. In the submillimetre wavelength range, where ALMA stands out, this allows delving deeper into the origins of galaxies and performing much faster astrochemical surveys of a spectrum plagued with a forest of lines which provide invaluable information about the physical-chemical conditions in the objects observed.

The major millimetre radio telescopes, including the Institute de Radioastronomie Millimétrique (IRAM) Northern Extended Millimetre Array (NOEMA) and the Submillimeter Array (SMA), are implementing this increased bandwidth upgrade. The Atacama Large Millimeter/submillimeter Array (ALMA) will also follow this strategy, as set out in its Development Roadmap 2030 (Carpenter et al., 2019) and detailed in the Wideband Sensitivity Upgrade (WSU) initiative (Carpenter et al., 2022).

Figure 1 is a generic, simplified block diagram of a typical receiver architecture as used in submillimetre radio telescopes like ALMA bands 3 and up. It is based on the heterodyne principle whereby the incoming submillimetre radio frequency (RF) signal is down-converted to a lower frequency, the intermediate frequency (IF), which is typically below 20 GHz, and which can be more easily amplified before being sampled and quantised by room-temperature electronics to establish a digital representation of the input signal. The mixing and first stages of IF amplification are carried out by devices developed specifically for this application and cooled to cryogenic temperatures to minimise the self-generated noise.

The sensitivity of the receiver is directly impacted by the noise generated in the signal chain. The cascaded noise performance is given by the expression (Friis, 1946):

$$T_{RX} = T_{SIS} + \frac{T_{IF_1}}{G_{SIS}} + \frac{T_{IF_2}}{G_{SIS} \times G_{IF_1}} + \ldots$$

Where T_{SIS}, T_{IF_1}, ... and G_{SIS}, G_{IF_1}, … represent the equivalent noise and gain respectively of the components in the signal chain of Figure 1. The formula provides insight into how the noise contributions of those components close to the input are dominant. Considering that the typical submillimetre-wave mixing devices[a] attenuate the incoming signal ($G_{SIS} < 1$), the noise contribution of the first IF low-noise amplifier (LNA) becomes even more pronounced and should be minimised to obtain a more sensitive receiver.

The other crucial parameter, the instantaneous bandwidth, is very much determined by the components in the analogue signal chain, in particular the IF amplifiers

Figure 1. Generic block diagram of a typical submillimetre heterodyne receiver signal chain. There is usually one channel per polarisation.

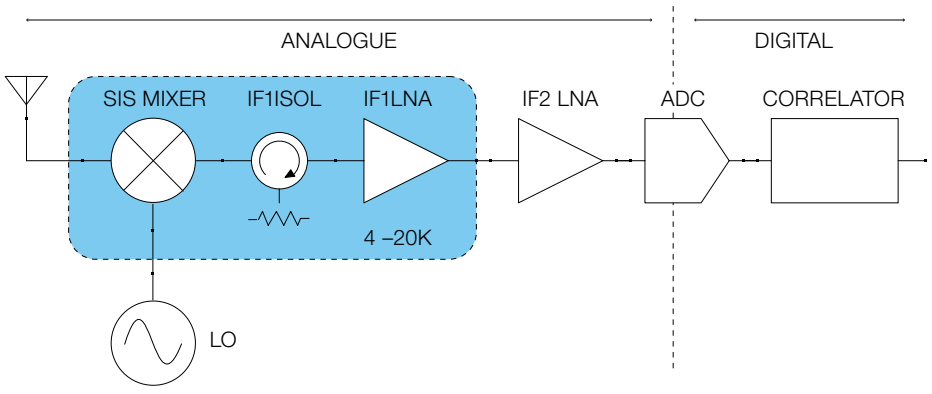

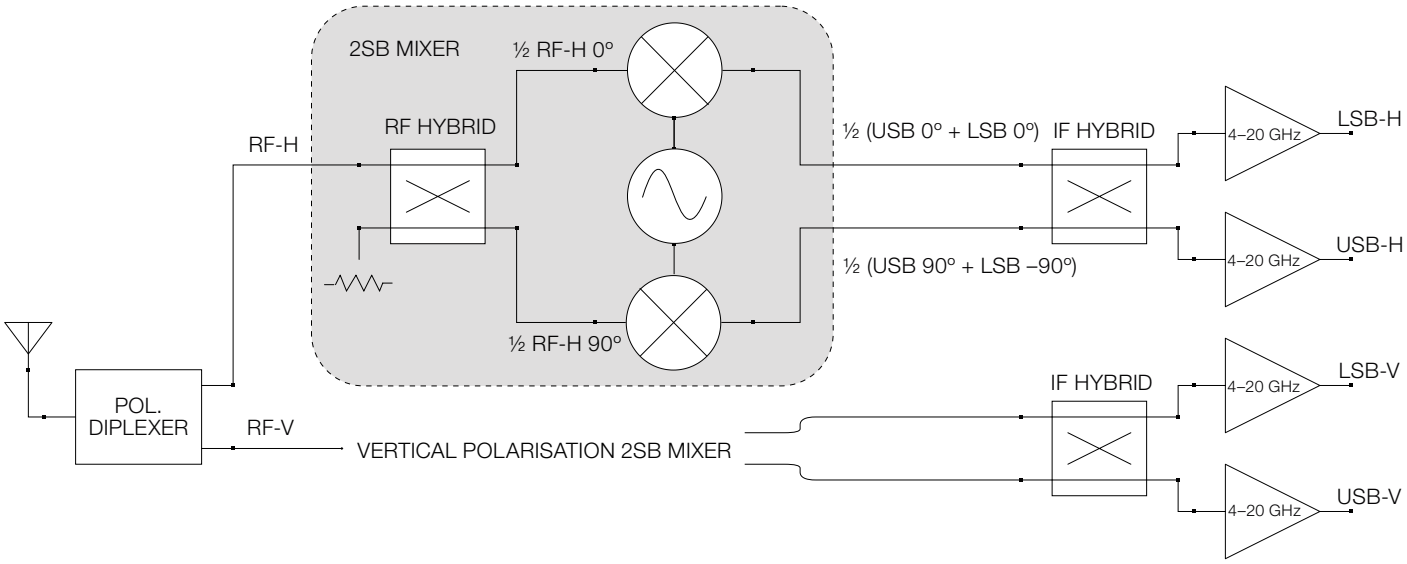

Figure 2. Simplified block diagram of a submillimetre receiver front-end based on 2SB mixers. The RF and IF quadrature hybrid couplers introduce a 90° phase delay in the coupled paths. USB and LSB refer to the upper and lower IF sidebands respectively. Note that the instantaneous bandwidth available to be processed is four times the IF bandwidth, totalling 64 GHz.

and the analogue-to-digital converters (ADCs).

Analogous to the visible spectrum, which extends over one octave, the maximum RF bandwidth that can be processed by the input mixer is usually limited in practice to less than one octave in frequency by the physical constraints of the components (waveguides, for example). The problem with a heterodyne receiver that is intended to cover a large bandwidth, comparable to that which could be handled by the input mixer, is that the number of octaves to be processed at the IF can be prohibitively high and this becomes a challenge for the design of the components in the IF chain.

The ALMA strategy to multiply by four the present instantaneous bandwidth consists of (a) doubling the present maximum 8 GHz bandwidth per IF channel to achieve 16 GHz, and (b) extending the use of sideband separating or 2-sideband (2SB) mixers to all ALMA bands[b]. Figure 2 presents a block diagram of a submillimetre receiver front-end based on 2SB mixers. This scheme can separate the upper and lower sidebands generated in the mixing process into two IF channels by means of two mixers and two quadrature hybrid couplers which introduce selective 90° phase delays to finally cancel the undesired sideband in each channel. The ALMA upgrade aims for a 64-GHz band to be processed in the correlator (2 polarisations × 2 sidebands × 16 GHz).

State of the art and requirements

The struggle to increase instantaneous bandwidth has been going on for the last few decades. Figure 3 shows how the instantaneous bandwidth of the most advanced instruments at each epoch has been evolving. In the 1990s the typical value for the first IRAM receivers was of the order of 1 GHz. The development of the HIFI submillimetre receivers for ESA's Herschel mission set the ambitious (at that time) goal of 4 GHz per channel. A few years later, in 2005, an even more ambitious target of twice that value (8 GHz per channel) was established for ALMA and most bands still retain that value.

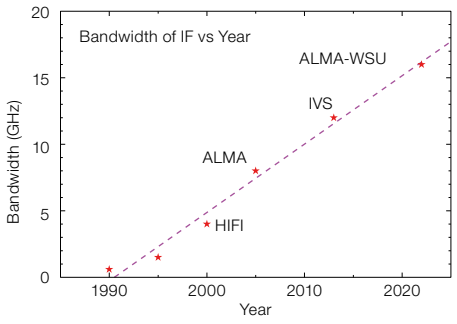

Figure 3. Evolution of the typical instantaneous bandwidth of state-of-the-art radio telescopes over the last 30 years.

The LNA laboratories at Yebes Observatory have promoted this evolution, developing, among others, the cryogenic amplifiers that set the standards in the aforementioned instruments. ALMA bands 5, 7 and 9 are equipped with cryogenic LNAs (CLNAs) designed in Yebes (López-Fernández et al., 2006). Although a significant number were manufactured in its labs, most of the production was completed by a firm that received expertise and technology transfer from Yebes.

However, to be effective the LNA bandwidth expansion should be accompanied by other performance benchmarks. Obviously the noise temperature of the amplifier has to be as low as possible, given its prominent role in the overall receiver sensitivity. Its gain must be high enough that the contribution to the receiver noise from warm electronics is negligible (following equation 1) and sufficiently flat to cope with the limited dynamic range of the ADCs. The power dissipation is restricted by the cooling power of the refrigerator. This fact is especially critical for submillimetre-wave receivers with superconducting mixers which only operate below 4.2 K, or in case of focal-plane arrays (multipixel receivers) with a large number of cryogenic amplifiers.

Finally, a crucial but frequently overlooked parameter is the degree to which the amplifier is matched to its input and output loads, usually measured by the reflection coefficients. A poorly matched amplifier would reflect a relevant fraction of the incident power, producing standing waves along the input line which will translate into a ripple in the output noise temperature and power. This problem was traditionally solved by introducing an isolator between the mixer and the CLNA, as in most of the current ALMA bands (see Figure 1). However, ultra-wideband isolators (Zeng et al., 2018) are critical components to avoid in cryogenic receivers, as they are bulky and introduce significant losses, degrading the system noise temperature. Additionally, a 2SB mixer scheme relies heavily on a well-matched amplifier to achieve a high image rejection ratio (IRR), that is, a proper cancellation of the image (upper or lower) frequency band, as illustrated in Figure 2.

When ESO, in the framework of its Technology Development Programme, set the goals for the next generation of ALMA CLNAs, it became clear that some trade-offs would be necessary, as the requirements far exceeded the state of the art. The challenge was not only to design a CLNA with twice the maximum bandwidth of the current generation ALMA amplifiers, but also to do so with numbers for noise temperature, gain flatness and input reflection typical of narrower-band cryogenic amplifiers.

The most competitive published ultra-wideband cryogenic amplifier results with similar noise temperature lack sufficient bandwidth and, moreover, have their Achilles heel in a poor input reflection: see, for example, Nilsson et al. (2014) for the 6–20-GHz band, later improved by the Low Noise Factory AB in Sweden, or Cha et al. (2018) for the 0.3–14-GHz band. These two conflicting requirements, namely noise and input reflection, are possibly the most difficult to meet in a wide-band LNA.

Transistor development

The key component in any modern microwave amplifier is the active semiconductor device, which is usually some type of transistor. A successful amplifier design revolves around making a number of cascaded stages of these devices operate as close as possible to their optimum to obtain their maximum gain and minimum added noise. Other cryogenic amplifying technologies with near quantum-limited noise are either intrinsically narrowband (solid-state masers) or still not sufficiently mature (travelling-wave kinetic inductance parametric amplifiers).

Since the turn of the century the devices of choice for extremely low-noise amplification at microwave frequencies are either GaAs or InP high-electron-mobility transistors (HEMTs), a type of field-effect transistor based on heterostructures with enhanced electron transport properties. InP is an exotic material that is difficult to handle and not easily available commercially. The mainstream GaAs HEMTs were developed first, and there is a prosperous semiconductor industry mass-producing them for many commercial and military applications at an affordable cost. However, the very best results we need are consistently reported using InP technology. Cooling these transistors to cryogenic temperatures further boosts electron transport and reduces the thermal noise generated by parasitic elements, and when combined with a careful design, enables an order of magnitude improvement in the equivalent noise temperature of the amplifier (see the excellent review by Pospieszalski, 2005).

A breakthrough in cryogenic amplifier performance such as demanded by ALMA is not possible without a substantial development of the present InP HEMTs. Very few foundries in the world are capable of producing InP devices. All current ALMA amplifiers feature transistors from the two US foundries (Northrop Grumman Space Systems and HRL Laboratories). With the aim of having an independent, flexible, and accessible supplier of InP transistors in Europe (without the severe import restrictions on US InP technology), Yebes Observatory began a partnership with the Swiss Federal Polytechnic Institute (ETH) 25 years ago that has found its natural continuation with Diramics AG, a spin-off from ETH that produces InP transistors using the same facilities. This collaboration was initially financially supported in part by several ESA projects and more recently by ESO.

Over the past five years we have focused on the development of transistors for the IF range, trying to improve the noise performance and to solve the chronic problem of very high-frequency oscillations. This issue tends to be worse for the best devices and it is aggravated at cryogenic temperatures. Through a slow iterative process, changes in the epitaxial material and the layout structure were proposed, implemented, and tested. On-wafer cryogenic noise measurements of transistors are not accurate enough, hence the devices were evaluated and modelled by testing them in the first stage of a well-known LNA in the Yebes labs. The resulting optimised devices are clearly less prone to auto-oscillation, avoiding the need to only use certain stable bias points that are not necessarily the best in other respects. Furthermore, a very considerable reduction in noise temperature was confirmed, between 15% and 20% depending on the frequency. An additional advantage of these improved devices is that the optimum noise is reached at a lower bias setting, thus dissipating less power. It is typical of well-behaved transistors to display their best performance for lower drain currents. These results put Diramics at the forefront of InP transistor development for IF, ahead of the traditionally superior American foundries.

Figure 4 shows a picture of an optimised device with a gate geometry appropriate for use in the first stage of the ultra-wideband amplifier (the first stage is the most important in terms of noise). It is presented in die form, suitable for wire bonding and independent testing.

LNA design

As regards the fabrication and assembly technology used, microwave amplifiers can be implemented in hybrid circuits (also known as ‘chip & wire’) or in monolithic microwave integrated circuits (MMIC). The former make use of microwave substrates and chip passive components interconnected by bond wires to achieve the matching of the different transistor stages and to realise the DC bias circuits, while the latter integrate most of this circuitry in a single chip. The MMIC option has advantages, especially at the higher microwave frequencies, where size

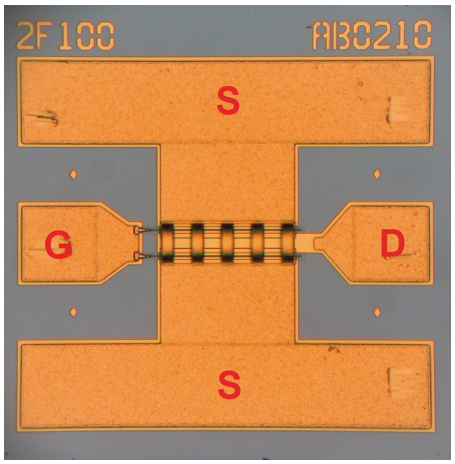

Figure 4. Microphotograph of the 350 × 350 × 100 μm die of the Diramics InP HEMT with 2 × 100 μm gate finger in 100-nm technology. This device is used in the first stage of the 4–20-GHz amplifier and was the outcome of a long term joint development effort between Diramics and Yebes. The transistor terminals (gate, drain and source) are labelled with their initials. Note the five air bridges connecting the source pads.

is a problem owing to the parasitics, and for applications for which a large number of units is demanded. However, for our prototype it is much more convenient to rely on a hybrid design because it is cheaper and faster to produce, modify and tune (an MMIC requires a complete iteration cycle with the foundry). It also allows different transistor technologies to be used for each stage and presents lower losses in the critical input matching circuit, usually implemented by microstrip lines.

Another important design choice is where to place the targeted 16-GHz-wide band. At the present development stage of the ALMA WSU (Carpenter et al., 2022) we are still on time to influence this system-level decision. On the one hand, the upper band limit is constrained by the noise temperature achievable, since it increases almost linearly with frequency. On the other hand, the lower band limit restriction comes from the maximum fractional bandwidth (FBW, defined as the ratio between the central frequency and the bandwidth, usually expressed as a percentage) that permits matching at the level required for this project. The input impedance of HEMT devices is very reactive at low frequencies. Matching in a wide band becomes increasingly difficult for large FBWs. A reasonable compromise was found in the 4–20-GHz band. Note that this represents an FBW of 133% or 2.3 octaves.

The problem of matching is pivotal in the design of an ultra-wideband CLNA. The conditions required by the first stage transistor to minimise the reflected power and deliver the minimum possible noise are different and the strategies for designing a matching network that transforms and brings them together are frequency-dependent and fail in such wide bands. Therefore, to address the stringent requirements for noise and input reflection, the first-stage transistor gate size was carefully selected to favour the matching in the 4–20-GHz band, and a very simple input network was devised. A progressive compromise for the noise mismatch at the lower band end must be tolerated to ensure an acceptable noise performance at the higher end. The other stages can compensate the gain rolloff; nevertheless, it is difficult to separate the role of each stage in this design, as opposed to narrower-band amplifiers.

The intensive use of simulation tools required was supported by a systematic and painstaking process of selection and modelling of components at cryogenic temperature.

The bias networks feed the extremely sensitive HEMT devices with DC power and protect them from electrostatic discharge. They also contribute to the stability of the transistors with high-value resistors that usually dissipate a significant amount of power. We have been able to reduce this fraction to just 15% while still ensuring that the amplifier is unconditionally stable.

A picture of the final prototype is provided in Figure 5, where it is compared with the three times bulkier CLNA used in ALMA bands 5 and 7. Nevertheless, the identical assembly processes, the use of similar microstrip substrates, similar connectors and equivalent gold-plated aluminium modules make them quite alike.

Results in the 4–20-GHz band

The results shown in Figure 6 demonstrate that it is possible to achieve state-of-the-art noise temperature in a 16-GHz-wide band with an input reflection low enough to guarantee excellent matching with the mixer and high IRR without the need for an isolator, which would penalise the system in complexity and sensitivity.

Noise temperature is compared at 15 K ambient with the current ALMA CLNAs. The measurements at 5 K ambient are more representative of the operating conditions of the amplifier, which will be placed in the 4-K stage of the cartridge, and yield an average of 3.7 K, below the goal of 4 K. It is remarkable that comparable noise values are obtained for an upper passband frequency extending to frequencies two to four times higher than current band 9 and 5/7 amplifiers, and with an input reflection below –15 dB, to our knowledge never before achieved in this frequency range. The noise results were confirmed using two independent methods. Yebes Observatory has a long history as a reference lab for cryogenic noise measurements, a slippery field where all too often numbers coming from different institutions differ significantly because of the difficulty of performing accurate measurements.

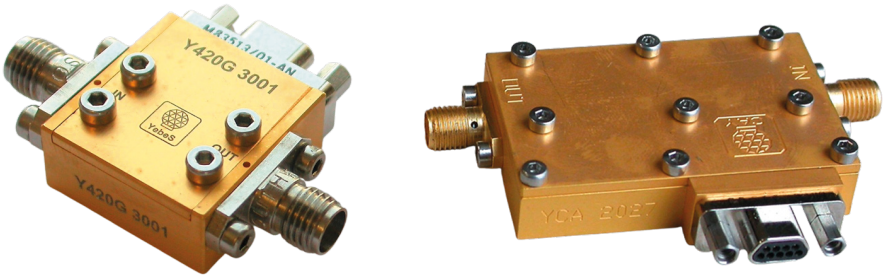

Figure 5. Comparison of the newly developed 4–20-GHz CLNA prototype for the next generation of ALMA receivers (left) with one of the 4–8-GHz CLNAs actually installed in ALMA band 5 and 7 cartridges (right). Both are made of gold-plated aluminum and their sizes are 21 × 20 × 9 mm and 46 × 29 × 9 mm, respectively.

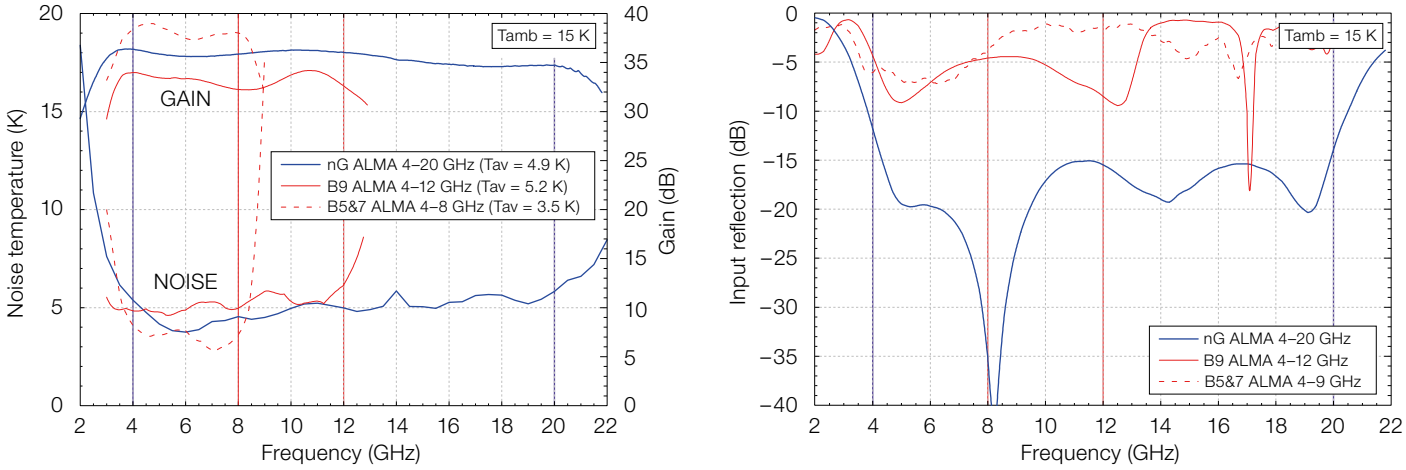

Figure 6. Performance at 15 K ambient of the prototype developed in the 4–20-GHz band (in thick blue) compared with a typical current 4–8-GHz CLNA of ALMA bands 5 and 7 (in dashed red) and 4–12-GHz CLNA of ALMA band 9 (in solid red). Left: noise temperature and gain. Right: input reflection. Average noise temperature at 5 K ambient is 3.7 K. The noise performance of the new amplifier is similar, despite its much wider bandwidth and being designed to achieve excellent input reflection.

The prototype also met the expectations in power dissipation (8 mW), gain flatness (< 1.8 dB_{pp}) and output reflection (< –15 dB).

Future prospects

ESO has recently awarded Yebes Observatory its proposal of a new ALMA Development Study for the "Development of InP MMIC based Wideband Low-Noise Amplifiers for the Next Generation ALMA Receivers" within which we plan to advance Diramics MMIC technology and translate the current design into a monolithic circuit. If successful, the resulting chips could be useful for a prospective production phase of ALMA receivers. Furthermore, considering our recent and promising results of performance with ultra-low power dissipation, they could enable the implementation of ultra-wide band focal plane arrays.

Acknowledgements

This work was supported in part by ESO Collaboration Agreement 79226/17/81324/ASP and in part by the Multiregional Operational Programme for Spain 2014-20 (ERDF) under project ICTS-2018-01-CNIG-11.

This study is part of the ESO Technology Development Programme (ESOblog - Shaping the future | ESO). We are indebted to the Programme Manager, Norbert Hubin, for his continued support and encouragement.

References

Carpenter, J. et al. 2019, arXiv: 1902.02856
Carpenter, J. 2022, ALMA Memo 621
Cha, E. et al. 2018, IEEE Trans. Microw. Theory & Techn., 66, 4860
Friis, H. T. 1946, Proc. IRE, 34, 254
López-Fernández, I. et al. 2006, IEEE MTT-S Int. Microw. Symp. Digest, 1907
Nilsson, P. A. et al. 2014, IEEE Compound Semicond. Integr. Circuit Symp., 1
Pospieszalski, M. W. 2005, IEEE Microw. Mag., 6, 62
Quertier, B. et al. 2021, The Messenger, 184, 20
Tan, G. H. et al. 2004, The Messenger 118, 18
Zeng, L. et al. 2018, IEEE Trans. Microw. Theory & Techn., 66, 2154

Notes

[a] Superconductor-Insulator-Superconductor (SIS) tunnel junction mixers.

[b] Presently, ALMA bands with 4-GHz IF channels have 2SB mixers, while bands with 8-GHz channels have classical DSB mixers. The total IF band to process is 16 GHz in both cases. See Tan et al. (2004).

ESA/NASA

This image from the NASA/ESA Hubble Space Telescope shows the central region of the rich globular star cluster NGC 3201 in the southern constellation Vela (The Sails).

A star that has been found to be orbiting a black hole with four times the mass of the Sun lies close to the centre of this picture.

DOI: 10.18727/0722-6691/5341

VIRCAM Operations End at VISTA

Jim Emerson[1]
Valentin D. Ivanov[2]
Thomas Szeifert[2]
Boris Haeussler[2]
Juan Carlos Muñoz Mateos[2]
Marina Rejkuba[2]
Magda Arnaboldi[2]
Monika G. Petr-Gotzens[2]
Michael Hilker[2]
Mike Irwin[3]
Nick Cross[4]

[1] Queen Mary University of London, UK
[2] ESO
[3] Cambridge Astronomical Survey Unit, University of Cambridge, UK
[4] Wide Field Astronomy Unit, Royal Observatory Edinburgh, UK

The VISTA InfraRed CAMera (VIRCAM) at the Visible and Infrared Survey Telescope for Astronomy (VISTA) made its last observation on the night of 5/6 March 2023 after more than a decade of infrared surveys. Its place at VISTA's focal plane is soon to be taken by the 4-metre Multi-Object Spectroscopic Telescope (4MOST) working in the visible region. Here we look back and summarise the experience gained and the great legacy of VIRCAM.

Introduction

The Visible and Infrared Survey Telescope for Astronomy (VISTA) was conceived in the UK and in late 1998 a consortium of UK universities, led by Queen Mary University of London (PI: J. Emerson), successfully applied for funding from the UK's Joint Infrastructure Fund. The original proposal envisaged constructing VISTA, equipped with interchangeable infrared (IR) and visible-light cameras, near Gemini South at Cerro Pachón in Chile. It later became clear that Cerro Paranal, also in Chile, was a better option for the location of VISTA. ESO was originally prepared to host VISTA for the UK university consortium, in exchange for telescope time. As interactions with ESO progressed very well the consortium later agreed that VISTA could became an ESO telescope as part of the UK's in-kind contribution when the UK joined ESO in 2002. This played a key financial role in enabling the UK to realise its long-held wish to join ESO. As the VLT Survey Telescope (VST) was being built for ESO surveys in the visible wavelength regime it was decided to forego the visible camera on VISTA in favour of using funds to fill more of the field of view in the IR camera.

Building VIRCAM

VISTA was designed, at the UK's Astronomy Technology Centre at the Royal Observatory Edinburgh, not as a general purpose telescope, but rather was optimised to host a wide-field near-infrared camera, the VISTA InfraRed CAMera (VIRCAM), operating in the *J*, *H* and *Ks* filters. It turned out that the system response was also good at shorter wavelengths so *Z* and *Y* filters were later added, along with NB118 for the UltraVISTA

Figure 1. VIRCAM insertion into M1 of VISTA.

ultra-deep survey. VIRCAM was built at the Space Science division at the UK's Rutherford Appleton Laboratory (RAL) and arrived at Paranal on 28 January 2007. It is described by Dalton et al. (2010), and, more accessibly along with the telescope, by Emerson et al. (2004) (design) and by Sutherland et al. (2015) (as built).

Although almost everything else was ready to start system integration and testing, the polishing of VISTA's 4-metre primary mirror (M1), in Russia, took very much longer than advertised, mainly because it was the most curved large mirror that had ever been polished. It finally arrived in Paranal on 27 March 2008, during the making of the James Bond movie *A Quantum of Solace*. After the M1 had been coated and installed, the camera was mated to the telescope (Figure 1). The first infrared light for VIRCAM followed on 24 June 2008. Finally the UK team integrating, testing, and commissioning the whole VISTA system could begin its year-long task of dealing with the various issues, mostly mechanical, that arose during testing. Following reviews of the operation of all parts of the system, and closing off all the outstanding actions, the UK team's final task was to ensure that ESO had all the necessary information to successfully operate VISTA.

System verification was carried out by ESO in August–September 2009 and Science Verification between 15 October and 3 November 2009 (Arnaboldi et al., 2010). The first VIRCAM data in the ESO Science Archive are from Science Verification on the night of 15/16 October 2009.

Impact on ESO operations

VISTA's surveys required new observing concepts to be developed for the survey telescopes (Bierwirth et al., 2010). To define the pointings of tiles that create a contiguously surveyed area of the desired shape, and efficiently identify suitable stars for guiding and active optics corrections, the VISTA project developed the Survey Area Definition Tool. This tool was subsequently adapted to enable quick tiling of large areas with the OmegaCAM camera at the VST as well (Arnaboldi et al., 2008). To enable the generation of many hundreds of similar Observation Blocks (OBs) as well as implementing machine-readable observing strategies with concatenated, grouped or time-linked observations, new observation preparation and short-term scheduling tools were developed by ESO (Arnaboldi et al., 2008). These tools, originally implemented on VISTA, were subsequently ported to also support operations at ESO's Very Large Telescope (VLT) and the VLT Interferometer and were further developed, adding programmatic interfaces and new services (Beccari et al., 2022).

Many changes in the day and night operations were implemented to allow on-site operations with only one telescope instrument operator shared between VISTA and the VST. Telescope presets for short observations, such as for the VVV (VISTA Variables in the Via Lactea) survey, which requires six presets in less than five minutes, were then executed automatically. The connection of the scheduler to the atmospheric site monitor enabled further streamlining of survey operations. To do that the scheduler automatically reads ambient conditions and filters executable observations for the current conditions, ranking the OBs such that the most difficult observations that fulfill all the constraints are scheduled first. The top-ranked OB gets automatically pulled and its acquisition starts as soon as the previous OB is executed. On-the-fly automatic analysis of the resulting data allows the telescope instrument operator to assess whether the conditions requested by the PI were met.

VIRCAM created very little work on daytime operations, requiring only a minimum of additional calibrations. The only necessary data taken were some dome flats and a linearity test once a week. Named 'barbecue flats' since they were taken parallel to the weekly barbecue on Sundays, they became a tradition and fixed point in the weekly schedule on Paranal.

VISTA's large data volumes were a strong driver for the installation of a fast fibre data link to Paranal through the EU-funded EVALSO programme. This enabled VISTA's raw data to be shipped to Garching each night over the internet instead of being shipped on hard disks (Comerón et al., 2012).

Observations

VISTA was designed to enable high survey speed in the near-IR and most of its time was dedicated to large-scale public surveys. The Public Survey Panel (PSP), composed of experts from the community, recommended an initial set of six such surveys to the Observing Programmes Committee (OPC), which were then scheduled by ESO for execution: VVV, a multi-purpose, multi-epoch survey of the inner Milky Way; VMC (VISTA near-IR YJKs survey of the Magellanic Clouds system); VHS (the VISTA Hemisphere Survey); VIKING (the VISTA Kilo-degree INfrared Galaxy survey); VIDEO (VISTA Deep Extragalactic Observations); and UltraVISTA, an ultra-deep survey with VISTA. See Arnaboldi et al. (2007) for a brief description.

'Dry run' observations of these public surveys started on 4 November 2009; the survey teams were told that in the first months ESO would be further optimising the instrument and telescope (hence 'dry run'), training staff and implementing operations processes and tools to make efficient survey operations. Nevertheless, it was expected that the time would be used to start advancing the survey observations.

The first night VISTA was operated after being "provisionally accepted by ESO and handed over by STFC to ESO on December 10" was 11 December 2009. The official start of public survey operations was in P85 (April 2010), but effectively several hundreds of hours (per survey) had been observed before then. P85 was the first time VISTA was also offered to the community for shorter 'normal' programmes. Over the years these amounted to around 9% of VISTA time.

In 2015, as the initial set of six public surveys approached its sixth year of operations and some surveys were approaching completion, ESO issued a call for Letters of Intent for the second cycle of public surveys with VIRCAM@VISTA. Following a competitive process with Letters of Intent and then review of proposals by the PSP, the OPC recommended extending VVV (as VVVx) and UltraVISTA and adding five new surveys, as described by Arnaboldi et al. (2017).

The second set of surveys included: GCAV (Galaxy Clusters at VIRCAM), VEILS (VISTA Extragalactic Infrared Legacy Survey), SHARKS (Southern H-ATLAS Regions *K*s-band survey), VISIONS (VISTA Star Formation Atlas), and VINROUGE (VISTA Near infrared Observations Unveiling Gravitational wave Events).

The sky coverage, in any filter, of each survey is shown in Figure 2 which, unsurprisingly, shows that VHS has the greatest coverage by area in both *J* and *Ks*. Other surveys have targeted smaller areas to greater depth and sometimes in more filters, with the UltraVISTA survey going deepest on the smallest area of just one fully covered field of view of VIRCAM.

By the end of VIRCAM operations in March 2023 all public survey observations had been completed.

Data products

VIRCAM was always intended to produce large-scale surveys with continuing archival value. Whilst the *JHK*s 2MASS survey has a much more uniform three-band sky coverage to its (shallower) survey depth, VIRCAM surveys at VISTA go much deeper and have higher image quality. Therefore, for many purposes users may find much more useful data in the VIRCAM archives.

All VIRCAM raw data are in the ESO archive and were also automatically transferred to the Cambridge Astronomical Survey Unit (CASU). At CASU a pipeline reduced and calibrated all VIRCAM data, both for public surveys and any other observations, using all the knowledge gained from processing all data produced by the instrument. This pipeline was developed by CASU's Jim Lewis who also delivered and maintained a version based on ESO's Common Pipeline Library for ESO's VIRCAM Quality Control and health monitoring process. The calibration method is described by González-Fernández et al. (2018). The reduced calibrated data were routinely

Figure 2. VIRCAM public surveys coverage (any filter) in Aitoff projection. For a breakdown of coverage by filter, or for a different projection, see CASU's survey progress page[1] or the ESO Science Archive[3].

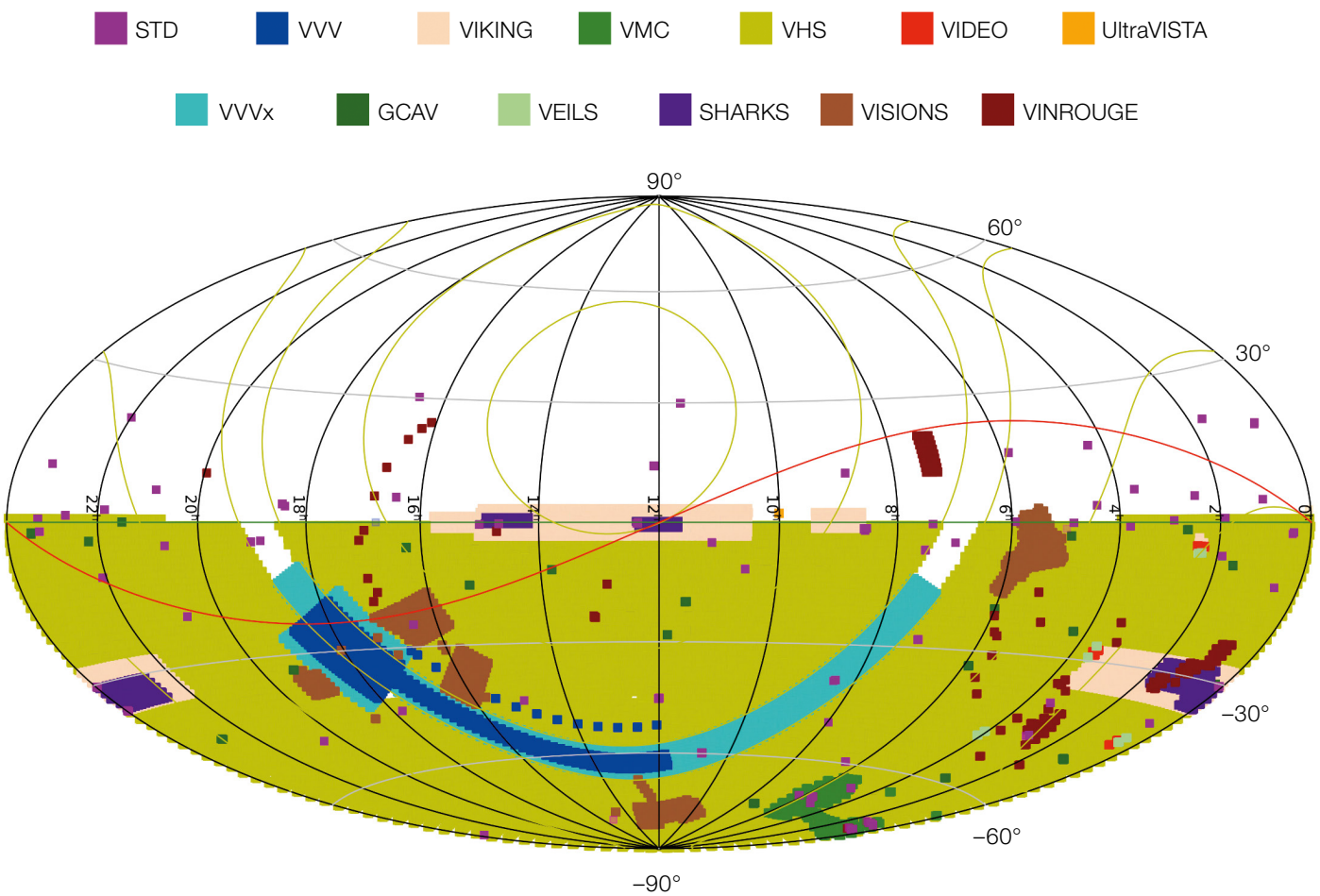

Observing dates: 20091015–20230305
Cambridge Astronomy Survey Unit

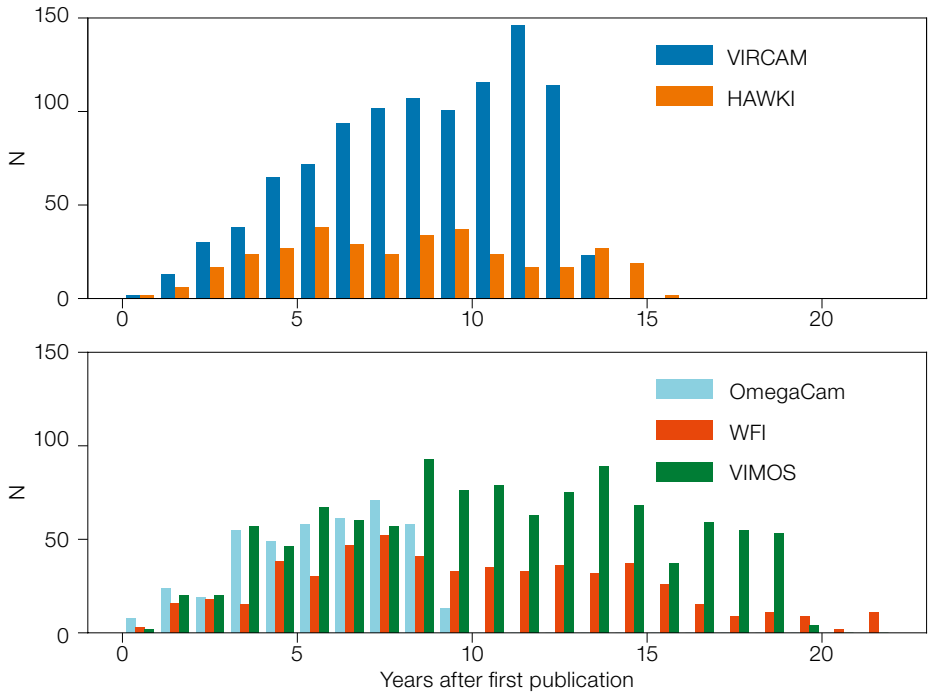

Figure 3. VIRCAM's publication history compared with another ESO IR imager (upper) and some visible wide-field cameras (lower).

uploaded to the VISTA Science Archive (VSA)[2] at the Wide Field Astronomy Unit at the Royal Observatory Edinburgh where it is archived. The VSA worked with five of the six first-generation VISTA surveys to help deliver their data products to ESO's Science Archive[3], and also to external archive sites like VizieR[4]. ESO's list of public VISTA survey data releases[5] is the route to finding reduced observations, and in some cases object catalogues, to download. UltraVISTA and some of the second-generation public surveys have done their own data processing.

The final images and catalogues for the public surveys can be downloaded by users from the ESO archives and the VISTA science archive.

Although all the VIRCAM public surveys have finished taking data, several of the teams are continuing to work on the data releases. Thus, although raw data are publicly available immediately, more and more data products, including higher-level catalogues are becoming available in the ESO archive.

Subject to resource availability, calibrated images and catalogues may be provided for individual VISTA pawprints and tiles not included in the public survey releases, on request to casuhelp@ast.cam.ac.uk or vsa-support@roe.ac.uk

Publications

At the time of writing there are 1029 refereed publications using VISTA data in the ESO Telescope Bibliography system[6] Most come from the original six public surveys with two having over 250 publications each (VVV 316, UltraVISTA 266). Figure 3 shows that the annual number of publications (N) from VIRCAM compares well with those from related ESO imaging instruments. The most cited VIRCAM paper, with nearly 800 citations, is by Minniti et al. (2010), describing the VVV survey.

The future

ESO is organising a workshop entitled A Decade of ESO Wide-field Imaging Surveys[7] from 16 to 20 October 2023 with invited talks covering all VISTA (and VST) public surveys, which will further explore the legacy of VIRCAM.

VIRCAM is soon to be replaced by the 4-metre Multi-Object Spectroscopic Telescope (4MOST; de Jong et al., 2019). For now, VIRCAM is kept as a backup instrument for VISTA, but once 4MOST is in full operation, it is hoped that VIRCAM will become its own legacy and will be put on display for visitors to Paranal, showcasing and highlighting large-scale surveys, which form an important part of astronomy research these days and are often forgotten about at a time when many telescopes concentrate on more detailed views of galaxies/objects, with small fields of view.

VIRCAM has been a great success and the legacy of its infrared imaging data will continue to be mined for many years. 4MOST will finally deliver the V in VISTA's name and is shaping up to make a big impact (see articles in The Messenger 175 and 190).

References

Arnaboldi, M. et al. 2007, The Messenger, 127, 28
Arnaboldi, M. et al. 2008, The Messenger, 134, 42
Arnaboldi, M. et al. 2010, The Messenger, 139, 6
Arnaboldi, M. et al. 2017, The Messenger, 168, 15
Beccari, G. et al. 2022, Proc. SPIE, 12186, 121860N
Bierwirth, T. et al. 2010, Proc. SPIE, 7737, 77370W
Comerón, F. et al. 2012, The Messenger, 147, 2
Dalton, G. B. et al. 2010, Proc. SPIE, 7735, 77351J
Emerson, J. et al. 2004, The Messenger, 117, 27
de Jong, R. S. et al. 2019, The Messenger, 175, 3
González-Fernández, C. et al. 2018, MNRAS, 474, 5459
Minniti, D. et al. 2010, New Ast., 15, 433
Sutherland, W. et al. 2015, A&A, 575, A25

Links

[1] VISTA public surveys progress: http://casu.ast.cam.ac.uk/vistasp/overview
[2] VISTA Science Archive: http://vsa.roe.ac.uk
[3] ESO Science Archive: http://archive.eso.org/scienceportal/home
[4] VizieR archive: https://cdsarc.u-strasbg.fr/
[5] Overview of Phase 3 data Releases: www.eso.org/rm/publicAccess#/dataReleases
[6] ESO Telescope Bibliography: https://telbib.eso.org
[7] A Decade of ESO Wide-field Imaging Surveys workshop: https://www.eso.org/sci/meetings/2023/surveys.html

This image shows Aurélio Barrera, a staff member at APEX, appearing to embrace the Milky Way as it arches above the Atacama desert.

The spectacular dark skies at the APEX site allow unsurpassed astronomical observations, and permit such stunning details of the Chilean night sky to be photographed.

DOI: 10.18727/0722-6691/5342

Celebrating 25 Years of Remarkable Science and Engineering with the VLT

Itziar de Gregorio-Monsalvo[1]
Michael Hilker[1]
Bruno Leibundgut[1]

[1] ESO

Twenty-five years ago, on 25 May 1998, a significant milestone was reached for ESO and for European astronomy as the Very Large Telescope (VLT) captured its first images. On the occasion of its first light, the 8-metre Unit Telescope UT1 offered impressive images of our Universe. These included a successful tracking test in the globular cluster Omega Centauri, detailed images of the central region of another globular cluster, Messier 4, the fine structure of the Butterfly Nebula, high-velocity ejecta near Eta Carinae, and a captivating picture showcasing stars, dust, and gas in Centaurus A.

Over the past 25 years the VLT has made an extensive and outstanding contribution to scientific research. More than 10 000 scientific publications have been published to date, utilising data collected from these telescopes. The VLT facility has been continuously developed, with the addition of new instruments, the combination of the unit telescopes to form a powerful interferometer, the addition of adaptive optics with lasers and the expansion of the end-to-end operations model. All VLT data are available through the ESO Science Archive Facility. Several remarkable scientific achievements have been recognised with two Nobel prizes. The VLT's exceptional instrumentation played a crucial role in establishing the accelerated expansion of the Universe and confirming the existence of a compact object at the centre of our own Galaxy. Additionally, the VLT achieved the groundbreaking feat of capturing the first direct image of an exoplanet and it has significantly contributed to our understanding of the diverse architectures of exoplanetary systems.

As part of the commemorative activities to acknowledge the construction of the VLT, on 4 December 1996 President Eduardo Frei Ruiz-Tagle of the Republic of Chile deposited a time capsule within the walls of VLT Enclosure 1 (Giacconi, 1997). This capsule, filled with nitrogen gas and hermetically sealed, contained outstanding scientific papers from every ESO member state, the host country Chile, and ESO itself, intended to be preserved for an extended period[1].

To celebrate the 25th anniversary[2] of this significant moment for ESO and the VLT the Offices for Science in Chile and Germany organised an internal event on 26 May 2023, inviting all ESO staff. This event aimed to reflect on the remarkable achievements of the VLT in scientific, technical, operational, logistic, and human aspects throughout these two and a half decades of teamwork. For this occasion, a group of ESO Students and Fellows on both sides of the Atlantic teamed up with ESO staff astronomers and science visitors to present the evolution and state of the art of nine different science topics included in the time capsule: the Galactic centre, exoplanets, degenerate stars, distant supernovae, microlensing, chemical evolution of the Galactic disc, galactic X-ray sources, gravitational lensing and nearby radio galaxies.

In addition, experts in lasers and adaptive optics provided a historical summary of, and a forward look at, one of the most significant technical achievements at the VLT. Live presentations were given from Vitacura, Paranal and Garching on the achievements and current status of VLT Science Operations and Data Flow, respectively. The event commenced with a brief summary of the historical first-light event by the ESO VLT Programme Scientist, the current ESO Director for Science Bruno Leibundgut. The closing remarks from the Director General Xavier Barcons highlighted the significance of the VLT and its leadership position in the context of international astronomy. He emphasised the human aspect, the contribution of logistics and administration, the international cooperation needed to make the programme a reality, the operational model, data flow, technical development, cutting-edge instrumentation, and continuous updates that have made

Figure 1. A lot can change in more than two decades — just take a look at these pictures of ESO's Very Large Telescope (VLT)! On the left we see the VLT when it was still under construction atop Cerro Paranal in Chile, while on the right we see it in all its glory as it stands today.

the VLT one of the most productive telescopes on Earth.

The VLT's remarkable contribution to science through superb instruments

More than three decades ago the discovery of the first Type Ia supernova at high redshift (z = 0.31) with the Danish 1.5-metre telescope on La Silla was reported in the journal Nature. These supernovae, identified as standard candles for estimating cosmological distances, have been extensively studied with the VLT. In 2011 the Nobel Prize in Physics was awarded "*for the discovery of the accelerating expansion of the Universe through observations of distant supernovae,*" in which the 8.2-metre VLT telescopes at Paranal, the 3.6-metre and the New Technology Telescope (NTT) on La Silla and ESO staff played a major role.

Observations of the proper motions of stars near the centre of the Milky Way have provided evidence in recent decades for the existence of a supermassive black hole at the Galactic centre. Over the course of 26 years, observations carried out with sensitive instruments at the NTT at La Silla and at Paranal, such as the Nasmyth Adaptive Optics System – COudé Near-Infrared CAmera combination (NAOS–CONICA, or NACO) and the Spectrograph for INtegral Field Observations in the Near-Infrared (SINFONI) at the VLT, and the GRAVITY instrument at the VLT Interferometer, contributed significantly to the Nobel Prize in Physics in 2020. These observations, including 16 years of tracking stars orbiting Sagittarius A*, provided empirical evidence for the existence of the supermassive black hole at the centre of our galaxy. GRAVITY has been fundamental in studying at high-precision orbits of stars near Sagittarius A* and testing general relativity, providing images 20 times sharper than those from individual VLT telescopes.

The VLT has played a leading role in the direct detection and characterisation of exoplanets. In 2004 the adaptive optics-supported NACO facility provided the first image of a planet outside our Solar System. To date more than 5000 exoplanets have been discovered and there are over 4000 known planetary systems.

Figure 2. This splendid colour image of a famous southern Planetary Nebula, NGC 6302 or the Bug Nebula (sometimes nicknamed the Butterfly Nebula), was obtained by combining blue, yellow and red images obtained on May 22, 1998, with 10 minute exposures and an image quality better than 0.6 arcseconds.

Instruments like the Spectro-Polarimetric High-contrast Exoplanet REsearch instrument (SPHERE) have revealed a variety of exoplanet architectures, including the first-ever image of two planets orbiting a Sun-like star. The new Echelle SPectrograph for Rocky Exoplanet and Stable Spectroscopic Observations (ESPRESSO) instrument is focused on determining the composition of exoplanet atmospheres, paving the way for future studies with ESO's Extremely Large Telescope (ELT). The combined capabilities of the VLT and the Atacama Large Millimeter/submillimeter Array (ALMA), in which ESO is a partner, and the forthcoming ELT, will make ESO a unique observatory with the ability to study the formation and evolution of planets and their atmospheres in unprecedented detail.

Entering the era of gravitational wave astronomy, multi-epoch data from the Fibre Large Array Multi Element Spectrograph (FLAMES) enabled the discovery of a stellar-mass black hole in the Large Magellanic Cloud. In 2017 ESO's telescopes, including the VLT, characterised the first visible counterpart of a gravitational wave source.

Advanced engineering systems: adaptive optics and laser guides at the VLT

The technology of the VLT has been continuously adapted and improved. The VLT Interferometer employs larger individual telescopes than any such instrument anywhere in the world and combines the light from them better. New instruments have provided new observing capabilities and the facility has grown to include adaptive optics with natural guide stars and artificial stars created by powerful laser beams.

ESO has remained at the forefront of adaptive optics and laser guide star technologies in astronomy for the past three decades. The adaptive optics technique plays a crucial role in correcting the distortions introduced by atmospheric turbulence in real time, rapidly adapting the mirror shape to counteract the blurring effect caused by the atmosphere. To achieve this, a bright star close to the astronomical target is required as a reference. However, such bright stars may not always be available in the vicinity, necessitating the creation of 'artificial' stars using lasers.

By exciting sodium atoms in the mesosphere, approximately 90 kilometres above Earth's surface, lasers generate artificial stars. Initial experiments in this area commenced in 1998, with the first light of the single laser guide star in UT4 in 2006. In 2016 the VLT further enhanced its Adaptive Optics Facility by installing the 4 Laser Guide Star Facility, each laser producing 22 Watts of power. This cutting-edge facility will serve as a crucial testbed for the ELT, which represents ESO's next major astronomical endeavour and which is already halfway through its completion process.

Operations model and end-to-end data flow

Science operations have played a crucial role in the success of the VLT. Over 25 years the facilities have continuously evolved, requiring the management of three different generations of instruments at the observatory, all adhering to the highest standards. As complexity has increased over time, science operations have adapted to new needs and circumstances, including the challenges posed by the COVID-19 outbreak, which led to the only long-term suspension of science operations at Paranal in 25 years.

The VLT Data Flow System effectively manages the complexity of handling multiple instruments and observing modes. This closed-loop software system consists of various subsystems that ensure a smooth flow of data, from proposal submission by scientists all the way to the final storage of the collected data in the ESO Science Archive Facility.

The remarkable achievements of the VLT over the past 25 years were the result of the team spirit, dedication, and international collaboration at ESO. Together, we have pushed the boundaries of astronomical exploration. As we look to the future with the construction of the ELT, the enhancement and future development of ALMA and another suite of new instruments for the VLT, exciting times lie ahead, which will ensure the success of ESO as a world-leading observatory.

References

Giacconi, R. 1997, The Messenger 87, 1

Links

[1] ESO Time Capsule Press Release: https://www.eso.org/public/news/eso9710/
[2] VLT 25th anniversary Announcement: https://www.eso.org/public/announcements/ann23009/

This photograph captures the Unit Telescope 4 of ESO's Very Large Telescope, located in Chile's Atacama Desert, and its four-laser system, which is used to excite sodium atoms in the atmosphere. The atoms excited by the lasers emit light that is affected by the atmosphere in the same way as the light emitted by real stars. The emitted light is collected by the telescope and can be used by the adaptive-optics system to measure the distortions introduced by the atmosphere and then to correct for them. This advanced system, combined with the excellent dark-sky conditions of the Atacama Desert, ensure the telescope can obtain extremely sharp images.

DOI: 10.18727/0722-6691/5343

Report on the ESO workshop

VLTI and ALMA Synthesis Imaging Workshop

held at ESO Headquarters, Garching, Germany, 9–12 January 2023

Fabrizia Guglielmetti[1]
Antoine Mérand[1]
Markus Wittkowski[1]
Lukasz Tychoniec[1]
Gemma González-Torà[1]
Martin A. Zwaan[1]
Paola Andreani[1]
Carlos De Breuck[1]

[1] ESO

Supported by the EU-funded Opticon RadioNet Pilot (ORP), the VLTI and ALMA Synthesis Imaging Workshop was held at ESO Headquarters on 9–12 January 2023. The hybrid format of the workshop allowed one hundred registered participants from six continents to gather, bringing with them a wide range of expertise: theorists, observers and data scientists. The need for such a broad range of skills originates in the workshop's focus on interferometric image-reconstruction algorithms applied to data from instruments across the optical/infrared and millimetre/radio domain, allowing the diverse communities to build synergies and explore innovative techniques applicable to both regimes. The three-day workshop was organised into six topics, each followed by discussion. Four distinguished lecturers established a shared understanding of data analysis processes (including data characteristics, handling and reduction) and presented innovative techniques employing artificial intelligence used by the two communities. Traditional imaging methods, as well as techniques for morphology fitting and other popular tools and methods, were presented and discussed by keynote speakers. Given the nature and goals of the workshop, most of the speakers were invited. ORP supported a number of speakers as well as students to allow growth within a young community in the rapidly evolving area of image analysis.

Motivation

The Very Large Telescope Interferometer[1] (VLTI) and the Atacama Large Millimeter/submillimeter Array[2] (ALMA) are two leading facilities employing synthesis imaging. Their data require extensive processing and analysis to align and combine the signals from multiple telescopes so as to produce high-quality images. Both observatories deliver high-resolution imaging of celestial objects and multi-wavelength observations. VLTI and ALMA data alone have provided breakthroughs in astronomy, widening our knowledge of the Universe in regards to several hot topics, such as the formation of stars and extra-solar planets, the distribution of molecular gas in the Universe, the evolution of galaxies, and the high-redshift Universe. Over the past five years interest has grown within the scientific community in employing VLTI and ALMA data to derive high-impact results (for example, Bohn et al., 2022).

Because of the low information content of interferometric data, the generation of images is a complicated and, in some cases, poorly defined procedure. VLTI images are typically reconstructed by minimising a cost function that includes both the data and some prior information on the object brightness distribution. ALMA data are characterised by a higher sampling of the uv plane compared to the VLTI, given the larger number of interferometric elements. ALMA's strategic design and location and its ability to track phases more accurately than the VLTI allow for a higher information content in the images. Nonetheless, images are reconstructed by converting the calibrated visibility data, often with iterative deconvolution algorithms to remove artefacts and to enhance the resolution of the final image. Challenges in image deconvolution include preventing thresholding in the deconvolution algorithm, continuum subtraction, the detection and deconvolution of extended emission, separating point-like sources from diffuse emission, and weak signal detection.

The VLTI and ALMA Synthesis Imaging Workshop[3] emphasised strengthening the links between the optical/infrared and radio/millimetre communities, with the aim of improving and exploring algorithms which allow imaging enhancements in both wavelength regimes, and which can be applied to multiple facilities. With this scope, sessions were structured around subject areas, including image deconvolution and enhancement, artificial intelligence, astrophysical parameter estimation and feature extraction, data visualisation and exploration, analysis and interpretation. It is worth mentioning that assessing the quality of the images is highly relevant to bench-marking image reconstruction algorithms. However, so far no systematic studies have been conducted on the selection of a robust metric for quality assessment, and no studies have been conducted that include similar algorithms applied to both optical/infrared and radio/millimetre data sets.

In the optical/infrared regime, experience of using Bayesian imaging techniques has been accumulated (for example, Buscher, 1994; Baron, Monnier & Kloppenborg, 2010; and see Thiébaut & Young, 2017 for a review), and they are now routinely applied. In the radio/millimetre, only the maximum entropy method of Cornwell & Evans (1985) has been employed within the 'tclean' task in the Common Astronomy Software Applications package (CASA; Casa Team et al., 2022). Other Bayesian estimation methods for imaging are advancing, and some packages based on artificial intelligence applied to ALMA (for example, Di Mascolo et al., 2023; Delli Veneri et al., 2023; Tychoniec et al., 2022) show promising results and are suited to the new generation of ALMA (Guglielmetti et al., 2022). One of the goals of this workshop was to explore the usability of such techniques in situations with very sparse sampling of spatial frequencies (for example, Arras et al., 2022), which is typically the case with optical interferometry observations, but also extends to the radio and millimetre, where the challenges lie mostly in reaching a high image dynamic range. In addition, developing procedures for speeding up the deconvolution algorithm is essential, especially for future facilities such as the Square Kilometre Array (Dewdney, 2009) and the forthcoming ALMA upgrade (Carpenter et al., 2023).

The objectives of the workshop were met. Collaboration was fostered among communities addressing similar problems and employing similar techniques, yet having limited practical overlap. The exchange of recent technical and scientific advances was facilitated, promoting knowledge-sharing and cross-pollination of ideas. Lively discussions about collaborative

initiatives were encouraged, leading to the identification of opportunities for joint efforts and endeavours. The groundwork for collaborative progress and mutual benefit in the field of synthesis imaging was laid and algorithms applicable to both regimes were identified.

Introduction to the VLTI and ALMA

The VLTI and ALMA observe in the wavelength ranges of about 0.002–0.013 millimetres and 0.3–8.6 millimetres, respectively.

The VLTI is composed of four 8.2-metre Unit Telescopes, supplemented by 1.8-metre movable Auxiliary Telescopes, at Paranal Observatory. The maximum distance (baseline) achievable by the Unit Telescopes is about 130 metres, while the Auxiliary Telescopes support a 200-metre longest baseline. These longest baselines allow us to detect astronomical objects with milliarcsecond resolution. The fields of view of the Unit and Auxiliary Telescopes are 30 arcminutes and 4 arcseconds, respectively. Adaptive optics technology is used to correct for atmospheric distortions, resulting in clearer and sharper images.

ALMA is equipped with 54 12-metre and 12 7-metre antennas located on the Chajnantor plateau in the Atacama Desert. The plateau has an extension of about 10 square kilometres, and the 12-metre antennas are sited on 'pads' — individual antenna stations that provide power, signal and network connection in addition to a stable foundation — such that they can be moved into different configurations. The dimensions of the most extended and most compact configurations are 16 kilometres and 160 metres, respectively. The longest baseline allows a resolution as sharp as 20 milliarcseconds to be achieved at a wavelength of 1.3 millimetres. The fields of view of the 12-metre and the 7-metre antennas are about 19 arcseconds and 33 arcseconds, respectively, at a wavelength of 1 millimetre. Mosaicking is used to achieve uniform sensitivity over larger regions. Atmospheric distortions are calibrated with water vapour radiometers that measure the amount of water in the line of sight, and a technique known as fast-switching phase referencing to mitigate the atmospheric phase fluctuations (atmospheric phase correction).

Complexities of image analysis

According to the Rayleigh criterion, the angular resolution, θ, of an imaging system (i.e., its ability to distinguish objects on the sky separated by some angular distance) is directly proportional to the observed wavelength (λ) and inversely to the antenna's diameter (D), such that $\theta \sim 1.22\ \lambda/D$. Therefore, for a given telescope size, higher resolutions are obtained in the optical/infrared regime than at millimetre/radio wavelengths. To obtain images at higher angular resolution, signals from several telescopes are

J.L. Dauvergne & G. Hüdepohl (atacamaphoto.com)/ESO

Figure 1. The VLTI is located on top of Cerro Paranal, in the Chilean Atacama Desert. The 8.2-metre UTs are visible at the image centre. On the right of the UTs, the 1.8-metre ATs are in their characteristic spherical dome shells. The ATs are movable and can be relocated on 30 different observing stations. To perform interferometry, the signals from the several telescopes are combined with varying array configuration and number of telescopes.

combined through interferometry, emulating a telescope with a larger diameter (aperture synthesis). Coherence theory, i.e. a statistical description of the electromagnetic radiation, is used to analyse the degree of correlation between pairs of measurements. Note that for N telescopes, there are N(N–1)/2 of those measurements, one for each baseline. The spatial coherence (correlation) of the signals illuminating telescope pairs is given by the van Cittert–Zernike theorem that provides a relation between the sky brightness and the spatial coherence function. Specifically, the geometrical (or time) delay of the signals from the pair of antennas is compensated for before reaching the correlator using a technique known as delay tracking. The correlator is a device capable of multiplying together the signal voltages produced by the antennas and time-averaging the signal, thereby producing the interferometer fringe pattern. The correlator output is proportional to the complex visibility function, which is the Fourier transform of the sky brightness integrated over the sky. Calibration procedures are applied to estimate the complex amplitude of the visibility function, which contains both the amplitude and the phase information of the correlation between the antennas. The amplitude of the complex visibilities is proportional to the brightness of the object being observed, while the phase is related to the position of the object in the sky. In the main, point sources of known flux density and position are used during the observation to allow the determination of the instrumental parameters for calibrating the visibility measurements.

Since the van Cittert–Zernike theorem provides the mathematical relationship between the detected complex visibility and the brightness distribution of the celestial source, this pivotal theorem forms the basis of Fourier synthesis imaging. It uses the inverse Fourier transform of the calibrated complex visibilities (in units of Jy, in the case of ALMA) to produce an image of the source brightness distribution (flux density per unit solid angle, or beam volume in the case of ALMA). An array of several antennas (or telescopes) measures the visibility function for each baseline. The sampling of the visibility function is limited by the number of antennas or telescopes, the observing time and the pervasive presence of noise in the measurements[a]. The inverse Fourier transform of the sampled (and noisy) visibility function provides an image I^D (the dirty image) that is corrupted by the instrumental point spread function, known as the dirty beam[b]. The sky brightness distribution, which is affected by the antenna’s primary beam, can theoretically be obtained by deconvolving I^D from the dirty beam. However, to control image formation, the sampling function is traditionally (density) weighted and tapered to constrain the shape of the dirty beam. While tapering implies smoothly weighting down the highest spatial frequencies to suppress sidelobe effects, the density weigthing is employed, for example, to optimise the density

Alma Observatory, Guy Wenborn

Figure 2. ALMA is located on the Chajnantor Plateau in Chile’s Atacama Desert. At the bottom-center of the image, one can see a set of the fifty-four 12-m atennas. To the left, in the bottom-center, the Atacama Compact Array (ACA) is composed of twelve 7-m antennas and four 12-m antennas. Triangular antenna stations are visible in the image. Each of the 192 available stations can house an antenna, allowing for several array configurations.

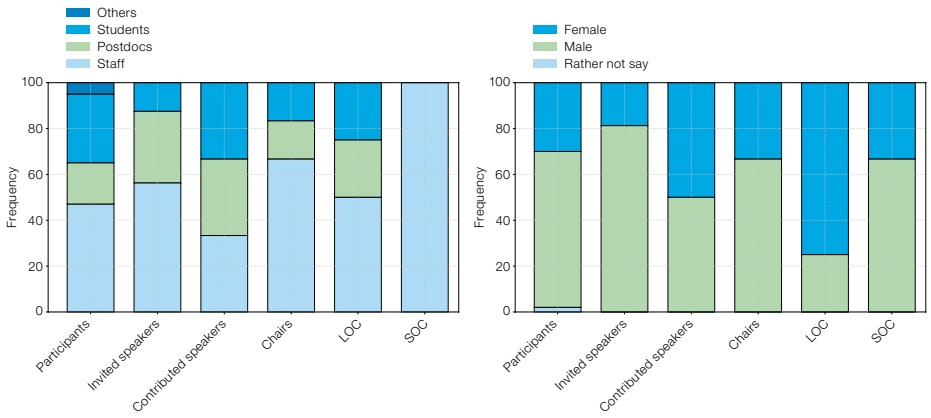

Figure 3. Demographic distributions of the career stage (left) and gender (right) between participants, invited and contributed speakers, Chairs, LOC and SOC.

of sparse sampling (long baselines) with respect to the dense sampling at the short baselines contributing to I^D. This uniform weighting scheme allows one to achieve an improved angular resolution compared to employing no density weights (a natural weighting scheme). Often tapering occurs at schemes in between these two extremes. Gridding is frequently used to calculate I^D as discrete representations in image pixels. The visibility measurements (sampled and weighted) are interpolated to a regular grid employing the Fast Fourier Transform algorithm, providing an estimate of I^D (the dirty map). The ill-posed problem in image reconstruction is summarised by the measurement equation $\tilde{I}^D = B * I + n$, where B, I and n are the dirty beam, the true sky representation and the additional noise, respectively. Additional imaging intricacies include, for example, the heterogeneous sensitivity of the instruments to point sources and extended emissions, chromatic aberration, azimuthal smearing, and position-shift as a result of distortion across the field of view.

Sparse sampling complicates the imaging process because of gaps in the visibility measurements. For this reason, VLTI measured visibilities are used to derive closure phases, combinations of phase differences between three or more telescope elements of the array. The closure phases are used as constraints in the image reconstruction process with the aim of improving image accuracy and quality. The interpretation of aperture synthesis data is a complex process, in which the uncertainties associated with image reconstruction are always present. Sparse sampling, instrumental responses and the pervasive presence of noise affect the data. The inverse problem of extracting astrophysically interesting information from the observed sky brightness is ill-posed, in the sense that the solution is not unique, or is not stable under perturbations in the data. Perturbation caused by noise can create large deviations in the solution being sought.

Major theme

On the first day of the workshop, proceedings were led by two keynote speakers, Urvashi Rao Venkata and Jean-Philippe Berger, who delivered an extensive retrospective of image reconstruction methods. Their presentations aimed to foster mutual understanding and facilitate the development of expertise in synthesis imaging within the two communities.

Because of the significant influence this groundbreaking research and its developments have had on various scientific domains, artificial intelligence was allocated two specialised sessions. Each of these sessions commenced with a keynote introductory talk aimed at offering a comprehensive grasp of machine learning and information field theory. Both Giuseppe Longo and Torsten Enßlin demonstrated the evolution of the field over the past decade and emphasised the importance of developing data scientists as an invaluable and essential resource for addressing contemporary astronomical challenges. Further themes included traditional reconstruction methods, advanced statistical methodologies, model fitting and tools at the interface between the data and imaging.

Half-day sessions comprised talks followed by 30–60-minute moderated discussions that all participants were invited to contribute to. The participants engaged in a hybrid format, and a dedicated Slack workspace facilitated further discussions, exchanges of ideas, and sharing of material. Synergies between different teams were forged and plans for collaborative surveys were developed.

Summaries of talks and highlights from sessions

Five sessions were organised over three days on a comprehensive range of topics.

Machine learning (ML) applications on the VLTI and ALMA were shown to successfully reconstruct high-resolution images from sparse and incomplete measurements. The CASSINI-Automap technique exploits the compressibility of a signal with neural networks. The networks are designed with adaptive activation functions to find an optimal mapping system between the infrared interferometric data and the reconstructed images. The ORGANIC method utilises generative adversarial networks for the reconstruction of objects from VLTI data. This class of deep learning models is used to learn the underlying distribution of the object being imaged from the interferometric data, while an input astrophysical prior is used for regularisation. DeepFocus is a high-performance and deep-learning pipeline, whose strength is shown when applied to ALMA cubes. By integrating images captured at different frequencies, DeepFocus effectively speeds up the deconvolution process and performs source detection and characterisation. It is capable of obtaining sharper and more detailed images of objects at different spatial frequencies. The ML algorithms have the potential to enhance the quality and fidelity of object reconstruction in interferometric imaging, enabling better understanding and analysis of astronomical data.

ML was shown to be used mostly as a supervised algorithm to infuse knowledge of the astrophysical object into the image reconstruction using mainly synthetic datasets generated from astrophysical simulations. A striking advantage resides in the increase in computation speed with respect to other methods.

Following this session, participants delved into traditional imaging techniques along with the latest developments in these historical methods: POLCA, OImaging, CASA, GILDAS, SQUEEZE are well-established numerical methods and integrated into user-friendly tools. Aspects of these techniques have been found to have usability in both regimes and to allow for the sharing of information and knowledge between communities, as OImaging can be customised for the use of ALMA, opening the doors for further implementations with other algorithms.

The subsequent half-day was specifically allocated to model fitting, an image reconstruction approach tailored for highly sparse data. During this session, various forward modelling algorithms were discussed, including PMOIRED, uvmultifit, RHAPSODY, and other techniques designed to address the challenges posed by interferometric data. These methodologies enable precise fitting of models to the data, offering valuable insights and enhanced reconstruction capabilities for sparse datasets. Also in this case, discussions revealed the potential for algorithms applicable to both observatories. The remaining day was fully reserved for information field theory (IFT), an artificial intelligence methodology to recover field-like quantities from finite and noisy data. IFT is based on Bayesian inference in the context of field theory. The Numerical Information Field Theory (NIFTy) library was shown to be a powerful computational tool, designed to handle and analyse numerical data within the IFT framework. This valuable resource provides a comprehensive set of functionalities to enable signal processing, including data manipulation, numerical operations, and advanced statistical modelling. Several presentations followed, on a large variety of applications: VLBI, ALMA, GRAVITY and direction- and time-dependent self-calibration. IFT came out as a strong candidate for a general algorithm applicable to VLTI and ALMA data.

The last day session was dedicated to popular tools (such as TP2VIS) and new methods. The TP2VIS software package is designed to effectively merge and analyse data from different observational techniques to achieve a more comprehensive view of astronomical sources. A very interesting assessment of imaging quality and parametric modelling for ALMA data showed valuable insights for VLTI data as well. The workshop concluded with applications of advanced statistical techniques to ALMA data. In a serendipitous search of high-*z* quasars in ALMA cubes, multiple algorithms are used and evaluated to detect and differentiate faint spectral lines employing a blind search technique. Moreover, the use of SupReMo enables the study of the early evolution of galaxy clusters using sparse data; supported by multiwavelength observations, SupReMo reconstructs the cluster properties, such as mass, velocity dispersion, and density profile, with the goal of improving our understanding of cluster evolution. Lastly, a regularised maximum likelihood approach to continuum data highlighted the significance of employing Graphics Processing Unit (GPU) for ALMA image deconvolution. The advancement of machine learning has played a pivotal role in fostering the development and applications of GPUs in astronomical data analysis. GPUs are known to improve the speed of image processing thanks to their performance in several concurrent calculations and to memory optimisation when handling large datasets. The first published application of GPUs on ALMA imaging is from Delli Veneri et al., 2023. The application of GPUs to VLTI data for image reconstruction is not a novelty (see Baron & Kloppenborg, 2010).

Main conclusions and ways forward

The workshop was successful in bringing together two communities working on related topics, but with few connections. The meeting exposed some methods used by one community which could be used by the other, with artificial intelligence techniques playing a significant role. For instance, regularised maximum likelihood has been used for 20 years in optical interferometric image reconstruction and provided popular imaging tools in multi-wavelength astronomy. During the workshop, an efficient regularised maximum likelihood approach applied to ALMA continuum observations was presented. The technique made use of GPUs for fast image reconstruction. Prior information

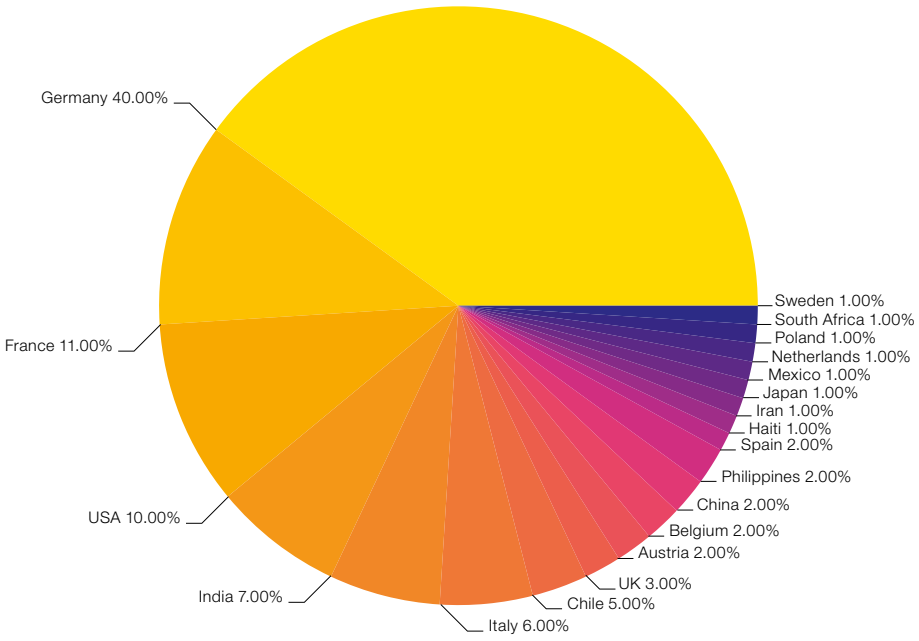

Figure 4. Geographical representation of attendees, highlighting the international diversity of the conference.

Figure 5. Participants at the VLTI and ALMA Synthesis Imaging workshop.

was incorporated in the image reconstruction process as a regularisation term to improve quality and reliability. The maximum likelihood approach has the advantage of providing a point estimate and its uncertainty, but in a parameter space of moderate size. Conversely, IFT (a Bayesian based technique) has the advantage of expanding the solution to a multi-dimensional parameter space and it is applicable to large data volumes. IFT computes the volume under the estimated parameters from which the covariance matrix is estimated to provide a robust uncertainty quantification. The IFT approach has been successful in radio imaging and can potentially be applied to optical data. Dissemination of ideas and methods can be achieved by fostering data format unification or developing data converters. These efforts would streamline the exchange of reference datasets and enable straightforward comparison of results. The advent of machine learning techniques requires large learning and control datasets and having fewer data formats ensures that datasets can be re-used in that context. Fewer data formats also make sure data challenges can be easily organised.

Demographics

The Scientific Organising Committee aimed at having a fair representation from the two communities in terms of speakers and genders, as well as including a wide range of techniques and research methodologies developed for aperture synthesis and their impact on scientific results. The cross-disciplinary programme was designed to combine insights and expertise from different communities to address the complex problem of image analysis and explore new paths to generate innovative solutions. For each of the six sessions, a reviewer led the discussions to promote a climate of creative collaboration and to support open-minded exploration of ideas. A well-balanced participation, including senior scientists, postdocs and students, was designed. Female participation and contributions reflected the overall demographic of the field — 31% of the participants, 20% of invited speakers, 30% of session chairpersons — and the distribution of speakers between young researchers, postdocs and staff was well balanced (see Figure 3). The attendees exhibited a diverse demographic composition, spanning five continents, with the following percentages (see Figure 4):

– 69% Europe (Germany, France, Italy, UK, Austria, Belgium, Spain, the Netherlands, Poland, Sweden)
– 13% Asia (India, Japan, Iran, China, Philippines)
– 12% North America (US, Haiti, Mexico)
– 5% South America (Chile)
– 1% Africa (South Africa)

The workshop had a high level of participation during each session, with 100 participants in total (Figure 5). Most of the in-person participants came from European countries, the extremes overall being 40% from Germany and 1% from Japan. The workshop was held in the second week of January, limiting face-to-face international participation. However, the hybrid format of the workshop allowed for a level of global participation that enriched the overall discussion and networking opportunities. We attribute this success both to the compelling nature of the subject matter, which draws researchers at all career stages, and to the generous support that kept the cost of attendance relatively low.

Acknowledgements

We wholeheartedly thank Elena Zuffanelli and Nelma Silva for their invaluable support and dedication to making this a successful workshop. We are grateful to Michiel Hogerheijde (Leiden Observatory) for his key contribution and insight as chair on key discussion sessions. Last but not least, it is a great pleasure to thank Michele Delli Veneri (INAF) for setting up the Slack workspace, allowing for many fruitful discussions. This event received funding from the European Union's Horizon 2020 research and innovation programme under grant agreement No 101004719 [ORP].

References

Arras, P. et al. 2022, Nature Astronomy, 6, 259
Baron, F. & Kloppenborg, B. 2010, Proc. SPIE, 7734, 7734D
Baron, F., Monnier, J. D. & Kloppenborg, B. 2010, Proc. SPIE, 7734, 77342I
Bohn, A. J. et al. 2022, A&A, 658, A183
Buscher, D. F. 1994, IAUS, 158, 91
CASA Team et al. 2022, PASP, 134, 114501
Carpenter, J. et al. 2023, Proc. of the 7th Chile-Cologne-Bonn Symposium, 304, arXiv:2211.00195
Cornwell, T. J. & Evans, K. F. 1985, A&A, 143, 77
Delli Veneri, M. et al. 2023, MNRAS, 518, 3407
Dewdney, P. E. et al. 2009, Proc. IEEE, 97, 1482
Di Mascolo, L. et al. 2023, Nature, 615, 809
Guglielmetti, F. et al. 2022, Phys. Sci. Forum, 5, 50
Thiébaut, É. & Young, J. 2017, JOSAA, 34, 904
Tychoniec, Ł. et al. 2022, Phys. Sci. Forum, 5, 52

Links

[1] VLTI webpage: https://www.eso.org/sci/facilities/paranal/telescopes/vlti.html
[2] ALMA webpage: https://www.eso.org/sci/facilities/alma.html
[3] Workshop website: https://www.eso.org/sci/meetings/2023/VLTI-ALMA-IW.html

Notes

[a] Earth's atmosphere may introduce phase errors, especially at longer wavelengths. ALMA mitigates this effect by employing atmospheric calibration and phase referencing. Other sources of random noise limiting the accuracy of the amplitude and phase information are thermal noise, shot noise, environmental noise, quantum noise, digitisation and crosstalk in addition to systematics.
[b] The dirty beam considers the source as a point of unit amplitude at the phase tracking centre and the visibility function is unity everywhere.

DOI: 10.18727/0722-6691/5344

Report on the ESO workshop

Disks and Planets across ESO Facilities

held at ESO Headquarters, Garching, Germany, 28 November – 2 December 2022

Antoine Mérand[1]
Michele Cirasuolo[1]
María Díaz Trigo[1]
Bruno Leibundgut[1]

[1] ESO

The observation of protoplanetary discs and exoplanets is a relatively recent and rapidly evolving research field. Many questions are still being posed, driven by both observations and theoretical developments. Discs and exoplanets now constitute a central observational field in astrophysics, and one of the main motivations for ESO and its community to build the Atacama Large Millimeter/submillimeter Array and the Extremely Large Telescope. They are also behind many recent and future developments at the Paranal and La Silla observatories. A workshop was held at ESO Headquarters in November/December 2022 to reflect on the role of ESO facilities (present and future) in this landscape.

Introduction

Observations of protoplanetary discs and exoplanets have always profited from progress in observational techniques: spectroscopic and photometric stability, high-contrast and high-resolution imaging, interferometry in the infrared and submillimetre and so on. ESO facilities played a key role in early observations of discs and planets. In 1996, newly available infrared sensors behind a coronagraph and adaptive optics on the 3.6-metre telescope allowed the first images of beta Pic and its disc[1]. ESO has been at the forefront of large-scale searches for exoplanets by velocimetry with the High Accuracy Radial velocity Planet Searcher (HARPS) since 2003 (Pepe et al., 2004), and with the Echelle Spectrograph for Rocky Exoplanet and Stable Spectroscopic Observations (ESPRESSO) since 2018 (Nielsen & Seidel, 2022). The first direct image of an exoplanet was obtained by the Nasmyth Adaptive Optics System – COudé Near-Infrared CAmera combination (NACO) at the Very Large Telescope (VLT) in 2005[2], followed by several more, recently with the Spectro-Polarimetric High-contrast REsearch instrument (SPHERE). One of the landmark results of the Atacama Large Millimeter/submillimeter Array (ALMA) was the stunning image of the dusty disc around HL Tau[3] in 2014, revealing unexpected ring structures that were interpreted as a signature of ongoing planet formation (ALMA Partnership, 2015).

Beyond these historical achievements, what is the future of observations of discs and planets using ESO facilities? What are the latest theoretical developments? How can they be addressed observationally? How are ESO facilities transitioning from making the first discoveries to surveying large populations? What are the latest observational techniques? How do ESO facilities play against and/or complement other facilities? What does the near future hold, in particular with the Extremely Large Telescope (ELT) on the horizon?

Following a recommendation by the Scientific Technical Committee (STC), the four ESO programme scientists (for the ELT, ALMA, the VLT and the VLT Interferometer) organised the workshop Disks and Planets across ESO Facilities[4] held at ESO's Headquarters from 28 November to 2 December 2022, in order to address these questions and invite community contributions. The workshop was organised in eight half-day sessions, each consisting of an invited review, contributed talks and a moderated discussion. The workshop focused on the following topics: Protoplanetary discs and evolution; Disc chemistry; Protoplanet detection; Planet atmospheres; Planet detection; Biosignatures; ESO opportunities; and Synergies with space missions.

The workshop showed that the community is currently in a privileged situation with access to a unique infrastructure for ground-based astronomy at the global level with facilities like ALMA, the VLT, the VLT Interferometer (VLTI) and the ELT. ALMA has revolutionised the study of discs in the submillimetre by improving by an order of magnitude or more the sensitivity and angular resolution of disc images. Since the first stunning image of gaps in the HL Tau disc, ALMA has provided insights into the architecture of gas and dust interaction. Understanding these observations is still an active research topic. The new frontiers lie in multi-band studies and increasing the sample of observed discs. Future directions require larger samples: expanding to fainter discs, more compact ones (where the dust has settled inwards) or discs in star-forming regions with more common environmental conditions. This requires more observing time via community organisation of surveys, as well as higher sensitivity (which is in part covered by the ALMA2030 development plan[5]) and higher angular resolution.

Protoplanets are hard to find because they are embedded in the discs. Only the exceptional case of PDS 70, where the protoplanets lie in an inner cavity, provides an observational example of interplay between the disc and the forming planets. This system has been discovered and observed by many ESO facilities: SPHERE, NACO, the Multi Unit Spectroscopic Explorer (MUSE; at the VLT), and GRAVITY (at the VLTI), as well as with ALMA, showcasing the suite of instruments ESO provides to its community. A promising technique to detect more protoplanets with ALMA is via perturbations in the Keplerian velocity field of a disc.

Obtaining a complete census of exoplanet demographics requires many observational techniques and facilities beyond even the rich palette offered by ESO. ESO has been at the forefront of planet discovery by radial velocity measurements and direct imaging. Remaining competitive requires observing time for large surveys and/or advances in instrumental technology. The current ESO operational model does not seem to be a limitation as it offers the possibility of large observing programmes and public surveys. The role of ESO facilities as discovery and/or follow-up machines was also discussed: some observations with ESO telescopes can lead to the discovery of discs or planets which can better be characterised by complementary facilities, in particular in space (the JWST, the CHaracterising ExOPlanet Satellite [CHEOPS] etc.) and vice-versa: other facilities (such as Gaia) can provide candidates which can be then observed more deeply with ESO facilities. There is no single recipe and ESO facilities have a significant role to play in both discovery and follow-up.

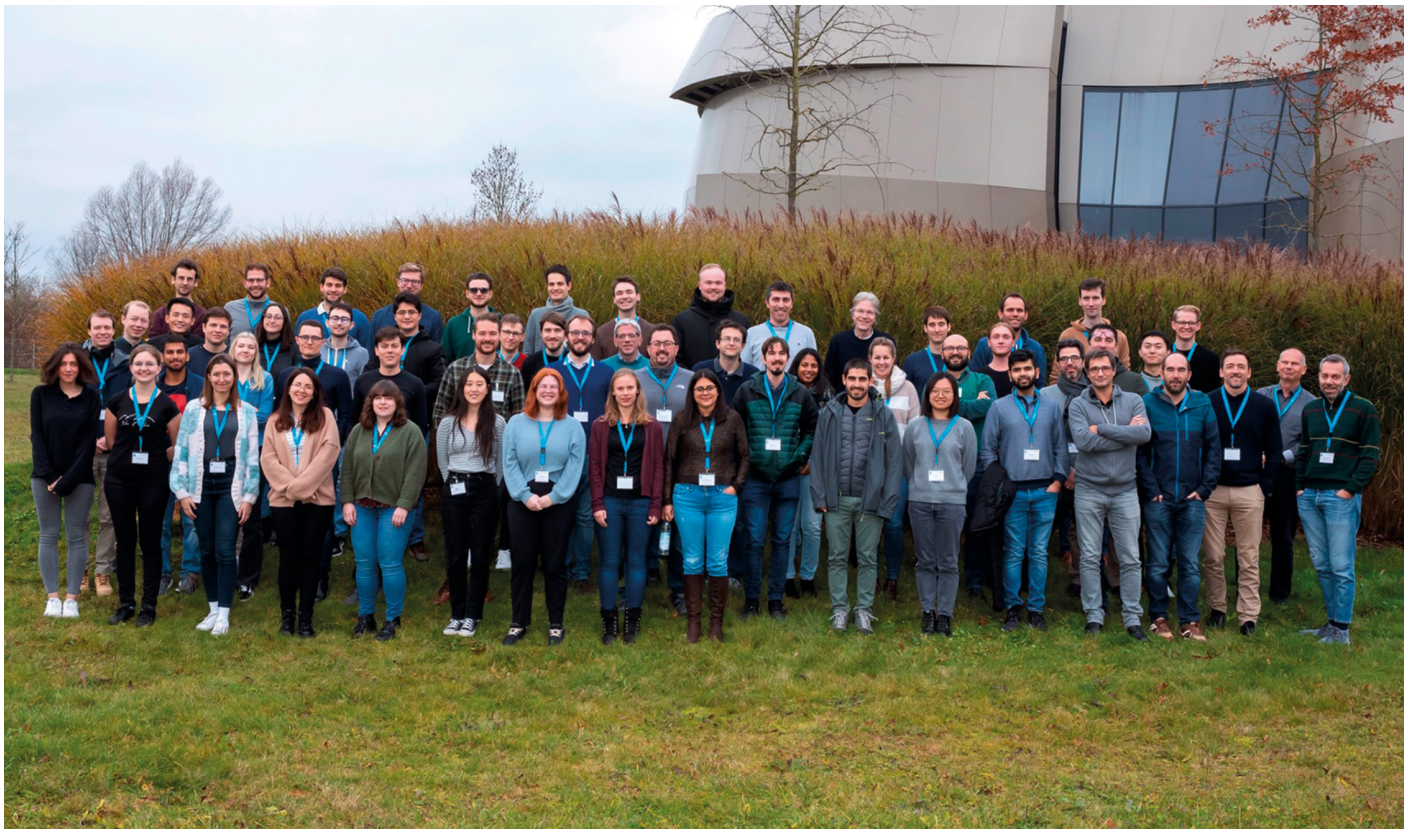

Figure 1. Group photo of the in-person workshop participants.

The search for biosignatures in the atmospheres of temperate rocky exoplanets is a major science driver in astronomy today. This, however, requires very demanding instrumentation. Two main avenues are being pursued: transmission spectroscopy for transiting planets, and spatially-resolved spectroscopy for non-transiting planets. The JWST is currently pushing the limits of transit spectroscopy towards habitable-zone planets, specifically in the TRAPPIST-1 system. Our next-best opportunity will likely come from reflected-light spectroscopy using ground-based instrumentation. Several ideas were proposed to enable the characterisation of the atmospheres and surfaces of habitable-zone planets in the next decade.

Finally, workshop contributions showed that the environment of technological and instrumental developments is a fast growing and rapidly evolving field, particularly in the context of integral-field spectroscopy, high spectral resolution, high-contrast imaging and interferometry. This requires the ability to support upstream critical developments to remain competitive and to prepare the development of ALMA, the VLT/I and particularly the ELT. These elements are already present in current developments (for example, ALMA2030[5] or VLT2030; Mérand & Leibundgut, 2019), and will continue for future exercises.

The workshop took place at ESO Headquarters in Garching, as well as online. The Scientific Organising Committee (SOC) was composed of the four ESO programme scientists and eminent members of the discs and exoplanets communities (including from ESO and the STC). Particular care was taken to balance gender, seniority and geographical origin of the SOC members, the eight invited speakers and the 68 contributors. In all, 135 participants registered and at any given time there were about 100 workshop participants present: 50 people in the conference room (Figure 1) and 50 online (some attendees only participated in the discs or planets sessions).

Acknowledgements

We thank Christophe Lovis for helping with the preparation of this report.

References

ALMA Partnership et al. 2015, ApJL, 808, L3
Mérand, A. & Leibundgut, B. 2019, The Messenger, 177, 67
Nielsen, L. D. & Seidel, J. V. 2022, The Messenger, 187, 8
Pepe, F. et al. 2004, A&A, 423, 385

Links

[1] Beta Pictoris image: https://www.eso.org/public/news/eso9714/
[2] First exoplanet image: https://www.eso.org/public/news/eso0515/
[3] HL Tauri image: https://www.eso.org/public/news/eso1436/
[4] Workshop webpage: https://www.eso.org/sci/meetings/2022/disks_and_planets_at_ESO.html
[5] ALMA Development Roadmap: https://almaobservatory.org/en/publications/the-alma-development-roadmap/

DOI: 10.18727/0722-6691/5345

Fellows at ESO

Julia Bodensteiner

Who would have thought that raspberry ice cream made with liquid nitrogen as a high school student would pave the way for me to become an astronomer. Certainly not me at the time, but it is true.

Although it is often a cliché for astronomers, it is true for me that I've always enjoyed the night sky. Its vast scope and tranquillity continually inspire me, despite only being able to see a handful of twinkling stars from Munich, Germany, where I grew up. I've also always enjoyed being outside, surrounded by nature, for example hiking or cycling. When I was a child, I often went to the mountains with my family. The highlight for me and my brother would always be when we camped outside at the foot of a mountain, where the view of sky was so much better than from the city of Munich.

Unfortunately, during high school the physics curriculum was not particularly inspiring. Physics is also usually not seen as the 'cool' subject, and kids who enjoy physics are often labelled as the weird ones, or the nerds. On top of that I was strongly lacking a female role model. Luckily, my parents kept nudging me towards my scientific interests, for example by gifting me books written by female astronomers.

Despite my interest in physics and astronomy, I never imagined that one day I would actually make a career out of it. And that brings me to one of the important milestone in my youth — a Germany-wide 'Girl's Day' for girls between 14 and 18, which I participated in. Instead of going to school, I spent the day at a solid-state physics lab in the Technical University of Munich (TUM). Not only did I learn a lot about microscopy and the surfaces of materials — but we also had fun doing it. One activity was making raspberry ice cream with liquid nitrogen. From this I realised two things: that physics can actually be really fun, and that 'real' physics is very different from what is taught in schools. I enjoyed the atmosphere of being surrounded by others, mainly girls, and I did not feel judged. So after high-school I decided to study physics at the TUM.

In all honesty, the first years of university felt more like I was more drifting in a river than actually steering a boat: I mainly tried to pass the first-year exams. The third year of my bachelor's degree, however, I spent at the Universidad Complutense de Madrid in the context of the ERASMUS programme, which is where I had my first astronomy lecture. I loved it, and when I came back I searched for a bachelor thesis about an astronomy topic. Specifically, I worked on massive stars in the high-energy group of the Max Planck Institute for Extraterrestrial Physics (MPE) in Munich. It was not only my interest in the topic, but also the welcoming, warm atmosphere in the group at MPE that made me stay on as a job student. In collaboration with a second supervisor at ESO, I continued there to do my master's thesis project investigating circumstellar nebulae around massive stars. Because massive stars, and in particular binaries, always interested me, I sought a PhD position in observational stellar astrophysics and was successful: I got a position to work on spectroscopic observations of massive binaries at the Institute of Astronomy at KU Leuven, Belgium.

A highlight of my career has been visiting La Silla observatory in Chile to observe during my time at MPE. I fell in love with the scenery of the Atacama Desert, the friendliness of the people working at the telescopes, and of course the stunning night sky. So I was very happy when during my PhD I could go observing to the KU Leuven Mercator telescope on the Roque de los Muchachos in La Palma, Spain. I went as often as I could, and so far I have spent more than 50 nights observing in different observatories. This was also one of my main drivers to apply for the ESO fellowship: the strong connection to the observatory, the proximity to telescopes, and the development of new instruments. Now, working at ESO, I have been able to visit Paranal and spend several nights at the telescope. This allowed me to gain invaluable insight into telescopes and how they work, and to better understand the observations themselves. Additionally, I think that Paranal is a really magical place.

What I really enjoy about the scientific environment, not only at ESO but also any other institute or research centre I've visited so far, is the international environment I am exposed to every day. This not only allows me to talk to and interact with many different people from different countries and diverse backgrounds, but also to learn more about other cultures. Most importantly, my research career has taught me openness and has provided me with a better understanding of different ideas and perspectives. In general, I've always enjoyed travelling, which is another aspect that I like about the scientific environment. Going to conferences or meetings at different institutes always means meeting new people and getting to know the world.

Something I am particularly grateful for is the scientific freedom afforded me so far in my career. I've always been able to follow my own curiosity and work on the questions that I find the most interesting. During my master's thesis, I wanted to work on a topic that was not particularly the focus of my supervisor. Instead of telling me to change it, he encouraged me to gain a second supervisor complementary in expertise for that topic. Similarly, during my PhD, when I devised a new project halfway through my PhD, my supervisor motivated me to follow my own interests and gave me the opportunity to work on new things that were originally not planned. As an ESO fellow, I enjoy similar scientific freedom: I applied to the ESO fellowship programme with my own project. My focus is the study of a particular type of massive star, classical Be stars, which are interesting because they are rapidly rotating and surrounded by a disc of gaseous material. During my fellowship at ESO, I am investigating whether their rapid rotation is linked to previous interactions in a binary system. For this, I am using spectroscopic observations with both ESO telescopes and the HERMES spectrograph on the Mercator telescope, which I analyse in collaboration with an international team of people. Given my fondness for nature, I called our collaboration HONEYBeeS (which stands for HERMES ObservatioNal survEY of BeOe Stars).

Now my career has brought me back to Munich, where it all began, and I still enjoy going to the mountains in south Germany and looking up at the night sky. I look forward to an exciting future, building on my experience in Germany and Belgium. My favourite flavour of ice cream may have changed, but I think back to that important milestone of how raspberry ice cream made me pursue a career in physics and astronomy. Today, I am grateful to have the opportunity to be involved in the Girl's Day from the other side, where I hope to inspire many girls to pursue a career in astronomy.

Melanie Kaasinen

Recently, my Dad asked me "What happens when light reaches the edge of the Universe? And anyway, why is the speed of light that value (no more, no less)?" I find these questions great fun to explore, which is lucky given that I am also often asked such mind-boggling questions when I do outreach. They are the kind of questions I thought about as a child, when I read books like Brian Greene's *A Fabric of the Cosmos*. At that time, astronomy was a form of escapism for me — beyond this tiny blue dot was an incredibly vast and wondrous Universe that had no concept of us humans and our insignificant problems!

Astronomy may have been an early interest, but it was not my first career goal. I moved from Germany to Brisbane (Australia) aged five and started swimming, which quickly turned into an obsession. A few years later, it was clear that I was far more talented at running. Later, in high school, I also started cycling seriously, leaving Wednesday school sport for my cycling session on the nearby cycling/criterium track. Obviously, I was going to be a triathlete... but alongside the focus on endurance sports, I also loved learning about astronomy. Luckily, my parents were incredibly supportive of both my sport and my education — even moving close to a high school with a focus on aviation. My passion for maths and science was also channelled early on by my wonderful maths teacher, who set me additional challenges. In the end, I was as ambitious academically as athletically and threw myself into my final years of high school to obtain a scholarship that would pay off my bachelor's degree.

After school I dived into an 'accelerated' science degree at the Queensland University of Technology. The challenge of the degree and interaction with like-minded people made me want to pursue astrophysics more seriously. I also realised during this time that I enjoyed outreach and I started to host astronomy workshops for high school students as part of my first paid job — as a STEM ambassador. Astronomy was looking more like a serious career, whereas sport was becoming the hobby. So I had to find a place where I could learn how to do astronomical research. Knock knock the Australian National University (ANU) in Canberra, where I spent the next two, hugely formative, years undertaking my master's.

The ANU's Research School of Astronomy and Astrophysics on Mt Stromlo is a magical place — a friendly astronomical community atop a hill that is home to

hundreds of vibrant birds and a few kangaroo mobs (including the local alpha male, Bruce). Working with Lisa Kewley (my supervisor, now director of the CfA), Brent Groves (now ICRAR) and Fuyan Bian (now ESO staff), I studied the conditions within the ionised interstellar medium (ISM) of $z \sim 1.5$ star-forming galaxies. This was a hot topic in galaxy evolution at the time; rest-optical lines at $z \sim 2$ had only recently become observable and there was much debate over the source of the 'more extreme' line ratios being observed. By analysing Keck/DEIMOS and Subaru/FMOS observations, I showed that these high line ratios arose in part from the high electron densities and ionisation parameters associated with the high specific star formation rates of $z \sim 2$ galaxies. Alongside my master's, I also continued doing astronomy outreach (night-sky tours, for example) and of course sport. After all, at the bottom of the hill there is a perfect cycling circuit and cross-country running track!

Having relished the supportive science environment of my master's, I was now serious about becoming an astronomer. I had heard about the exciting results coming from ALMA and was keen to jump on board. Luckily, I snagged a PhD with the supervisory dream team: Fabian Walter and Simon Glover, the first an expert on radio astronomy, and the second an expert on the chemistry of the cold ISM. So, I moved across the world to the stunningly picturesque city of Heidelberg — where I again worked at a vibrant institute atop a gorgeous, forest-covered hill (perfect to cycle and run up). During my PhD, I helped to accurately constrain the amount and distribution of molecular gas and dust in galaxies at $z = 1.5$–2. Yes, I was still stuck at Cosmic Noon, but I was studying a different gas phase and delving into VLA, NOEMA and of course ALMA data — gaining experience in millimetre- to radio-wavelength interferometry. I also continued with astronomy outreach, giving planetarium shows and public talks (this time in German) at the Haus der Astronomie.

Ten months before the end of my PhD, and during one of the worst lockdowns, I wrote my application for the ESO fellowship. And a few days before Christmas... I GOT THE ESO FELLOWSHIP!

My excitement was well placed. Since coming to ESO, I have worked on unexpected new projects, like searching for evidence of a $z \sim 13$ galaxy candidate in ALMA data with my ESO colleagues (spoiler alert — no evidence found). I have been lucky enough to help prepare for ESO's Extremely Large Telescope (ELT), working on finding faint new sky lines in VLT/CRIRES observations with fantastic colleagues I never would have worked with otherwise. I have also observed for the first time at a submillimetre telescope. Muchos gracias to Carlos De Breuck for enabling my trip to APEX! It was incredible to be part of this tight-knit community, to explore other people's data as it came in (what are these complex multi-peaked line profiles?!) and to see APEX and ALMA in person. Those antennas are simply surreal in that landscape. I was also lucky enough to visit Paranal for a whole week and receive a tour of the ELT site!

Being an astronomer has been an amazing adventure and I cannot wait to see where it takes me next. Thankfully, I still have the same sense of wonder about the Universe that I had when I was a child. But now I am fortunate enough to be able to share this wonder with others and answer a few of their burning questions.

Marco Berton

I loved science since I was a kid. When I was twelve, after watching a documentary on Italian television, I became certain: I wanted to become an astronomer. By the end of middle school, I had read the astronomy section of the science textbook so many times that I had memorised all the orbital parameters of the (back then) nine planets. I chose my high school because it offered basic astronomy classes in the fifth and final year. Of course, over time, my conviction wasn't as strong as when I began. However, in my last year of high school, I had the chance to participate in a project organised by the Department of Astronomy at the University of Padova, called Il cielo come laboratorio (The sky as a laboratory). Over three observing nights at the Asiago 1.22-metre telescope, we collected the optical spectrum of the spiral galaxy NGC 2748 and determined its gravitational mass from the Hα rotation curve. That was the turning point: observational astronomy truly was the right path for me.

The city of Padova, near Venice, is home to one of the oldest universities in the world, with a tradition of astronomy dating back to Galileo Galilei himself. The university offers a bachelor's and master's program entirely focused on astronomy: I couldn't have found a better place to pursue my interests. Having the opportunity to study the nature of various astrophysical objects was simply amazing to me, and I soon realised that active galaxies interested me the most. These accreting supermassive black holes, shining brighter than an entire galaxy, became the subject of both my bachelor's and master's theses. Initially, I analysed the physical properties of ionised gas in a sample of nearby active galaxies using archival data. However, for my master's, I finally had the chance to use new data from a real telescope, the 3.6-metre Telescopio Nazionale Galileo. While I managed to earn my degree, it was only after an incredibly challenging effort. For the first time, I doubted my decision: did I truly want to wrestle with data analysis for the rest of my life? I had to step back and seriously consider my options. Everyone, take note: pursuing a career in astronomy is not a decision to be taken lightly!

It took nearly two years for me to clear my mind once and for all, but my PhD adventure finally began on 1 January 2013. The topic? Active galactic nuclei (AGN), of course! My advisors were Stefano Ciroi in Padova and Luigi Foschini at the Brera Astronomical Observatory, and I couldn't have asked for better advisors. Working with them, I had the opportunity to delve into the physics of jetted AGN across all wavelengths, from radio waves up to gamma rays. I stayed in Padova for five years, completing my PhD and my first postdoc. During that time I spent over 250 nights observing with the Asiago telescopes, mainly to obtain optical spectra for my own work but also for other research groups. I also had my initial experiences of living abroad, with two periods at Purdue University and the University of California Santa Barbara in the USA. These were enriching experiences that introduced me to new people

and allowed me to grow not only as a scientist but also as a person. In terms of research, I continued to study a unique class of AGN known as narrow-line Seyfert 1 (NLS1) galaxies. While some of them do harbour relativistic jets, unlike 'normal' radio galaxies with black hole masses around a billion solar masses, NLS1s are powered by black holes a thousand times smaller that are rapidly accreting matter. In NLS1s, typically hosted in spiral galaxies, the AGN coexists with relativistic jets, star formation, and outflows of ionised and neutral gas. This uniqueness makes them valuable sources, possibly representing an early evolutionary phase in the AGN life cycle. Given the relatively unexplored radio properties of these objects, I undertook the largest and deepest survey in this wavelength range using the Very Large Array in New Mexico. As a fan of the movie Contact, having the opportunity to use such a massive array of 28 antennas was an unparalleled feeling.

In 2018 I eventually left Padova. I secured a fellowship at the Finnish Centre for Astronomy with ESO and worked at the Aalto University Metsähovi Radio Observatory for three years. I cherished every moment spent there. Finland, renowned as the happiest country in the world for good reason, offered wonderful people and nearly untouched natural beauty. Metsähovi, situated 30 kilometres from Helsinki in the heart of a forest, often led to encounters with deer and even moose during my commutes to the office. Unfortunately, I could fully enjoy this only for half of my time there, as the pandemic emerged. Nevertheless, even during those challenging times, taking walks in the woods provided a stress-relieving escape.

As the pandemic neared its end, the time for another move approached. I accepted a position as an ESO fellow in Paranal and relocated to Chile. Honestly, this wasn't an easy decision: I had never worked in such a large observatory before, and the prospect of spending 80 nights a year at Paranal initially seemed daunting. However, it took only a few months for me to realise how fortunate I am. My enthusiasm for the ESO life has grown, and I'm now grateful to be part of the expansive and diverse Paranal community, along with the dynamic scientific atmosphere at ESO Vitacura. Presently, when I'm not studying AGNs in Santiago, I work as a night astronomer on the UT4. With its advanced adaptive optics system, it's the closest approximation we currently have to the ELT. Specifically, I now serve as the second instrument scientist for MUSE, arguably the world's best integral-field spectrograph. The journey that brought me here was long and winding, but I would retrace each step. I now eagerly await what the future holds.

ESO/H. Heyer

This photograph shows the European Southern Observatory's Headquarters in Garching, near Munich, Germany. This is the scientific, technical and administrative centre for ESO's operations, and the base from which many astronomers conduct their research. The scientists, technicians and administrators who work here come from many different backgrounds, but all have one thing in common: a passion for astronomy.

This drone image, taken in late September 2023, captures an aerial view of ESO's Extremely Large Telescope (ELT) dome at night-time. It already has the recognisable spherical shape of a telescope enclosure with the construction of the frame well on its way to being completed by the end of 2023.

ESO/G. Vecchia